

INFORMATION TO USERS

This manuscript has been reproduced from the microfilm master. UMI films the text directly from the original or copy submitted. Thus, some thesis and dissertation copies are in typewriter face, while others may be from any type of computer printer.

The quality of this reproduction is dependent upon the quality of the copy submitted. Broken or indistinct print, colored or poor quality illustrations and photographs, print bleedthrough, substandard margins, and improper alignment can adversely affect reproduction.

In the unlikely event that the author did not send UMI a complete manuscript and there are missing pages, these will be noted. Also, if unauthorized copyright material had to be removed, a note will indicate the deletion.

Oversize materials (e.g., maps, drawings, charts) are reproduced by sectioning the original, beginning at the upper left-hand corner and continuing from left to right in equal sections with small overlaps. Each original is also photographed in one exposure and is included in reduced form at the back of the book.

Photographs included in the original manuscript have been reproduced xerographically in this copy. Higher quality 6" x 9" black and white photographic prints are available for any photographs or illustrations appearing in this copy for an additional charge. Contact UMI directly to order.

UMI

A Bell & Howell Information Company
300 North Zeeb Road, Ann Arbor MI 48106-1346 USA
313/761-4700 800/521-0600

University of Alberta

**Assembly and secretion of rubella
virus-like particles in mammalian cells**

by

Michael Garbutt



A thesis submitted to the Faculty of Graduate Studies and Research
in partial fulfillment of the requirements for the degree of
Master of Science

DEPARTMENT OF CELL BIOLOGY AND ANATOMY

Edmonton, Alberta

Fall 1997



National Library
of Canada

Acquisitions and
Bibliographic Services

395 Wellington Street
Ottawa ON K1A 0N4
Canada

Bibliothèque nationale
du Canada

Acquisitions et
services bibliographiques

395, rue Wellington
Ottawa ON K1A 0N4
Canada

Your file *Votre référence*

Our file *Notre référence*

The author has granted a non-exclusive licence allowing the National Library of Canada to reproduce, loan, distribute or sell copies of this thesis in microform, paper or electronic formats.

The author retains ownership of the copyright in this thesis. Neither the thesis nor substantial extracts from it may be printed or otherwise reproduced without the author's permission.

L'auteur a accordé une licence non exclusive permettant à la Bibliothèque nationale du Canada de reproduire, prêter, distribuer ou vendre des copies de cette thèse sous la forme de microfiche/film, de reproduction sur papier ou sur format électronique.

L'auteur conserve la propriété du droit d'auteur qui protège cette thèse. Ni la thèse ni des extraits substantiels de celle-ci ne doivent être imprimés ou autrement reproduits sans son autorisation.

0-612-22597-6

University of Alberta

Library Release Form

Name of Author: Michael Garbutt
Title of Thesis: Assembly and secretion of rubella virus-like particles in mammalian cells
Degree: Master of Science
Year this Degree Granted: 1997

Permission is hereby granted to the University of Alberta Library to reproduce single copies of this thesis and to lend or sell such copies for private, scholarly or scientific research purpose only.

The author reserves all other publication and other rights in association with the copyright in the thesis, and except as hereinbefore provided, neither the thesis nor any substantial portion thereof may be printed or otherwise reproduced in any material form whatever without the author's prior written permission.

M Garbutt

Michael Garbutt

#1-4420-102 Avenue,

Edmonton, AB

T6A 0M6

June 27, 1997

University of Alberta
Faculty of Graduate Studies and Research

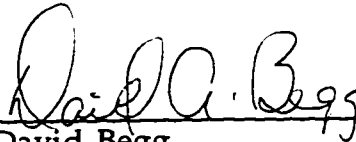
The undersigned certify that they have read, and recommend to the Faculty of Graduate Studies and Research for acceptance, a thesis entitled **ASSEMBLY AND SECRETION OF RUBELLA VIRUS-LIKE PARTICLES IN MAMMALIAN CELLS** submitted by **MICHAEL GARBUTT** in partial fulfillment of the requirements for a degree of **MASTER OF SCIENCE**.



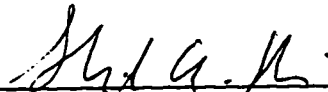
Dr. Thomas C. Hobman



Dr. Bruce Stevenson



Dr. David Begg



Dr. Stephen Rice

June 26, 1997

Nurse's elegy

You have the right to tread so softly
beside a couch of pain.
To smooth with loving fingers
those tangled locks again.
To kneel beside the dying
in the small hours of the night.
Then whisper a righteous blessing
as the spirit takes its flight.

Olive Lambert

ABSTRACT

To establish an *in vitro* model system to study RV assembly and secretion characteristics, MDCK II-24S, Vero C1008-24S and Caco-2-24S epithelial cells were derived by stably transfecting parental cells with 24S cDNA. 24S cDNA codes for rubella virus structural proteins NH₂-capsid-E2-E1-COOH, which assemble into rubella virus-like particles (RLPs). RLP secretion from Vero C1008-24S and Caco-2-24S cells resembled RV virion release from infected Vero C1008 or Caco-2 cells. EM analysis of all three transfected cells revealed that RLPs resembled RV virions in terms of size and morphology. In all three cell lines, RV structural proteins were targeted to the Golgi. However, RLPs were released in a polarized manner from MDCK II-24S cells and in a non-polarized manner from Vero C1008-24S and Caco-2-24S cells. Vero C1008-24S cells exhibited epithelial polarity, using inulin diffusion, dome formation, Na/K-ATPase distribution, EM morphology and biotinylation profiles to demonstrate tight junction formation. RLP assembly and secretion from stably transfected CHO cells was abrogated by replacing or removing the transmembrane and/or cytoplasmic domains of E1.

DEDICATION

I would like to thank Tom Hobman for giving me the opportunity to do the work presented in this thesis. Thanks Tom :-) Also, I would like to thank Margaret, Honey, Vera, Leigh Ann, Darren and Kevin for technical assistance. As well, I would like to thank Andrew Chau for technical and personal assistance.

I would especially like to thank Linda, Christopher and my mother, who tolerated my single-mindedness through the past six years. Their encouragement and support maintained my spirits through out this endeavor.

Table of contents

1. INTRODUCTION

1.1. Medical significance of rubella virus	1
1.2. Rubella virus characteristics	2
1.2.1. Capsid protein	3
1.2.2. Envelope glycoproteins, E2 and E1	5
1.2.3. 24S cDNA expression results in formation of rubella virus-like particles (RLPs)	8
1.3. Recombinant virus-like particles (VLPs) and their uses	9
1.4. RLPs as tools to study rubella virus assembly and secretion	10
1.5. Virus assembly and polarized secretion in mammalian cells	11
1.6. Rationale	12

2. MATERIALS AND METHODS

2.1. Reagents	14
2.2. Antibodies	15
2.3. Recombinant plasmids	16
2.4. Construction of recombinant plasmids	
2.4.1. Construction of pCMV5-24SE1-CD8tm	16
2.4.2. Construction of pCMV5-24SE1-CD8tmct	17
2.4.3. Construction of pCMV5-24SE2-Gtm	17
2.5. Cell culture, transfection and immunofluorescent screening	
2.5.1. Cell Culture	18
2.5.2. Stable transfection	18
2.5.3. Immunofluorescent Screening of clones	20
2.6. Metabolic labeling and immunoprecipitation	
2.6.1. Metabolic labeling	21
2.6.2. Immunoprecipitation	22
2.7. SDS PAGE and fluorography	23

2.8. Western blotting	23
2.9. Electron microscopy	24
2.10. Inulin diffusion and transepithelial resistance (TER)	
2.10.1. Inulin diffusion	25
2.10.2. Transepithelial resistance (TER)	26
2.11. Biotinylation of cell surface proteins	27
2.12.1. Virus plaque assay (agarose overlay)	27
2.12.2. Virus plaque assay (immunofluorescent)	28
2.13. Confocal microscopy	29
3. RESULTS	
3.1. MDCK II cells secrete RLPs in a polarized manner	31
3.2. Vero C1008 cells secrete RLPs and RV virions in a non-polarized manner	34
3.2.1. RLP secretion in polarized Vero C1008-24S cells	36
3.2.2. RV infection of Vero and Vero C1008 cells	39
3.3. Caco-2 cells secrete RLPs and RV virions in a non-polarized manner	40
3.4. Assembly of RLPs in stably transfected CHO cells	41
3.4.1. Characteristics of CHO24S cells	43
3.4.2. Characteristics of CHO24S E1 ct- cells	44
3.4.3. Characteristics of CHO24S Gtmct cells	45
3.4.4. Characteristics of CHO24S CD8tm and CHO24S CD8tmct cells	46
3.4.5. Characteristics of CHO24S E2Gtm cells	48
4. DISCUSSION	
4.1. Polarized secretion of RLPs in mammalian cells	50
4.2. Assembly of RLPs in mammalian cells	53
4.3. Future perspectives	55
5. FIGURES	57
6. BIBLIOGRAPHY	97

1 INTRODUCTION

1.1. Medical significance of rubella virus

Rubella virus (RV) causes a mild childhood disease known as rubella, three day measles or German measles. The notable characteristics of this disease include skin rash, occasional fever and lymphadenopathy (99). Most significantly, RV is a teratogenic agent that can cross the placenta of seronegative women who become infected during the first trimester of pregnancy. Subsequently, the virus replicates in the fetus leading to a disorder collectively known as congenital rubella syndrome (CRS). CRS in the newborn is characterized by defects of the heart, cataracts, deafness and mental retardation (20). RV also causes polyarthralgia and arthritis, more prevalent in adult women than in adult males (20). In addition, chronic arthropathy can occur following vaccination and to a lesser extent post infection (87). Autoimmune diseases such as insulin-dependent diabetes mellitus (IDDM), multiple sclerosis (MS), rheumatoid arthritis and thyroiditis have also been linked to RV infection (20). A mouse monoclonal antibody specific for RV capsid protein that cross-reacts with a 52 kD protein present in rat insulinoma cells, further implicates RV with autoimmune disease (44).

RV can persist in humans for many years (99), and is prevalent world wide. Epidemics occasionally occur, particularly in underdeveloped countries or in regions of developed countries where vaccination programs are not instituted, such as prisons or religious communities (20). 1964 marked the last major RV epidemic in the United States, where an estimated 20,000 children were infected *in utero* and contracted CRS (20, 99). Since then, other outbreaks in the United States and throughout the world caused CRS in large numbers of children. After a rubella outbreak in 1991 in the largely unimmunized Amish community in Pennsylvania, the annual CRS incidence was reported to be 2,130/100,000 live

births (61). More recently in Manitoba, RV infections reached epidemic proportions, and more than 1,900 cases were reported in a six month period ending April 1997, compared to just two cases in 1995 (73). Males who were not vaccinated against RV accounted for the majority of cases.

While vaccination is adequate to control RV infection, the finite lifetime and supply (29, 43) of the cells used to propagate the vaccine may ultimately lead to a problem in producing adequate amounts of vaccine. Obviously, eradication of RV would be most favorable, however, continued control of RV is a more realistic and essential goal. Unfortunately, no animal model exists to further the study of RV, and only a few *in vitro* cell culture systems support infection (20). For this reason it is important to develop new strategies to investigate RV infection either *in vitro* or *in vivo*. Once we understand the molecular basis of RV infection, we may discover ways to prevent some or all of the associated disorders.

1.2. Rubella virus characteristics

RV is the only member of the rubivirus genus in the *Togaviridae* family (80). Togaviruses are so named because of their lipid envelope or "toga," and are grouped based on serology and genomic organization (99). Alphavirus is the other genus in the *Togaviridae* family, and Sindbis virus is the type-specific member (80). Alphaviruses replicate in both insects and mammals, and cause a variety of diseases in humans and domestic animals (83). Rubella virus however only replicates in humans; no arthropod vector is known.

Rubella virions contain a single stranded, positive (+) polarity RNA genome encapsidated in an icosahedral protein shell surrounded by a host-derived lipid envelope. The envelope contains two glycoproteins, E2 and E1 (64).

Virions are approximately 60 nm to 65 nm in diameter, and mature by budding into the Golgi or plasma membrane depending upon cell type (48, 67, 93).

Some of the details of virion penetration and uncoating have been determined (figure 20). Phospholipids and glycolipids rather than proteins are believed to be involved in binding RV (55). Subsequent to attachment, virions are internalized and follow the endosomal pathway into the cell (70). The low pH of the endosome is believed to cause capsomere solubility after fusion of the viral envelope with the endosome. Consequently, the viral RNA is released into the cytoplasm (56). Once the genomic RNA is released into the cytoplasm, the 5' proximal ORF is translated by host enzymes to produce non-structural (NS) RV proteins. NS proteins putatively use the genomic RNA as a template to transcribe negative-polarity RNA (20), which is subsequently used as a template to make full length and subgenomic positive-polarity RNAs (see figure 1) (30). The RV genome has been cloned and sequenced, and is 9756 nucleotides in length and sediments with a coefficient of 40S (20). A subgenomic 24S RNA, while more prevalent in infected cells, can also be isolated from RV virions (65, 96). The 3' one-third of the genome and the subgenomic 24S RNA, which corresponds to the 3' one-third of the genomic RNA, contains a 3183 nucleotide ORF (15, 16), which codes for the structural proteins NH₂-capsid-E2-E1-COOH in the form of a polyprotein (63, 65). E2 and E1 signal peptides direct the translocation of the polyprotein into the endoplasmic reticulum (ER), where it is cleaved by resident signal peptidase on the C-terminal side of both signal peptides (34, 39).

1.2.1. Capsid protein

Capsid (C) protein is 299 amino acids long (15), and remains on the cytoplasmic side of the ER membrane, the C-terminus being anchored to the ER by virtue of the E2 signal peptide (figure 2) (84). Capsid proteins spontaneously

form noncovalent homodimers which become disulfide-linked after virus budding (4). These proteins are phosphorylated (54), are rich in arginine and bind to the viral genomic RNA (99). The molecular weight (MW) ranges between 33 kD and 38 kD, depending upon the gel system used, with a mean of 34.5 kD. Capsid proteins assemble into the virion core, which are thought to have $T = 3$ icosahedral symmetry, reviewed in (20). RV capsid assembly is synchronized with budding, unlike alphavirus, where preformed nucleocapsids interact with virus glycoproteins at the site of budding (80). The mechanism of capsid assembly at the molecular level remains to be determined, and little information about transport of capsid from the site of synthesis (ER) to the site of budding (Golgi) is available. When capsid is expressed alone in COS cells, a diffuse cytoplasmic staining pattern is seen (36). Similarly, when capsid is expressed along with E2, a diffuse capsid staining pattern can be seen. When C/E2 cleavage is inhibited, i.e., by mutating the cleavage site, capsid is seen to concentrate in the ER, as co-localization with ER marker con-A is predominant (58). Contrary to the findings of McDonald et al., Baron et al., found that capsid was localized to the ER when expressed alone in COS cells (3). One possible explanation for these different findings could be heterogeneity within cell lines, i.e., different culture conditions can produce variants with characteristics different to the parental type (18). Another explanation, while less likely, could be the level of expression of the protein due to the length of the construct within the expression vector; while translation was driven by the SV40 late promoter in both expression vectors, insert lengths were different (3, 16). Baron et al. used an insert coding for capsid with a stop codon immediately after the E2 signal peptide sequence, while McDonald et al. used an insert coding for capsid and the first one-third of E2; an amount sufficient to permit cleavage between capsid and E2 (58). Capsid localization may be affected by the position of the stop codon in each construct.

A pause in protein translation occurs when signal-recognition particle (SRP) binds to the nascent protein signal sequence that emerges from a ribosome (1). While both constructs contain the hydrophobic domain, only McDonald's construct allows for the nascent protein/ribosome complex to be guided to the ER by SRP. Baron's construct would facilitate the nascent protein's release from the ribosome into the cytoplasm before SRP mediated targeting to the ER could occur (84). However, capsid protein containing the stop codon after the 23 amino acid signal peptide is integrated into microsomes during *in vitro* translation experiments, probably by a SRP independent means (84).

Capsid is localized to the Golgi in CHO or COS cells coordinately expressing C/E2/E1 (37, 58), indicating that E1 facilitates capsid egress from the ER. Metabolic labeling studies correlate with immunofluorescent staining, indicating intracellular degradation occurs when capsid is expressed alone and secretion occurs when capsid is expressed with E2 and E1. However, degradation is not rapid, as ³⁵S labeled capsid is present within CHO24S cells for at least 8 h, while labeled E2/E1 is seen to be almost completely secreted by this time (37). These results indicate capsid protein stability (possibly in association with a cellular protein) and non-concerted assembly of structural proteins (presuming 1:1:1 ratio of assembled structural proteins (7)). Often, capsid is seen to migrate as a doublet on polyacrylamide gels under reducing conditions. However, this phenomenon cannot be attributed to alternate translation initiation (16) or differential phosphorylation (54) of capsid.

1.2.2. Envelope glycoproteins, E2 and E1

Both E2 and E1 are type I membrane spanning glycoproteins, whose nascent polypeptides are 281 amino acids (E2) and 481 amino acids (E1) in length. After cleavage of the polyprotein within the lumen of the ER, E2 and E1

ectodomains are core glycosylated (36, 51, 64). E2 is N-glycosylated at three or four sites (strain specific) (71) and is O-glycosylated (51). E1 is N-glycosylated at three sites (38). E2 is predicted to be attached to the ER by a transmembrane region and the signal peptide of E1; a short cytoplasmic region separates the two hydrophobic domains. E2 and E1 both incorporate palmitic acid (36, 97). A single transmembrane region attaches E1 to the ER (15). The MW of the mature form of E2 ranges from 42 kD to 47 kD, because of heterogeneous O-linked glycosylation, and the MW of the mature form of E1 is 58 kD to 62 kD (20, 99). (figure 2)

E2 and E1 form heterodimers (4, 41), and confer the virion with hemagglutination, fusogenic and infectivity properties. Hemagglutination is associated with glycosylated E1 (31), and is nullified by trypsin treatment (32). Fusion of the virus with membranes is dependent upon a pH induced conformational change in E1 (20). Monoclonal antibodies that react with regions of E1 can block infection by neutralizing the binding sites of the virus (86, 100). Some of the molecular details of E2/E1 maturation and assembly are known.

The signal peptide of E2 has been shown to target translocation of E2 into the lumen of the ER (34, 84). Signal peptidase cleaves E2 from capsid, and this cleavage is essential for E2 transport beyond the ER (58). E2 containing Golgi specific glycan modifications can be detected after 30 min in COS cells transiently expressing 24S cDNA or E2E1, and to a lesser degree at 60 to 120 min in cells transiently expressing E2 only. The fastest rate of Golgi specific glycan modification occurs in E2E1 transfected cells, suggesting that E1 facilitates E2 egression from the ER (36). This also indicates that capsid slows down E2E1 transport to the ER, consistent with the finding that capsid localization to the Golgi is dependent upon coordinated E2/E1 expression, and lends support to the hypothesis that E1 modulates a C/E2 interaction in RLP assembly. Palmitic acid is incorporated into E2, but predominantly ER or precursor type E2 is present in

cells expressing only E2. Consequently, palmitylation occurs before E2 reaches the Golgi (36). M33 strain of E2 is N-glycosylated at three sites, N-53, N-71 and N-115 of the ectodomain. Removal of either one of these sites by mutagenesis, impairs ER to medial Golgi transport in transiently transfected COS cells, and non-glycosylated mutants are degraded completely within 4 h (71). When secretory forms of E2 are constructed, i.e., the transmembrane domain is removed, only endo-H resistant forms of these anchorless E2 glycosylation mutants are secreted, and the amount of protein secreted is dependent upon the site that is deleted. Expression of E2E1 in CHO cells results in Golgi localization and retention of both glycoproteins, and brefeldin-A (BFA) and nocodazole treatment reveals that E2 and E1 behave as integral Golgi membrane proteins (41). Some E2 and E1 reaches the cell surface by an as yet unidentified means, however, most remains Golgi-associated. E2 and E1 form a dimer within the ER within 5 min of synthesis even though E1 does not reach its fully folded form for 1 h. Because endo-H resistance occurs in E2 and E1 at the same time, it is believed that E1 folding within the ER is the rate limiting step before egress of the E2/E1 heterodimer to the Golgi (41). The E2 transmembrane region contains a Golgi retention signal, and is required for transport of the E2/E1 spike complex from the ER (42).

E1 is translocated into the ER by virtue of a signal peptide located after and continuous with, the E2 cytoplasmic domain. Without this signal peptide, E1 is degraded within the cytoplasm (39). Coordinate expression of E2 with E1 optimizes E1 egress from the ER, and capsid expression seems to slow the rate of ER to Golgi transport (36). These findings are based upon E2 and E1 glycoproteins becoming endo-H resistant more quickly when expressed as NH₂-E2-E1-COOH than as NH₂-capsid-E2-E1-COOH. Assembly of RLPs in cells expressing 24S cDNA may therefore occur prior to the medial Golgi,

consequently slowing down E1 and E2 progress. On the other hand, cells expressing E2E1 only, encounter no delays due to particle assembly, therefore E2 and E1 glycoproteins proceed to the medial Golgi unhindered. E1 is N-glycosylated at three sites, but unlike E2, glycosylation mutants of E1 expressed in COS cells can be found to localize to the juxtannuclear region (38). CHO cells expressing E1 only, show staining predominantly in a post-rough ER pre-Golgi structure (40). COS cells expressing E1 also show juxtannuclear staining, but a higher level of expression may occur in COS cells resulting in aberrant localization.

E1 contains 24 cysteine residues, 20 of which are believed to be involved in folding of the extracellular domain (25). As the quality control system of the ER allows only fully folded proteins to exit (28), the slow folding rate mentioned above and quality control likely account for the delay in mature E1 egress to the Golgi. Also, chimeric molecules incorporating the E1 transmembrane and cytoplasmic domains exhibit ER retention (35). However, the E1 ER retention signal most likely is inactivated after heterodimeric E2E1 formation and folding.

1.2.3. 24S cDNA expression results in formation of rubella virus-like particles (RLPs)

24S mRNA was originally transcribed into cDNA to delineate the nucleotide sequence, with a view towards *in vitro* expression and a better understanding of the processing of RV structural proteins (15). Subsequent to these initial experiments, individual expression of the structural proteins facilitated the study of intracellular processing and transport properties of capsid, E2 and E1 (34, 36, 38-41, 49, 51, 54). Ultimately, Hobman et al. showed that coordinated expression of RV structural proteins results in the formation of rubella virus-like particles (RLPs) in the Golgi of CHO cells (37). Particle diameters range from 50 to 60 nm, with a buoyant density of 1.16 to 1.18 g/ml

(37). These particles are not seen in the absence of capsid, suggesting that expression of all three structural proteins is required for particle assembly. Rubella virus-like particles are similar to RV virions in terms of size, morphology, buoyant density and antigenicity (37).

1.3. Recombinant virus-like particles (VLPs) and their uses

Virus-like particles (VLPs) may form when cDNA coding for viral structural protein(s) is expressed in cultured cells. Resulting particles generally resemble native virions but lack the viral genome. Numerous reasons for studying VLPs are cited in recent literature. These include VLPs as potential human vaccines, e.g., against HIV infection. A cell mediated immune response is essential for protection against HIV, but the use of a live vaccine may facilitate integration of viral RNA into the recipients genome (82). Currently, VLPs are used as vaccines against several animal papillomaviruses (19). VLPs can also be used to study viral morphogenesis. For instance, tick-borne encephalitis (TBE) virus VLPs are proposed as a model for investigating envelope glycoprotein functions (78). As well, VLPs can be used to study immunological aspects of infection and autoimmune diseases. Several examples of the many types of virus-like particles produced from recombinant cDNA are presented here.

Morphologically normal virus-like particles bud from QT6 (quail tumor) cells, coexpressing Rous sarcoma virus *gag/pol* genes from one plasmid and *env* gene from another plasmid (17). Virus-like particles also bud from African green monkey kidney cells CV-1, when cells are transfected with simian immunodeficiency virus (SIV) mutant *gag* gene coding for matrix protein (23). However, these particles appear morphologically different from typical lentivirus particles. Expression of corona viral envelope proteins leads to assembly and budding of viral envelopes from cultured cells (92). In addition,

rabies VLPs can be produced from recombinant plasmids encoding rabies virus cDNA expressed from a vaccinia virus expression system (60).

1.4. RLPs as tools to study rubella virus assembly and secretion

We were primarily interested in capsid and envelope glycoprotein interactions during budding, so we chose to use RLPs to investigate this development. Our initial goal was to determine if RLP secretion and RV virion release were similar, then to determine the domains within E2 and E1 essential for RLP assembly. If RLP secretion from stably transfected cells paralleled RV virion release from infected cells, we felt confident that RLPs would provide a suitable model system for our purpose. RLPs hold several advantages over infectious virions. First, stably transfected cells constitutively and reproducibly express RLPs whereas continuous virus cultures produce increasing numbers of defective interfering (DI) particles over time (21). Second, RV titers are low in cells with an active interferon system, and RV replicates efficiently only in BHK-21 cells or Vero cells (20). Third, Hobman et al. have shown that three times as much RV antigen per milliliter is released from stably transfected CHO24S cells than from Vero cells infected with wild type M33 virus (37). As well, working with RLPs would obviate the need to work with live virus whose cytopathic effects may mask or alter normal cellular function (50). In addition, RV structural proteins, capsid, E2 and E1 migrate to the Golgi when coordinately expressed in transfected cells, the same as wild type structural proteins in RV infected cells.

Presuming that RLP and RV virion assembly and secretion pathways are the same, we could use mutational analysis to determine the structural protein domains essential for RLP assembly. The putative domains could then be

introduced into cDNA constructs from which infectious mRNA can be transcribed (96), and recombinant virus infection studied.

1.5. Virus assembly and polarized secretion in mammalian cells

The well characterized MDCK II cells were chosen to conduct experiments. Unfortunately, they did not support RV infection very well, so two other more susceptible cell lines were chosen. In all, three epithelial cell lines with different origins were used: MDCK II, Vero C1008 and Caco-2. MDCK II cells were identified in 1981 from high passage MDCK cells, initially isolated from the kidney of a normal cocker spaniel. MDCK II resemble the transporting epithelium of proximal tubules in terms of electrical resistance and enzyme markers alkaline phosphatase and gamma-glutamyl transferase (72). Vero C1008 cells were established from Vero 76 cells, and both were verified by cytogenetic analysis as belonging to African green monkey, and have a hypodiploid number of chromosomes. Vero 76 derived the name from pool #76 of Vero cells passage number 124, developed from kidney tissue (18). Caco-2 cells are derived from colon adenocarcinoma. Although they express some enzymatic markers of normal small intestinal villus cells, they more closely resemble enterocytes from a normal 15-week old human fetal colon. In addition, they share similarities with colonic crypt cells in terms of electrical parameters, ion conductance and permeability (62).

All cells have been used previously to demonstrate virus infection and polarized secretion of progeny virions. Virions usually leave different cells by the same secretory pathway, e.g., respiratory syncytial (RS) virus exits both Vero C1008 and MDCK from the apical surface (74), and measles virus exits Vero C1008 and Caco-2 cells from the apical surface (6). As well, MDCK cells secrete influenza virus exclusively from the apical surface while vesicular stomatitis

virus (VSV) is sorted exclusively to the basolateral surface (75). However, the same virus may exhibit different secretion pathways in different cells, e.g., Sindbis virus and Semliki Forest virus (SFV) bud from the apical surface of Fischer rat thyroid (FRT) cells and from the basolateral surface of Caco-2 cells (102). Similarly, poliovirus while not enveloped, is released from the apical surface of Caco-2 cells and from both surfaces of Vero C1008 cells (90).

The type of disease caused by a virus can often be correlated with its mode of infection and subsequent release from infected cells. Sendai virus is released from the apical surface of cultured epithelial cells, and causes a localized respiratory infection *in vivo* (85). However, measles virus (6) and influenza virus (75) are both released from the apical surface of cultured cells but cause systemic infections *in vivo* due to necrosis of the infected epithelium (81). Establishing a systemic viremia may not depend upon epithelial necrosis. Coronavirus mouse hepatitis virus (MHV) establishes an infection in the upper respiratory mucosa, then becomes disseminated throughout the body. Cell culture studies reveal that the cells are preferentially infected from the apical surface, but virion release occurs primarily from the basal surface (77).

1.6. Rationale

The primary goal of this study was to determine the molecular basis of rubella virus particle assembly. Capsid and envelope glycoprotein interactions drive the assembly process, but the molecular interaction(s) between the proteins remains to be determined. I used recombinant DNA techniques to replace the transmembrane and cytoplasmic domains of E1 to determine any involvement of these domains with RLP assembly. Previous recombinant DNA experiments established the use of RV structural proteins as efficient and effective tools to study intracellular transport pathways. I hoped to advance this knowledge and

to learn the molecular basis of structural protein assembly. As a preliminary study, I proposed to compare the secretion characteristics of RV virions and RLPs from three polarized epithelial cell lines, MDCK II, Vero C1008 and Caco-2. If secretion pathways paralleled one another, then I could confidently presume that RLPs would serve as an adequate tool to study virion assembly. Results from these preliminary investigations may endorse the use of RLPs as a suitable *in vitro* system to study RV assembly and secretion characteristics. Also, results from such experiments could indicate how RV crosses the epithelial boundary and causes a systemic infection. This work could serve as a starting point for future studies with cultured placental cells, with a view to understanding *in vivo* fetal RV infection.

2 MATERIALS AND METHODS

2.1. Reagents

Tissue culture reagents including media Opti-MEM, MEM-alpha (minimum eagle's medium without nucleosides) and DMEM (Dulbecco's modified eagle's medium), Transferrin, Lipofectin, Sodium Pyruvate 100 mM, L-Glutamine 200 mM, 100X Antibiotics/antimycotics (10000 units/ml penicillin G sodium, 10000 µg/ml streptomycin sulfate and 25 µg/ml amphotericin B as Fungizone in 0.85% saline), 100X Antibiotics (10000 units/ml penicillin G sodium, 10000 µg/ml streptomycin sulfate), HEPES (N-2-Hydroxyethylpiperazine-N'-2-Ethane Sulfonic Acid), G418, Fetal Bovine Serum (FBS) and hypoxanthine-thymidine (HT) supplement were purchased from GIBCO BRL (Burlington, ON).

Dialyzed FBS, Fibronectin and Western blotting paper were purchased from Sigma (St. Louis, MD).

Tissue culture plastic ware including $\approx 4.7 \text{ cm}^2$, high pore density, $0.4 \text{ }\mu\text{m}$ pore diameter, cell culture inserts, were purchased from Falcon, Becton Dickinson, Canada and Corning Costar, Fisher Scientific (Edmonton, AB).

Vero cells were a kind gift from Dr. Stephen Rice, Department of Biochemistry, University of Alberta, and Vero C1008 cells were purchased from ATCC (Rockville, MD) or were a kind gift from Dianna Blau Department of Microbiology and Immunology, Emory University School of Medicine (Atlanta, GA). MDCK II cells and Caco-2 cells were a kind gift from Dr. Bruce Stevenson, Department of Cell Biology and Anatomy, University of Alberta. CHO DG44 cells were obtained from Dr. Erkki Ruslati, La Jolla Cancer Foundation (La Jolla, CA).

(^{35}S methionine/cysteine) PRO-MIX (7.15 mCi/500 µl [5.0 mCi (265 MBq) methionine/2.15 mCi (185 MBq) cysteine]) and ^{14}C protein molecular weight markers were purchased from Amersham Canada Ltd. (Toronto, ON).

^{14}C Inulin: Inulin-Carboxyl, [Carboxyl- ^{14}C]-, 0.060 GBq/g, 1.62 mCi/g was purchased from NEN, Du Pont, Canada. (Inulin was reconstituted in DMEM to 20 $\mu\text{Ci/ml}$)

(^{32}P orthophosphate) Phosphorus-32 H_3PO_4 in H_2O , HCl free (concentration = 500 mCi/ml; specific activity = carrier free), was purchased from ICN Biomedicals, Canada (Montreal, HQ).

PVDF (polyvinylidene fluoride) 0.20 μm pore size was purchased from Bio-Rad Laboratories (Hercules, CA), or Immobilon-P, 0.45 μm pore size, from Millipore Corporation (Bedford, MD).

EZ-Link Sulfo-NHS-Biotin was purchased from Pierce (Rockford, IL).

2.2. Antibodies

H4C52 mouse anti-E1, H46C64 mouse anti-E2 and H15C22 mouse anti-capsid antibodies were provided by Dr. John Safford, Abbott Laboratories (North Chicago, IL). Human anti-RV was provided by Dr. Aubrey Tingle, University of British Columbia (Vancouver, BC). 1B9 mouse anti-E1 was provided by Dr. Chris Mauracher, F. Hoffmann La-Roche (Basel, CH). B2 anti-E1 was a kind gift from B. Pustowoit (Leipzig). C1 mouse anti-capsid was provided by Dr. Jerry Wolinski, University of Texas (Houston, TX). Rabbit anti-Manosidase II and rabbit anti- βCOP were provided by Dr. Marilyn G. Farquhar, University of California, San Diego (La Jolla, CA). Texas red conjugated goat anti-mouse IgG, FITC (fluorescein isothiocyanate) conjugated donkey anti-rabbit IgG and rhodamine (tetramethylrhodamine isothiocyanate; TRITC) conjugated goat anti-mouse IgG were purchased from Jackson ImmunoResearch Laboratories (West Grove, PA). Goat anti-mouse HRP conjugated antibodies were purchased from Bio-Rad Laboratories, Hercules, CA.

2.3. Recombinant plasmids

The pCMV5 vector contains the transcription promoter from the human cytomegalovirus (CMV, Towne strain) major immediate early gene, a synthetic polylinker, the human growth hormone (hGH) transcription termination and poly-adenylation signals and an ampicillin-resistance gene. These features allow for transcription in eukaryotic cells, as well as selection of plasmid carrying bacteria (2). Recombinant 24S cDNA constructs (see figure 3) were subcloned between the *Eco* RI and *Hind* III or *Bam* HI sites of the polylinker, downstream from the CMV promoter.

The plasmids pCMV5-24S, pCMV5-24SE1ct- and pCMV5-24SE1-Gtmct were constructed as described (37). Briefly, pCMV5-24S codes for RV structural protein NH₂-capsid-E2-E1-COOH. pCMV5-24SE1ct- codes for unaltered capsid and E2 but only the E1 ectodomain and transmembrane (tm) region and one amino acid of the cytoplasmic tail (ct), which is normally 13 amino acids long. pCMV5-24SE1-Gtmct codes for unaltered capsid and E2 but only the E1 ectodomain; VSVGtmct replaces E1tmct.

Three new constructs were made (see figure 3): pCMV5-24SE1-CD8tm codes for unaltered capsid and E2 but only the E1 ectodomain and cytoplasmic tail; the CD8tm replaces the E1tm. pCMV5-24SE1-CD8tmct codes for unaltered capsid and E2 but only the E1 ectodomain; CD8tmct replaces E1tmct. pCMV5-24S-E2Gtm contains the VSVGtm in place of the E2 tm domain; capsid, E1 and the remainder of E2 are unaltered.

2.4. Construction of new recombinant plasmids

2.4.1. Construction of pCMV5-24SE1-CD8tm (figure 17)

To construct this plasmid, pCMV5-CD8-E1ct was digested with *Eco* RV and *Bam* HI, and the ≈160 bp *Eco* RV/*Bam* HI, CD8tmE1ct fragment purified by

agarose gel electrophoresis and elution. pCMV5-24S-Gtmct was digested with *Bam* HI and *Eco* RV and the 415 bp *Bam* HI / *Eco* RV fragment purified by agarose gel electrophoresis and elution. pCMV5-24S-Gtmct was digested with *Bam* HI only, and the large fragment, i.e., the vector-NH₂-capsid-E2-and the N-terminal part of the E1ecto domain, was purified and treated with Shrimp Alkaline Phosphatase (SAP; USB, Cleveland OH). Ligation of the three fragments resulted in a construct which contained pCMV5-24S with the transmembrane region of CD8 in place of the transmembrane region of E1 (CD8tm underlined).

NH₂-...WADYTWAPLAGTCGVLLLSLVITLYCNHKCLYYLRGAIAPR

2.4.2. Construction of pCMV5-24SE1-CD8^{tmct} (figure 18)

To construct this plasmid, pCMV5 was digested with *Eco* RI and *Bam* HI; this opened up the 4.7 kb vector at the polylinker. pCMV5-CD8 was digested with *Eco* RV and *Bam* HI, and the 900 bp (approx.) *Eco* RV/*Bam* HI, CD8^{tmct} fragment purified by agarose gel electrophoresis and elution. pCMV5-24S-Gtmct was digested with *Eco* RI and *Eco* RV, and a 3.0 kb (approx.) fragment purified by agarose gel electrophoresis and elution, i.e., NH₂-capsid-E2-E1ecto domain. The three part ligation of these fragments resulted in a construct which contained pCMV5-24S with the transmembrane and cytoplasmic regions of CD8 in place of the transmembrane and cytoplasmic regions of E1 (CD8^{tmct} underlined).

NH₂-...WADYTWAPLAGTCGVLLLSLVITLYCNHRNRRRVCKCPRPVVKSGDKPSLSARYV

2.4.3. Construction of pCMV5-24SE2-Gtm (figure 19)

pCMV5-E2-Gtm-EI was digested with *Eco* RI and *Bst* EII, and the 7 kb large fragment containing the pCMV5 vector and all except the first 26 N-terminal amino acids of NH₂-E2-E1-COOH was purified by agarose gel electrophoresis and elution. pCMV5-24S was digested with *Eco* RI and *Bst* EII,

and the 1 kb fragment containing NH₂-capsid and the first 26 amino acids of E2 was purified by agarose gel electrophoresis and elution. These two fragments were ligated together to produce pCMV5-24S-E2Gtm which contained NH₂-capsid-E2Gtm-E1-COOH, i.e., E2 tm was replaced by VSVGtm (VSVGtm underlined).

NH₂-...SLDSSIASFFUIGLIIGLEFLVLRRA...-COOH

2.5. Cell culture, transfection and immunofluorescent screening

2.5.1. Cell Culture

All cells were normally cultured at 37° C, 5% CO₂ with the following growth media. **MDCK II** and **Vero** cells were grown in DMEM containing 5% FBS, 1X antibiotic/antimycotic solution, 20 mM HEPES and 2 mM L-Glutamine. **Vero C1008** cells were grown in DMEM containing 10% FBS, 1X antibiotic/antimycotic solution, 20 mM HEPES and 2 mM L-Glutamine. **Caco-2** cells were grown in DMEM containing 20% FBS, 1X antibiotic/antimycotic solution, 20 mM HEPES, 1X pyruvate, 2 mM L-Glutamine and 10 µg/ml Transferrin. **CHO DG44** cells were grown in MEM-alpha containing 10% FBS, 1X antibiotic solution, 20 mM HEPES, 0.5X HT supplement and 2 mM L-Glutamine. Stably transfected **CHO** cells were grown in media containing MEM-alpha, 10% dialyzed FBS, 1X antibiotic solution, 20 mM HEPES and 2 mM L-Glutamine.

2.5.2. Stable transfection

MDCK-II, **Vero C1008** and **Caco-2** cell lines were stably transfected with pRc/CMV-24S, a plasmid containing a G418 resistance gene and 24S cDNA, which codes for Rubella virus structural proteins NH₂-capsid-E2-E1-COOH, following Gibco BRL's, "Guide to Eukaryotic Transfections with Cationic Lipid Reagents" protocol. 5 X 10⁵ cells were plated onto 60 mm tissue culture dishes

and grown overnight. For each transfection, 20 μg (approx. 4.0 pmol) of plasmid DNA was mixed with 300 μl of Opti-MEM, and 30 μl of Lipofectin was mixed with 300 μl of Opti-MEM, for 30 min. These two mixtures were combined for 15 min before being mixed with 2.4 ml Opti-MEM, and added to cells; cells were previously washed with PBS pH 7.4 and incubated with Opti-MEM for 15 min prior to the application of the Opti-MEM, Lipofectin/DNA mix. The cells were cultured for 6 to 16 h, then the media was replaced with normal growth media. Cells were cultured for 48 h, then split into 1:2, 1:5 and 1:10 dilutions and cultured in the presence of G418, approximately 480 $\mu\text{g}/\text{ml}$ (active) MDCK-II and 240 $\mu\text{g}/\text{ml}$ (active) Caco-2 and Vero-C1008. Fourteen to 21 d later isolated colonies were picked, and expanded in selective media containing G418; 240 $\mu\text{g}/\text{ml}$ (active) MDCK-II and 120 $\mu\text{g}/\text{ml}$ (active) Caco-2 and Vero-C1008. Ultimately, normal growth media was used to propagate stable clones.

Transfection of **CHODG44** cells (dihydrofolate reductase [DHFR] deficient) were stably transfected with pCMV5-24S (or 24S recombinants, see below) and pFR400. pCMV5-24S contains an ampicillin resistance gene and 24S cDNA, which codes for RV structural proteins NH₂-capsid-E2-E1-COOH. pFR400 contains the DHFR gene, and permits cells expressing the gene to grow in tissue culture media containing dialyzed FBS. For each transfection, 20 μg (approx. 4.0 pmol) of pCMV5-24S (or 24S recombinant) and 1.1 μg (0.4 pmol) pFR400 were mixed with 300 μl of Opti-MEM, and 30 μl of Lipofectin was mixed with 300 μl of Opti-MEM, and the procedure followed as described above. Cells were cultured for 48 h, split as above and cultured in selective media containing MEM-alpha with 20 mM HEPES, 2 mM L-Glutamine, 1X antibiotic solution and 10% dialyzed FBS. Fourteen to 21 d later isolated colonies were picked, and expanded in selective media.

2.5.3. Immunofluorescent Screening of clones

MDCK II, Vero C1008 and Caco-2, Colonies were screened by indirect immunofluorescence for the presence of rubella virus specific proteins capsid, E2 and E1, using mouse monoclonal antibodies B2 anti-E1 or H4C52 anti-E1, H46C64 anti-E2 and H15C22 anti-capsid, and co-stained for Golgi specific marker, Manosidase II (MDCK) or Golgi and cytoplasmic marker, β -COP (Vero and Caco-2), essentially as described by Hobman et al., 1992 (40). Cells grown on glass coverslips (20% to 90% confluent) were rinsed 2X with PBS containing 1.0 mM Mg and 0.5 mM Ca (PBSCM), 3 to 5 min each rinse, followed by fixation and permeabilization in cold methanol at -20° C for 6 min, then re-hydrated with two changes of PBSCM, 3 to 5 min each change. Alternatively, cells were fixed at 4° C in 2.5% paraformaldehyde (in PBS pH 7.4) for 30 min, then permeabilized with 0.2% Triton X-100 (in PBS pH 7.4) for 4 min at room temperature. The cells were then incubated with PBSCM/1% BSA for 15 min to block non-specific binding of primary antibodies. Coverslips were placed cell side down upon appropriate dilutions of 1° and conjugated 2° antibodies in PBSCM/1% BSA, for 30 to 60 min at room temperature; coverslips were washed three times over 5 to 15 min with PBSCM/0.1% BSA after each antibody. Finally, coverslips were mounted on glass slides using mounting media containing 80% glycerol in PBS and 1 mg/ml paraphenylenediamine.

CHO24S (and CHO24S recombinant) cells were screened by indirect immunofluorescence for the presence of RV specific proteins capsid, E2 and E1, and co-stained for Golgi specific marker, Manosidase II as described above, with the addition that all CHO cells were grown on fibronectin (10 μ g/ml) coated glass coverslips.

2.6. Metabolic labeling and immunoprecipitation

2.6.1. Metabolic labeling

Cells were seeded at 1.5×10^6 (MDCK II-24S) or 1.0×10^6 (Vero C1008-24S and Caco-2-24S) onto $\approx 4.7 \text{ cm}^2$, high pore density cell culture inserts (pore diameter of $0.4 \mu\text{m}$), and grown for 3 to 4 d (MDCK II-24S) or 4 to 8 d (Vero C1008-24S and Caco-2-24S). Cells were washed with PBSCM before cysteine/methionine (cys/met) free media (MEM/5% dialyzed FBS/2 mM L-Glutamine/1X penicillin/1X streptomycin) was added. Cells were then incubated at 37°C , 5% CO_2 for 30 min to deplete any stores of cys/met. The media was removed entirely from the basal surface but a small amount was left on the apical surface. $100 \mu\text{Ci}$ of PRO-MIX was mixed with $100 \mu\text{l}$ cys/met free media (per insert), then pipetted into a 100 mm tissue culture dish upon which the cell culture insert was placed for 15 to 30 min. The labeling media was removed from the cells by washing both surfaces of the insert twice with normal growth media containing 25X cys/met, and cultured for the desired times in this media.

For CHO24S (and CHO24S recombinant) cells, ^{35}S metabolic labeling was accomplished essentially as described by Hobman et al., 1992 (40). 2.0×10^5 cells were seeded onto 35 mm dishes, and grown overnight. Cells were washed with PBS pH 7.4, then incubated in cys/met-free media. Media was replaced with cys/met-free media containing $100 \mu\text{Ci}$ of PRO-MIX and culture continued for 30 min. Labeling media was removed and the cells washed twice with normal growth media containing 25X cys/met, and culture continued for the desired times with 25X cys/met media.

For ^{32}P labeling, cells were seeded at 2.0×10^5 onto 35 mm dishes, and incubated as for ^{35}S labeling. Cells were washed 2X with PBS pH 7.4 then incubated with phosphate-free media for 30 to 60 min followed by culture with

1.0 ml phosphate free media containing 500 μCi of ^{32}P orthophosphate for 16 to 18 h (54).

2.6.2. Immunoprecipitation

For MDCK II, Vero C1008 and Caco-2, the cells were rinsed three times with ice cold PBS, then lysed for 5 min with 1.0 ml cold RIPA buffer (50 mM Tris-Cl pH 7.5, 150 mM NaCl, 1% NP 40, 0.5 % sodium deoxycholate, 0.1 % SDS). The cells were scraped from the cell culture insert into a 1.5 ml ependorf tube using a rubber policeman, and centrifuged at 4° C in a fixed angle microfuge at 10,000 g for 5 min. Then the supernatant was incubated with 10 μl human anti-RV serum for 1 h or overnight. Media from the apical and basal chambers was centrifuged at 4° C in a fixed angle microfuge for 5 min at 10,000 g to remove any cells, then 10% Triton X-100 in PBS pH 7.4 was added to the supernatant to a final concentration of 1% before adding 10 μl human anti-RV serum for 1 h or overnight at 4° C. Immune complexes were adsorbed using 20 μl of Protein A sepharose beads, added to each tube and mixed for 1 h at 4° C on a rotating or rocking platform. Immune complexes were washed (5 min each time) 2X with RIPA buffer, 1X with high salt solution (50 mM Tris-Cl pH 7.4, 0.5 mM NaCl, 1% Triton X-100) and 1X with 10 mM Tris-Cl pH 7.4 plus 0.1% NP 40. Immune complexes from the media were washed 3X with 1% Triton X-100 in PBS pH 7.4, then 1X with H₂O. Proteins were eluted from beads by boiling for 5 min with 30 μl 2X SDS gel-loading buffer (100 mM Tris-Cl pH 6.8, 4% β -mercaptoethanol, 4% SDS, 0.2 % bromphenol blue and 20% glycerol), after which samples were centrifuged briefly at 10,000 g to pellet the beads.

^{35}S labeled CHO24S (and CHO24S recombinant) cells were immunoprecipitated as above except 15 μl human anti-RV serum was used. For immunoprecipitation of ^{32}P -labeled proteins, phosphatase inhibitors (1 mM

sodium orthovanadate, 50 mM sodium fluoride, 5 mM tetra-sodium pyrophosphate and 0.4 mM Pefabloc) were added to the PBS before washing, and to the RIPA buffer before cell lysis. 100 μ l of 10% Triton X-100 in PBS pH 7.4, containing 10 mM sodium orthovanadate, 500 mM sodium fluoride, 50 mM tetra-sodium pyrophosphate and 4.0 mM Pefabloc, were added to 900 μ l clarified media. Supernatants and media were incubated with 15 μ l human anti-RV serum and processed as above.

2.7. SDS PAGE and fluorography

Samples were electrophoresed through 10% SDS polyacrylamide gels. The gels were then fixed in 25% isopropanol/10% acetic acid for 30 min, then processed for fluorography in 50 ml of a 100 mM Sodium Salicylate solution containing 0.01% β -mercaptoethanol for a further 30 min. Gels were dried and exposed to Kodak XAR film (Eastman Kodak Co., Rochester NY) and processed through a Kodak M35AX-OMAT processor.

2.8. Western blotting

Western Blotting followed the ECL western blotting protocol described by Amersham Life Science (Buckinghamshire, UK). **Vero C1008-24S** and **Caco-2-24S** cells were cultured on ≈ 4.7 cm², high pore density cell culture inserts (pore diameter of 0.4 μ m), and **CHO24S** and CHO24S recombinants were grown in 35 mm dishes. Cells were washed 2X with PBSCM to remove RLP-containing media, then fresh media was added for the desired times. RV antigens were immunoprecipitated and electrophoresed as described above. The proteins were transferred from the gel to a polyvinylidene fluoride (PVDF) membrane using a semi-dry electrophoresis technique (Tyler Research Instruments, Edmonton).

PVDF membranes were equilibrated in methanol, H₂O and transfer buffer (25 mM Tris, 150 mM glycine pH 8.3, 20% [v/v] methanol) respectively. Similarly, SDS polyacrylamide gels and blotting papers were equilibrated in transfer buffer. Proteins were transferred at 250 mA for 30 min. Non-specific antibody binding to membranes was blocked using TBS/TWEEN 20 (0.05%)/5% skim milk, after which mouse anti-capsid antibody was added to the blocking solution at 1:1000 dilution, and incubation continued for 1 h. Membranes were washed with TBS/TWEEN 20 (0.05%), then incubated for 1 h with horseradish peroxidase conjugated, goat anti-mouse antibody at 1:3000 dilution in blocking solution. Enhanced Chemiluminescence was used to detect any signal. Reagents for ECL were as follows: Stock solutions; 250 mM luminol (3-amino-phthalhydrazide) in DMSO, 90 mM paracoumaric acid in DMSO, 1.0 M Tris-HCl pH 8.5, 30% (8.82 M) H₂O₂. Working solutions: solution #1. 2.5 mM luminol, 400 μ M paracoumaric acid in 100 mM Tris-HCl pH 8.5; solution #2. 5.4 mM H₂O₂ in 100 mM Tris-HCl pH 8.5. Equal volumes of solution #1 and #2 were combined just before use. Membranes were overlaid onto the solution for 1 min, followed by exposure to Fuji film (Fuji Photo film Co. TOKYO). Films were processed through a Kodak M35AX-OMAT processor.

2.9. Electron microscopy

Cells grown on ≈ 4.7 cm², high pore density, 0.4 μ m pore diameter, cell culture inserts (PET; Falcon [MDCK] or polycarbonate; Costar [Vero and Caco-2]), were fixed in 2.5% glutaraldehyde with or without 2% paraformaldehyde in 0.1M cacodylate buffer (pH 7.3) for 1 h. After washing with three changes of 0.1 M cacodylate, the cells were either processed immediately or left overnight at 4° C to be processed the next day. Cells were post-fixed in 1% osmium tetroxide in 0.1 M phosphate buffer (pH 7.3) for 30 min and dehydrated in 60%, 80%, 95%,

98% and 100% ethanol. Infiltration were performed in 1:1 mixture of ethanol and EPON resin for 1 h and in fresh mixture of resin for 4 h. The inserts were cut into thin strips and polymerized in fresh resin at 60° C for 48 h. Sections about 60-80 nm thick perpendicular to the filters were collected on grids, stained with uranyl acetate and lead citrate and examined at 80 KV using a Philips 410 electron microscope.

2.10. Inulin diffusion and transepithelial resistance (TER)

Monolayer permeability was measured using inulin diffusion or TER.

2.10.1. Inulin diffusion

Inulin is a 11-15 Å diameter molecule with a M_r 5000 Daltons (11, 52), and was used essentially as described by Caplan et al. to measure monolayer integrity (11). Apical and basal chambers were equilibrated with 1.0 mM unlabeled inulin, after which the apical chamber was spiked with 2 µl (40 nCi/89K dpm) ^{14}C labeled inulin. 100 µl aliquots were removed from both the apical and basal chambers (with replacement where necessary) and radioactivity measured by Liquid Scintillation Counting (LSC). The flux formula devised by Madara and Hecht (53) was used to calculate the inulin diffusion rate, and the percentage of inulin diffused was calculated by measuring total counts in each chamber at the end of the desired time periods.

$$J = \frac{(X)(DPM)_2 - (X-Y)(DPM)_1}{\frac{DPM_H/ml}{\mu mol/ml} \cdot T \cdot A}$$

Where J is flux in $\mu mol \cdot hr^{-1} \cdot cm^{-2}$

X is volume of cold reservoir (expressed as "1.0")

Y is volume of sample removed (% of X removed, expressed as a decimal)

DPM₁ volume at beginning of flux period

DPM₂ volume at end of flux period

DPM_H is hot reservoir counts

μmol is concentration of unlabeled solute (1.0 mM)

T is time in hours

A is area in cm^2

NOTE, CPM = 0.8 X DPM

2.10.2. Transepithelial resistance (TER)

TER was measured using a Millicell-ERS resistance apparatus (Millipore Corp., Bedford, MA) and Endohm measuring chamber (World Precision Instruments, Inc. (Sarasota, FL), essentially as described in the operators' manuals. Briefly, epithelial monolayers on cell culture inserts were rinsed with PBSCM pH 7.4, placed into a previously equilibrated Endohm measuring chamber containing PBSCM pH 7.4, then a small current passed through the monolayer to determine the resistance to current flow. Values were expressed as ohms. cm^2 .

2.11. Biotinylation of cell surface proteins

Biotinylation followed the protocol described by Rodriguez-Boulan et al. (76). Vero, Vero-C1008 and Vero-C1008-24S cells (1×10^6) were seeded on Costar $\approx 4.7 \text{ cm}^2$, high pore density ($0.4 \text{ }\mu\text{m}$ pore diameter) cell culture inserts, and grown for 6 d. Cells were washed four times with ice cold PBSCM pH 7.4, then either the apical or basal surface was exposed to 1 mg/ml Sulfo-NHS-Biotin in ice cold PBSCM pH 7.4 for 30 min at 4°C ; inserts were rocked gently. The non-biotinylated surface was exposed to ice cold PBSCM pH 7.4 only. After 30 min, the biotinylating reagent was removed and both surfaces were exposed to DMEM without FBS for 5 min to inactivate any remaining Sulfo-NHS-biotin. Insert were then washed 3X with ice cold PBSCM pH 7.4. Cells were lysed in 1% SDS, 10 mM Tris-Cl pH 7.5 and 2 mM EDTA, then the DNA was sheared using a 27 gauge needle.

Samples were boiled in 2X SDS gel loading buffer and 5 to 20 μl were electrophoresed on a 10% SDS polyacrylamide gel. Proteins were blotted onto a PVDF membrane, and the membrane was blocked for 15 min with TBS pH 7.4/TWEEN 20 (0.05%)/5% skim milk with gentle rocking at room temperature. Horseradish peroxidase conjugated to streptavidin (Bio-Rad) was added to the blocking solution to a final concentration of $0.5 \text{ }\mu\text{g/ml}$, and allowed to bind to the biotinylated proteins for 40 min. Blots were then washed for 15 min in TBS pH 7.4/TWEEN 20 (0.05%), and ECL was used to detect biotin/streptavidin complexes.

2.12.1 Virus plaque assay (agarose overlay)

Virus plaque assay was performed using Vero cells essentially as described (5). For titration of virus stock (M33), Vero cells were plated at a

density of 1.0×10^6 / 9.6 cm^2 well of a six well dish, and grown until confluent (next day). Viral stocks were diluted in serial 10 fold dilutions, ranging from 10^{-1} to 10^{-6} . Cells were infected with 200 μl of inoculum for 1 h at 37°C , 5% CO_2 , with gentle rocking every 10 min. Inoculum was removed, then 2.0 ml of prewarmed media containing 4% agarose was added to each well, allowed to solidify, and culture continued. After 3 d, 2.0 ml of media was added to the top of the agarose overlay of each well and incubation continued. After 6 d, media was removed and 1.0 ml media (no FBS) containing approximately 0.02% neutral red was added and incubation continued for 4 h to overnight. Plaques appeared clear in a red background.

2.12.2. Virus plaque assay (immunofluorescent)

Virus plaque assay was performed essentially as described by Hobbins and Kendall (33). For titration of virus stock (M33), Vero cells were plated, infected and cultured as above, with the exception that after infection, 2.0 ml growth media (without agarose) was added. After 3 d, medium was removed from each well and cells were processed for immunofluorescence as described above.

For infection of cells grown on cell culture inserts, cells were seeded at 1.0 to 1.5×10^6 and grown for 2 d (MDCK II), 5 d (Caco-2) or 7 to 9 d (Vero and Vero C1008), on $\approx 4.7 \text{ cm}^2$, high pore density cell culture inserts, $0.4 \mu\text{m}$ pore diameter. Cells were infected on the apical surface with 200 μl of inoculum (M33 RV, approx. $\text{MOI} = 0.1$) and virus free medium was added to basal surface for, 1 h at 37°C , 5% CO_2 , being gently rocked every 10 min. Inoculum was removed and both surfaces of the monolayer were washed 2X with PBSCM, then growth medium was added and cell culture continued. After 48 h, the media from the apical and basal chambers were collected, centrifuged for 2 to 5 min at 10,000 g to

remove cellular material, and titered out in serial 10 fold dilutions. 100 μ l of each dilution was placed onto Vero cells, grown in a 12 well multi chamber dishes, for 1 h (as above). After 1 h, inoculum was replaced with 2.0 ml growth medium then culture continued for 3 d. Cells were then processed for immunofluorescence (as above).

While virion release was non-polar, with apical counts greater than basal counts, a broad range of apical to basal ratios was noted. In an attempt to quantitate virion release, only wells with four or more plaques were used to assay viral titers, and highest and lowest apical to basal ratios were discarded prior to preparing histograms.

2.13. Confocal microscopy

The basic principal of confocal microscopy is that one and the same point in the object is optimally illuminated by a point light source as well as imaged on a point detector (8). A Leica confocal laser scanning microscopy (clsm) system was used in our studies. Leitz Aristoplan fluorescence microscope was used for direct observation and focusing of cell monolayer in the epi fluorescence mode. The system is fitted with Argon/Krypton ion gas laser which excites with major emission lines of 488, 568 and 647 nm. The following physical parameters were used: The objective was the PLANAPO 100/1.32 oil immersion lens. The fluorescein (FITC) and rhodamine (Rh) in single labeled specimen were scanned using the following filter settings excitation short pass SP 510 and band pass BP 568, beam splitter TK 510 and TK 580 and emission long pass OG 515 and OG 590, respectively. Simultaneous scanning of the specimen labeled with two fluorochromes FITC and Rh was carried out using the excitation short pass KP 590 filter, the dual dichroic mirror and the barrier filters LP 590 in detector 1 and band pass BP 530 in detector 2. Thus, the excitation of the two fluorochromes was

achieved using two laser lines in the same time, and the separation of the FITC and RH emission spectra was improved by the use of band pass filter to minimize the cross talk from the FITC region. The 512x512 pixel images of the horizontal sections 0.5 microns deep were acquired using the line accumulation high quality scanning algorithm. The image acquisition was optimized with the pinhole, photomultiplier gain and offset settings.

Acquisition of images, visualization and necessary processing of the images like background fluorescence removal, scale bar measurements and double labeled images processing was done using the Multi-user Multi-tasking Image Analysis software developed by Leica Lasertechnik GmbH (Heidelberg, Germany) which was run on the Motorola 68030 CPU workstation using OS9 operating system.

The z-series of optical sections recorded on the clsm system at given vertical distances were processed and 3D reconstructed using the comprehensive volume rendering software VoxelView 2.1.2 from Vital Images and the Silicon Graphics Iris Indigo XS24 (California) workstation. Precise alignment of sections, interpolation of additional sections to ensure real world measurements of the volume, mathematical algorithms based on thresholding and opacity were applied during the volume rendering.

3 RESULTS

3.1. MDCK II cells secrete RLPs in a polarized manner

Hobman et al. have shown that RLPs in stably transfected CHO cells bud into the Golgi (37), as do RV virions in infected cells (48, 93). Immunofluorescent staining of stably transfected CHO cells expressing 24S cDNA reveals that vesicular structures dispersed throughout the cytoplasm also stain for capsid, E2 and E1.

MDCK II cells were stably transfected with 24S cDNA or infected with rubella virus to determine if RLP and RV virion secretion characteristics were similar. Double indirect immunofluorescent staining was performed on transfected MDCK II cells to determine if capsid, E2 and E1 were localized to the Golgi. A number of clones expressing capsid, E2 and E1 were obtained, but only one was used for further study and subsequently renamed MDCK II-24S. RV structural proteins were seen to overlap with Man II, indicating that they were present in the Golgi. Capsid was also within vesicular structures throughout the cytoplasm (figure 4). The vesicles containing capsid did not contain Man II, and their identity is unknown.

Transmission electron microscopy (EM) revealed the presence of 50 to 60 nm diameter particles with an electron dense core surrounded by an envelope, similar to particles observed by Hobman et al. (37) in CHO24S cells (figure 5A). RLPs were seen budding into or within cytoplasmic vesicles (figure 5A iii), and were also detected at the apical surface (figure 5A i). Occasionally, RLPs were seen at the basolateral surfaces of cells grown on $\approx 4.7 \text{ cm}^2$, high pore density cell culture inserts, or glass coverslips. Basolaterally located RLPs were rare for MDCK II-24S cells, and a distinctly polarized secretion of radiolabeled RV structural proteins was observed (see below). Specimen processing for EM likely removes any accessible cell surface RLPs, and basolateral RLPs would be less

accessible during washing steps, consequently a less pronounced increase for the apical to basal ratio of RLPs may be observed by EM. RLPs were also noted in large intracellular bodies, possibly endosomes, and being endocytosed in what may be a clathrin coated vesicle (figure 5A ii). Studies have ascertained that the apical to basolateral surface area ratio for MDCK II varies depending upon type of support, but is believed to be 1:1 on polycarbonate (9), compared with 1:4 for nitrocellulose (94).

Metabolic labeling with ^{35}S cys/met revealed a distinctly polarized release of RV structural proteins into the apical chamber of MDCK II-24S cells (figure 5B). Cells were grown to confluence on $\approx 4.7 \text{ cm}^2$, cell culture inserts, (0.4 μm pore diameter). The presence of tight junctions was confirmed by measuring the transepithelial resistance (TER) across the monolayers and EM (not shown). Electrical resistance gives information primarily on individual junctions (53). The TER for MDCK II-24S cells grown on cell culture inserts, was measured 2 to 4 d after seeding, and was 50 to 70 ohms. cm^2 in four separate experiments. MDCK II cells have measurably low TER of 70 ohms. cm^2 using Ussing chambers (72), and a TER greater than 50 ohms. cm^2 using Millicell-ERS resistance apparatus is indicative of tight junction formation (Bruce Stevenson, personal communication). In duplicate assays, ^{35}S -labeled structural proteins were released primarily into the apical chamber in a time-dependent manner (figure 5B). Notably, only the mature form of E2 (figure 5B asterisk) was present in the media, indicating that proteins had passed through the Golgi during secretion. At 24 h post labeling, all of the labeled RV proteins were in the media, although $\approx 50\%$ less E1 label was present when compared with the 3 h sample. The decrease was probably due to endocytosis and subsequent degradation of RLPs. It is important to note that expression of all three structural protein is required for protein secretion (37). Implicitly, RV structural proteins must

assemble into RLPs, before they are secreted into the media. Consequently, any apical targeting signal must lie within the ectodomain of the E2E1 heterodimeric complex on the surface of RLPs (figure 3), as this is probably the only accessible structure within the Golgi lumen. Whether RLPs are targeted primarily to the apical surface, or sorted to all surfaces then transcytosed to the apical surface remains to be determined. Interestingly, the default secretory pathway for MDCK II cells is to both the apical and the basolateral surfaces (10, 12).

Productive infection of MDCK II cells with RV, as described in methods and materials, proved unsuccessful. In duplicate assays, less than 100 infectious virions were released into the apical chamber. The TER at the beginning and end of the infection period in both cases was 47 ohms.cm^2 . If nothing else, this experiment served as a negative control for the infection protocol, i.e., washing removed non-adsorbed virus, thereby preventing false positives.

Taken together, these results indicate that RLPs are secreted primarily into the apical media from MDCK II-24S cells grown on cell culture inserts. RLPs form by budding into the Golgi, as evidenced by EM and immunofluorescent staining of RV structural proteins' co-localization with the Golgi marker, Man II. Capsid is present in locations distinct from E2 and E1, possibly sites of degradation, i.e., proteasomes (after synthesis) or endosomes (after endocytosis of RLPs). E2 and E1 may be present in endosomes also, but epitopes may be denatured.

Unfortunately we were unable to compare virion and RLP secretion in this cell line. We therefore chose two other polarized cell lines, Vero C1008 and Caco-2, to further our studies. Vero C1008 were derived from Vero cells which support RV infection. RV infection of Caco-2 cells had not previously been demonstrated.

3.2. Vero C1008 cells secrete RLPs and RV virions in a non-polarized manner

Vero C1008 cells, stably transfected with 24S cDNA, were grown on glass coverslips, fixed and permeabilized with methanol and processed for indirect immunofluorescence as described above. Cells grown as a confluent monolayer for 2 to 3 d would not remain attached to the coverslip during processing for immunofluorescence (probably due to N/K-ATPase mediated water build up at the basolateral surface). Cells were therefore grown for shorter periods to facilitate staining, consequently, not all cells display cell-cell contact. Capsid could be seen in the Golgi, as determined by co-localization with β -COP (figure 6, panel A and B). Capsid staining was also apparent throughout the cells in a diffuse pattern, and staining at the peripheral surface of several cells was noted (figure 6, panel A arrowhead). E2 could be found in the Golgi, as well as in vesicular structures throughout the cells (figure 6, panel C and D). E2 was also noted within the ER, as evidenced by the perinuclear halo. E1 was also found to co-localize with the Golgi, and was also seen in vesicular structures throughout the cell (figure 6, panel E and F). This cell line was named Vero C1008-24S to reflect that it expressed capsid, E2 and E1. Further staining with endosomal, lysosomal or secretory vesicle markers will have to be done to determine the nature of the vesicular staining. Also, because the cells selected for photographing E2 and E1 do not display the same level of cell-cell contact as the cells stained for capsid, a time course for E2 and E1 staining will have to be done to optimize staining conditions and ascertain peripheral surface localization of these antigens. Peripheral staining with capsid may be due to intercellular accumulation of RLPs (noted during EM examination). However, the absence of corresponding staining patterns for E2 or E1 in cells studied to date, does not substantiate this idea.

Transmission electron microscopic studies of Vero C1008-24S grown on cell culture inserts revealed RLPs within cytoplasmic vesicles, presumably the Golgi (figure 7 arrowhead). RLPs were also noted at the apical (figure 7 asterisk) and basal (not shown) surfaces. In addition, RLPs were noted within multi-vesicular bodies (not shown), and were noted at the lateral surfaces (not shown), more so than at the lateral surfaces of MDCK II-24S or Caco-2-24S (see below) cells. No visible clumps of RLPs within the pores of the cell culture insert membrane were seen. The RLPs diameter appeared to be 1/6 to 1/8 of the pore diameter (not shown). Tight junctions, apical microvilli and smooth basolateral membranes were present, but cell-cell contact between Vero C1008-24S cells was not as distinct as between MDCK II-24S or Caco-2-24S cells (see below). Also, cell-cell contact of Vero C1008-24S cells appeared in some cases to only occur at the tight junction. This may be an EM processing artifact, or it may be a feature of the clone or parental cell type.

For metabolic labeling with ^{35}S cys/met, cells were grown to confluence on cell culture inserts, and the presence of tight junctions was demonstrated by measuring the resistance to inulin diffusion across the monolayers (not shown). Inulin diffusion measures the average junctional permeability (53), and a diffusion rate of less than 1%/h is indicative of tight junction formation in Vero C1008 cells (14, 89). Capsid, E2 and E1 were shown to be released into the media in a time dependent manner. E2 and E1 could be detected by fluorography as early as 3 h after labeling in the apical and basal media (figure 8A), and were found almost exclusively in the media at 24 h in monolayers grown for 3 d or 9 d. In a replicate of three assays, metabolic labeling with ^{35}S cys/met showed almost 75% of E2 and E1 could be detected in the apical and basal media by 6 h. Capsid could be also be detected by Western blot analysis in the apical and basal media (see below, and figure 8B). This clone did not express RV structural proteins in

100% of the cells. Also, it was thought that the cells were a mixed population and that transfection caused the cells to revert to a non-polar phenotype. Consequently, limiting dilution was used to obtain a clone that expressed all proteins in 100% of the cells, and this clone was subject to experiments to determine whether the cells were indeed polarized.

3.2.1. RLP secretion in polarized Vero C1008-24S cells

Biophysical confluency (tight junction formation between cells), was determined using EM morphology, inulin diffusion, dome formation, biotinylation assays and N/K-ATPase distribution as indicators of cell polarity. EM analysis, as described above, revealed tight junctions, apical microvilli and smooth membrane adjacent to the insert, consistent with the characteristics described by McRoberts et al. for structural polarity of transporting epithelium (59). From a replicate of three inulin diffusion assays of Vero C1008-24S cells, flux rates more closely represented impermeable monolayers of Vero C1008 cells than the permeable monolayers of Vero cells (figure 9). Also, ^{14}C inulin levels in the apical and basal chambers of Vero C1008-24S cells were shown to equilibrate within 1 h after the addition of 30 mM EGTA to the media, indicating calcium-dependent tight junctions were present (not shown). Similarly, Vero C1008-24S dome formation of cells grown on plastic tissue culture dishes was disrupted within minutes after the addition of EGTA (not shown). Domes form due to ion induced water build up under the basal surface, a consequence of N/K-ATPase distribution on the basolateral surface (13).

Biotinylation of cell surface moieties, as described in Materials and Methods, revealed distinctly different profiles for Vero, Vero C1008 and Vero C1008-24S cells grown on cell culture inserts. Biotinylation occurs as a result of

nucleophilic attack by a deprotonated primary amine present on the cell surface, i.e., lysine, on the ester bond of Sulfo-NHS-biotin (NHS/N-hydroxysulfosuccinimide). An end product, N-hydroxysulfosuccinimide is released, and biotin is attached via the primary amine to the cell surface moiety. Apical or basolateral biotinylation of Vero cells revealed similar patterns, unlike Vero C1008-24S, in which apical and basal biotinylation profiles were markedly different (figure 10A). Typically after 6 d, distinct apical and basolateral high molecular weight bands were apparent in Vero C1008-24S cells. In addition, numerous low molecular weight bands showed distinctly different apical and basolateral profiles. We can infer from this data that an impermeable cell surface boundary was present in the Vero C1008-24S cells, and that different proteins are biotinylated at the apical than at the basolateral surface of Vero C1008-24S cells. The impermeable boundary was not present in Vero cells, since all cell surface proteins were biotinylated, whether Sulfo-NHS-biotin was added to the apical or basolateral surface. Hence, for the purpose of biotinylation, Vero cells serve to display all cell surface markers, and Vero C1008-24S cells display apical and basolateral differences in these surface markers.

N/K-ATPase was shown by confocal microscopy to be distributed only on the basolateral surface of Vero C1008-24S cells, whereas the complete cell surface of Vero cells appeared to contain N/K-ATPase (figure 10B). Vero C1008-24S cells were grown for 7, 8 or 9 d on cell culture inserts, then processed for immunofluorescence as described in Materials and Methods. Serial sections were taken from above the apical cell surface through to the basal cell surface and into the insert, to ensure the cells were completely analyzed. Hammerton et al. showed that N/K-ATPase is selectively retained at the basolateral surface of MDCK cells for >36 h or 40 times longer than on the apical surface, 6 d after cell-cell contact (27). N/K-ATPase in Vero C1008-24S cells was limited to the

basolateral surfaces. In contrast, Vero cells presented a diffuse or non-polar distribution of the same protein (figure 10B). TER values for Vero cells are low (not shown), and inulin diffusion values for confluent Vero cells grown on cell culture inserts for up to 7 d indicate that monolayers remain permeable during this time (figure 9). These results indicate that Vero C1008-24S, but not unpolarized Vero cells, selectively retain N/K-ATPase at the basolateral surface.

Double indirect immunofluorescent staining with E1 and N/K-ATPase revealed some co-localization at the lateral surface, probably due to intercellular RLPs (not shown). Vero cells were noted to grow in multiple layers during the conditions selected for surface confocal microscopy, i.e., 4 d at confluency, and at least four layers of cells were noted in selected fields. In contrast, Vero C1008-24S cells grew in a monolayer displaying contact inhibition, 7, 8 or 9 d post seeding (not shown). The results thus far, i.e., inulin diffusion, biotinylation, confocal microscopy and contact inhibition, infer that Vero C1008-24S cells are indeed polarized, and grow as simple epithelium.

Western blot analysis performed on 6 d old monolayers of Vero C1008-24S cells, revealed capsid protein in the apical and basal media by 3 h, with distinctly higher levels of capsid protein in the apical chamber (figure 8B). Domes were visible on cells grown for 6 d on tissue culture dishes in parallel with cells cultured on inserts, with domes implying the polarized distribution of N/K-ATPase (13). Capsid protein distribution appeared to equilibrate in both chambers by 24 h in other assays (not shown). The latter result may be indicative of pronounced endocytosis of RLPs at the apical surface, or may be due to obstruction of RLP diffusion through the permeable insert. Media collected after 24 h from Vero C1008-24S and immunoprecipitated with human serum, seronegative for RV, was negative for capsid (not shown). Similarly, media from Vero C1008 cells, immunoprecipitated with human anti-RV then probed for

capsid was negative by ECL (figure 8B). These results demonstrate that RLPs are released from both cell surfaces of polarized Vero C1008-24S cells, and that RLPs can pass through the 0.4 μm pores of the cell culture insert.

3.2.2. RV infection of Vero and Vero C1008 cells

Vero and Vero C1008 cells were infected as described in Materials and Methods, and the media processed for immunofluorescent plaque assay. In three separate experiments of RV infected Vero C1008 cells and a replicate of four RV infected Vero cells grown on cell culture inserts, infectious virus was shown to be secreted into both the apical and basal media (figure 11). The plaque forming units (PFU) released per cell for the apical media were consistently greater than basal PFU, by approximately ten fold. Approximately 10^6 virus were released from Vero cells grown on cells culture inserts, while 10^5 were released from Vero C1008 cells. It is important to note that Vero cells do not exhibit contact growth inhibition, confirmed by the fact that four or more layers of cells could be observed by confocal microscopy after 4 d growth at confluent density. Similarly, when Vero cells were scraped from inserts and centrifuged, the pellets were much larger than were Vero C1008 cells, pelleted under the same conditions. Consequently, the higher number of virus may be attributed to increased number of cells rather than increased PFU released per cell. Based on these observations, approximately 0.1 PFU were released per cell over the 48 hour infection period, similar to the multiplicity of infection (MOI). Its interesting to note that the TER for Vero C1008 cells did not decrease during infection, but in fact increased through the course of the infection period on all three occasions, indicating that the monolayer remained intact during the infection period.

3.3. Caco-2 cells secrete RLPs and RV virions in a non-polarized manner

Caco-2 cells stably transfected with 24S cDNA were processed for immunofluorescent staining as described in Materials and Methods. Even though staining of Caco-2 transfected cells was poor, overlap could be seen between capsid and β -COP and E1 and β -COP (not shown). While overlap with β -COP was noted, perinuclear or Golgi localization was not obvious. This clone expressed capsid, E2 and E1 in greater than 70% of the cells, and was named Caco-2-24S. Interestingly, cells at the peripheral surfaces of clumps appeared to stain more than cells at the centers of the clumps, irrespective of how large the clumps were. This may be a characteristic of the cell, i.e., prolonged cell-cell contact alters the growth characteristics of cells, or it may be that cells need to be fixed and permeabilized under different conditions to facilitate optimum staining of all cells. Staining differences may be due to morphological and possibly functional features of the cells, i.e., cells at the peripheral surface may be more squamous-like, whereas cells at the centers of clumps may be more columnar-like. Subsequent to cell-cell contact, 24S gene transcription may be affected, i.e., reduced, due to the nature of the cDNA integration site and activity of the chromosome at different times during the life cycle of the cell. One salient feature of this clone and the parental type is that cells took three to four times longer to reach confluent density than either MDCK II or Vero C1008 cells. Several different growth conditions are described in the literature, so conditions may have to be altered to facilitate optimum growth, and possibly expression of the RV proteins in Caco-2-24S cells. Alternatively, a new clone may need to be selected.

EM analysis of Caco-2-24S cells grown on cell culture inserts was performed. As for MDCK II-24S and Vero C1008-24S cells, RLPs were found at both the apical (figure 12A i) and basolateral surfaces (not shown). RLPs were

also noted within cytoplasmic vesicles (figure 12A ii and iii). The diameter of the RLPs (asterisk) is less the diameter of the membrane pores (arrowhead)(figure 12A iii). No studies were done to ascertain an apical to basolateral surface area ratio.

Cells were grown to confluence on $\approx 4.7 \text{ cm}^2$, high pore density cell culture inserts, $0.4 \text{ }\mu\text{m}$ pore diameter, and the presence of tight junctions was determined by measuring the TER across the monolayers. The TER average was 190 ohms.cm^2 over four independent experiments. Metabolic labeling with ^{35}S cys/met revealed capsid, E2 and E1 in the cells, and E2 and E1 in the apical and basal media 24 h post labeling (figure 12B). Capsid protein was shown by western blot to be in the apical and basal media at 24 h (figure 12C).

Although preliminary, these results indicated that RLPs were successfully assembled in Caco-2-24S cells, albeit less efficiently than in MDCK II-24S or Vero C1008-24S cells. Similarly, these results showed that RLPs were released in a non-polar fashion from a polarized cell line in which the default pathway is thought to be to the basolateral surface (62).

Caco-2 cells were successfully infected with RV from either the apical surface or the basal surface. Infectious particles were released into both the apical and basal media, although the PFU per cell was 10 fold less than for Vero C1008 cells (not shown). As with Vero C1008 cells, no loss of TER was observed after the infection period.

3.4. Assembly of RLPs in stably transfected CHO cells

Assembly and secretion of RLPs has been demonstrated in CHO cells stably transfected with 24S cDNA (CHO24S) (37). To summarize, RLPs were shown by EM to bud into the Golgi, and E1 was shown by immunoperoxidase staining to be present within multivesicular bodies (mvb) throughout the

cytoplasm. Immunofluorescent staining of stably transfected CHO24S cells revealed Golgi localization of capsid, E2 and E1. Vesicular structures dispersed throughout the cytoplasm also stain with capsid, E2 and E1. The vesicular structures stained for E1 do not contain detectable Golgi marker (Man II), nor do they contain early (transferrin receptor) or late (mannose-6-phosphate receptor) endosome markers, lysosome marker (lpg-120), pre-and intra-Golgi transport vesicle (B-COP) or post-Golgi transport vesicle (VIP21/caveolin) markers (37). As virus infection is mediated via the endosomal pathway (70), E1 may be expected to co-localize with transferrin receptor or mannose-6-phosphate receptor if these vesicles contained endocytosed RLPs. Similarly, secretory vesicle markers may be expected to co-localize with E1 if RLPs egressed via a characterized secretory pathway. Possibly the vesicular structures corresponded to unidentified and uncharacterized secretory vesicles, unique to RV infected or transfected cells. ³⁵S methionine labeled CHO24S cells secrete RV structural proteins into the media as early as 2 h post labeling, whereas CHO cells expressing E2E1 or capsid only do not secrete detectable amounts of RV structural protein into the media within 8 h of labeling. In fact, labeled E2 and E1 are almost completely degraded by 8 h in CHO E2E1 cells. When pCMV5-24SE1ct- or pCMV5-24SE1Gtmct were transiently expressed in ³⁵S cysteine labeled COS cells, no labeled RV structural proteins were detected in the media at 5 h post label, whereas RV structural proteins were present in the media of COS cells transfected with pCMV5-24S (23). These results imply that RLP secretion only occurs when all wild type proteins are coordinately expressed, either in COS cells or CHO cells.

To determine the effect of E1 mutations on RLP secretion and viral protein targeting in stably transfected CHO cells, CHO24S-E1tmct recombinant clones were established. Two plasmids, pCMV5-24SE1ct- and pCMV5-24SE1Gtmct were constructed previously (37). However, two new constructs were made,

pCMV5-24SE1CD8tmct and pCMV5-24SE1CD8tm, to further substantiate the effect of E1tmct substitution on RLP secretion.

3.4.1. Characteristics of CHO24S cells

CHO24S cells were established by Hobman et al. (37) by transfecting CHODG44 cells with the plasmid pCMV5-24S, as described (36). Immunofluorescent staining revealed Golgi localization of capsid, E2 and E1, as determined by overlap with Man II, and vesicular staining (figure 13 and 14, 24S row). Capsid was also detected throughout the cytoplasm in cells with higher expression levels. Golgi and vesicular staining of capsid was often masked by the high levels of cytoplasmic staining. It is possible that capsid moves independently throughout the cell, and that C/E2 interactions are not stable. Two lines of evidence support this idea. The capsid protein anchor (E2 signal peptide) is not sufficient to prevent release of some capsid from microsomal membranes, when capsid is expressed with E2 in *in vitro* pelleting assays (84). Also, Hobman et al. have previously shown that COS cells expressing capsid only, display a diffuse cytoplasmic staining pattern (36). Presumably, capsid only associates with mature E2/E1 heterodimers undergoing ER to Golgi egress. Thus, prior to this event, some capsid is released from the ER by an as yet unidentified means, possibly proteolysis. Consequently, the diffuse cytoplasmic pattern is a result of antibody/capsid-peptide interaction. Alternatively, a capsid/HSP complex may occur to facilitate protein folding and to prevent proteolysis, and this complex may account for the cytoplasmic staining pattern. Notably, labeled capsid is still prevalent within CHO24S cells at 8 h post labeling, whereas the bulk of labeled E2/E1 is secreted (37).

To determine the secretion characteristics of RV structural proteins, cells were labeled with ³⁵S cys/met or ³²P orthophosphate, and the media

immunoprecipitated with human anti-RV (figures 15A and 15C). Proteins were separated by SDS PAGE, and the resulting fluorographs examined. After a 6 h chase period, ^{35}S labeled E2 and E1 could be detected in the media (figure 15A, lane 4). Similarly, after an 18 h chase period, ^{32}P labeled capsid protein could be detected in the media (figure 15C, lane 2). Western blots were performed in parallel with ^{32}P orthophosphate labeling. Media was immunoprecipitated with human anti-RV serum, and the resulting protein blot probed with mouse monoclonal antibody specific for capsid. ECL analysis of the blots revealed capsid protein in the media of CHO24S cells (figure 15B, lane 2). These results are consistent with the idea that coordinate expression of wild type capsid, E2 and E1 results in the secretion of detectable amounts of RV structural proteins into the media of stably transfected cells (37).

3.4.2. Characteristics of CHO24S E1ct- cells

CHODG44 cells were stably transfected with the plasmid pCMV5-24SE1ct- as described in Materials and Methods, and viral structural protein transport and RLP secretion were characterized. Indirect immunofluorescent staining revealed overlap between the Golgi marker Man II and capsid, however, cytoplasmic localization of capsid was more prevalent in cells with high levels of expression (figure 13, 24S E1ct- row). Capsid staining was also noted within vesicular structures. E2 and E1 were primarily located within the Golgi region as determined by co-localization with Man II. Very little, if any vesicular or cytoplasmic staining was noted with E2 or E1.

CHO24SE1ct- cells were labeled with ^{35}S cys/met or ^{32}P orthophosphate, and the media immunoprecipitated with human anti-RV. Proteins were separated by SDS PAGE, and the resulting fluorographs examined (figure 15A and 15C). ^{35}S labeled structural proteins were present in the cell lysates at 0 h

and at 6 h post labeling, albeit at reduced amounts at 6 h (figure 15A, lanes 11 and 12). After a 6 h chase period, ^{35}S labeled E2 and E1 could not be detected in the media (figure 15A, lane 13). Similarly, after an 18 h chase period, ^{32}P labeled capsid protein could be detected in the cell lysates but not in the media (figure 15C, lanes 5 and 6 respectively). Phosphorylation of capsid did not seem to depend upon interaction of capsid with E1ct, as intracellular capsid was phosphorylated. Western blotting was performed in parallel with ^{32}P orthophosphate labeling. Media was immunoprecipitated with human anti-RV serum, and the resulting protein blot probed with mouse monoclonal antibody specific for capsid. ECL analysis of the blot revealed capsid protein in the cell lysate but not in the media (figure 15B, lanes 3 and 4 respectively). These results present evidence to rule out E1ct in targeting of C/E2/E1 to the Golgi. The results do however implicate E1ct in assembly of RLPs as was found for transiently transfected COS cells (37). While a C/E2 association is implicated, the E2 signal peptide at the carboxy terminus of capsid may associate with E1tm in the plane of the membrane (figure 2). Secretion of RLPs appears to be dependent upon assembly, as no structural proteins could be detected in the media for up to 18 h post labeling.

3.4.3. Characteristics of CHO24S Gtmct cells

CHODG44 cells were stably transfected with the plasmid pCMV5-24SE1Gtmct as described in Materials and Methods. The transmembrane and cytoplasmic domains of E1 were replaced with the corresponding regions from another type I palmitylated glycoprotein, vesicular stomatitis virus G protein (VSVG) (95). Unlike E1 which behaves as an intracellular integral membrane protein (41), VSVG is normally expressed at cell surfaces, e.g., VSVG is expressed at the surface of stably transfected MDCK cells (24). Hobman et al. have

demonstrated that E2 and E1-Gtmct are targeted to the Golgi in CHO2E1-Gtmct cells (42), similar to E2 and E1 targeting to the Golgi in CHO24S cells (37). Results for immunofluorescent staining of capsid, E2 and E1 (figure 14, 24S Gtmct row), metabolic labeling with ^{35}S cys/met (figure 15A, lanes 14-16), ^{32}P orthophosphate labeling (figure 15C, lanes 3 and 4) and Western blot experiments (figure 15B, lanes 5 and 6) were identical to those for CHO24S E1ct-. To verify the presence of VSVGct, cells were stained with mouse monoclonal antibody P5D4 (46). P5D4 staining was seen to overlap entirely with Man II, confirming Golgi localization of E1Gtmct (not shown).

In this experiment, E1tmct is absent from this construct yet E2 and E1 are both transported to the Golgi, a feature known to be dependent upon E2/E1 heterodimer formation (40, 41). Consequently, these results implicate the E1 ectodomain with E2/E1 heterodimer formation. Also, C/E2 association is implicated since following removal of both the transmembrane and cytoplasmic domains from E1, capsid is seen within the Golgi, a feature known to be dependent upon C/E2/E1 expression (36). RLP assembly seems to be dependent upon E1ct (36, 58), and the absence of RLP secretion using this construct supports this hypothesis.

3.4.4. Characteristics of CHO24S CD8tm and CHO24S CD8tmct cells

CHODG44 cells were stably transfected with the plasmids pCMV5-24SE1CD8tm or pCMV5-24SE1CD8tmct, as described in Materials and Methods. The transmembrane or transmembrane and cytoplasmic domains of E1 were replaced with the corresponding region(s) from another type I palmitylated glycoprotein CD8, a human T cell surface marker (47, 69). Identical results were found as for CHO24S E1ct-. CHO24S CD8tm immunofluorescent staining of

capsid, E2 and E1 (figure 14, CD8tm row) showed Golgi overlap of capsid and E1 with Man II. Metabolic labeling with ³⁵S cys/met (figure 15A, lanes 5-7) and ³²P orthophosphate (figure 15C, lanes 9 and 10), and Western blot experiments (figure 15B, lanes 7 and 8) revealed no secretion of RV structural proteins into the media. CHO24S CD8^{tmct} results for immunofluorescent staining of capsid, E2 and E1 (figure 13, 24S CD8^{tmct} row) also showed Golgi overlap of capsid and E1 with Man II. Metabolic labeling with ³⁵S cys/met (figure 15A, lanes 8-10) and ³²P orthophosphate (figure 15C, lanes 7 and 8), and Western blot experiments (figure 15B, lanes 9 and 10) once again revealed no secretion of RV structural proteins into the media. The interpretation of results for CHO24S CD8^{tmct} is the same as for CHO24S G^{tmct}, i.e., the E1 ectodomain is implicated with E2/E1 heterodimer formation. However, the CHO24S CD8tm clone allows us to make further observations, namely, the involvement of E1tm in RLP assembly. In CHO24S CD8tm cells, all the RV specific predicted cytoplasmic elements are available for interaction, i.e., capsid, E2^{ct} and E1^{ct}. Surprisingly, RLPs do not assemble even though all proteins are targeted to the Golgi. One possible explanation for this is altered alignment of E1^{ct} with E2^{ct} and/or capsid, due to the nature of the amino acids in the CD8tm region. Another more plausible explanation is that E1tm is involved in assembly along with E1^{ct}. For instance, E1^{tmct} has recently been identified as an ER retention signal in CD8 chimeras (35). E1tm or E1^{ct} alone were not able to prevent maturation and cell surface expression of CD8. So possibly the attribute of E1^{tmct} that facilitates retention in the ER may afford E1 enough time to mature completely and associate correctly with E2. This is supported by another recent report regarding the alpha-helical properties of E1tm. An alpha-helical domain immediately preceding the E1 transmembrane and the transmembrane region itself, are predicted to be involved in helix-helix mediated protein oligomerization (25). So, by removing

the E1tm domain, this oligomeric association may be disturbed. Consequently, E1^{ct} is unable to facilitate RLP assembly in this construct.

3.4.5. Characteristics of CHO24S E2Gtm cells

CHODG44 cells were transiently transfected with pCMV5-24SE2Gtm. Preliminary indirect immunofluorescent staining of CHO24S-E2Gtm, showed that E2 was retained in the ER and E1 in a post ER pre Golgi compartment, consistent with previously published data by Hobman et al. (40, 42). Capsid was found throughout the cytoplasm. No co-localization was noted with the Golgi marker Man II and either capsid, E2 or E1 (not shown). Western blot analysis of transiently transfected CHOK1 cells revealed no capsid protein in the media (not shown). Media was collected from transiently transfected cells, 30 h after the start of transfection. Clarified media was immunoprecipitated with human anti-RV serum, and the resulting protein blot was probed with mouse anti-capsid. pCMV5-24S and pCMV5-24SE1^{ct}- were used as positive and negative controls respectively. Only CHOK1 cells transiently transfected with pCMV5-24S released capsid into the media (not shown). This result confirms previous reports that capsid egress from the ER to the Golgi is dependent upon C/E2/E1 association (36, 58), where E1^{ct} (or E1^{tmct}?) modulates a C/E2 interaction (37). E2tm facilitates E2/E1 egress from the ER to the Golgi (42). Based upon this data, it appears that E2/E1 form a complex that is dependent upon E2tm but not upon E1^{tmct}. The absence of Golgi or reticular staining allows us to propose that capsid's C-terminal hydrophobic domain (E2 signal peptide) associates with the E2tm region, thereby facilitating capsid egress along with E2/E1.

The results presented here confirm previous finding by Hobman et al. that expression of capsid, E2 and wild type E1 are required for secretion or RLPs into

the media (37). Both E1tm and E1^{ct} are required for assembly of RLPs as altered E1^{tm/ct} clearly abolished secretion. It is likely that virus like particles are the only secretory form of capsid-E2-E1 complexes. As E2 and E1 are type I membrane spanning proteins with cytoplasmic COOH domains, and capsid resides on the cytoplasmic side of the ER, capsid most likely interacts with one or both transmembrane/cytoplasmic domains. This capsid/E2/E1 interaction likely causes the E2E1 studded lipid membrane to envelope the capsid homodimers, which ultimately leads to oligomerization. The RLPs bud into the Golgi and are released from the confines of the membrane, enabling the RLPs to be secreted. Indeed, RLPs have been seen by EM within cytoplasmic vesicles and at the surfaces of polarized cells (see above) and Hobman et al. (37). Presumably alterations in E1^{tmct} hinders capsid association, therefore preventing RLP formation, which ultimately leads to degradation rather than secretion of E2 and E1 as evidenced above.

4 Discussion

4.1. Polarized secretion of RLPs in mammalian cells

The study of RV infection in polarized mammalian cells *in vitro* is hampered because RV will not efficiently infect cells with an active interferon system (20). Also, there is no reliable animal model available to study acquired or congenital rubella *in vivo* (99). For these reasons, it was important to develop a system to study the assembly and secretion characteristics of RV *in vitro*. Ultimately, these studies may contribute to our understanding of how RV crosses the placenta and causes the most serious of rubella infections, CRS. A novel approach was adopted that involved the use of RLPs as a means to study RV virion secretion characteristics. RLPs resemble RV virions in terms of size, antigenicity, buoyant density and morphology, and are secreted from transfected cells expressing C, E2 and E1 (37). As a first step in this process, we had to determine if RLPs behaved the same as RV virions in polarized cells, in terms of secretion characteristics. To do this, we employed transfection and infection studies of three polarized mammalian cells.

Obviously, human epithelium is different from cultured epithelium, being highly specialized and heterogeneous. As would be expected, epithelium in the respiratory tract for example, functions differently to epithelium in the urinary tract. Consistent with this idea, secretory epithelium transports secretory products to the apical cell surface, e.g., the mucus secreting epithelium of the gastric mucosa of the stomach, whereas absorptive cells transport to the basal surface, e.g., intestinal villi enterocytes. However, epithelial tissue do have some common features. All epithelial cells are closely bound to each other, are supported by a basement membrane and absorb nutrients from the underlying tissue (98). It seems likely therefore that common and specialized sorting or secretory pathways are prevalent in epithelium, and this fact is evident in many

of the commonly used *in vitro* cell culture systems used to study epithelial polarity. It is this commonality among epithelium that we had hoped to exploit to further our understanding of RV infection *in vitro*, which may ultimately lead to a working hypothesis of RV infection *in vivo*.

Clonal variety exists in transfected cells, and variants of MDCK cells with specific properties and characteristics (26), and Vero cells which differ in morphology, metabolism and contact inhibition (18), have been reported. While RLP secretion from a single clone may not represent the complete, heterogeneous parental population of MDCK II, Vero C1008 or even Caco-2 cells, it is possible to study polar or non-polar secretion in transfected epithelium (57). The information we gain may help us understand how RV causes a systemic infection *in vivo*.

The current belief is that secreted proteins are released by default at both the apical and basolateral domains of MDCK II cells (10, 12), which implies that proteins secreted from only one surface must be sorted to that surface. Accordingly, RLPs are released primarily from the apical surface of MDCK II-24S cells, which means they must be sorted to that surface. Conversely, proteins are reputed to leave the basolateral surface of Caco-2 cells by default (62), so on this premise RV virions and RLPs must be sorted to the apical surface. Although Vero C1008 cells are less well characterized than either MDCK or Caco-2 cells, polarized virus sorting has been demonstrated (6, 14, 74, 90), implying that targeting depends upon some virus encoded targeting signal. Presumably, RV virions and RLPs possess such a targeting signal as they do not appear to be secreted by the default pathway in MDCK II or Caco-2 cells. It will be interesting to learn how RV virions avoid contact with the putative cell surface RV receptor within the Golgi, as this must also be a molecule that traverses the secretory pathway of susceptible cells. Possibly RLP secretion exceeds rates of receptor

synthesis. A cartoon of cellular default and RV secretion pathways is shown in figure 16.

Because RLPs are free within the lumen of the Golgi and cytoplasmic vesicles, and therefore analogous to secretory proteins (77), it is possible that part of the ectodomains of the E2 or E1 act as a ligand for some putative trans-Golgi network (TGN) receptor with apical or basal membrane sorting properties (10). While this hypothesis may prove true for apical secretion of RLPs in MDCK II cells and RV virions in Caco-2 cells, it does not account for basolateral secretion of RV virions or RLPs in Caco-2, i.e., if there is a targeting signal, why do RV virions and RLPs also follow the putative default pathway in Caco-2 cells? Similarly in Vero C1008-24S cells, where RLPs are released at both surfaces, albeit qualitatively with a bias for the apical surface. Possibly the rate of RLP synthesis or secretion can saturate the apical or basolateral receptor system in these cells. Clearly, a complicated task is at hand, but fortunately the tools are available to attempt to unravel the complicated pathways of polarized secretion of RV virions; RLPs, more magnet than divining rod.

If RLPs follow any intracellular pathway, it is likely to be a constitutive secretory pathway, since constitutive viral particle or protein secretion has been shown to diverge from regulated secretion at the TGN in AtT-20 cells (rat pituitary cells with regulated and constitutive secretory pathways) (66, 88). It is unknown whether RLPs are secreted via acidic compartments. However, treatment of monolayers with acidotropic agents has been shown to affect virus release from both Vero C1008 and Caco-2 cells (90), and E2E1 degradation is inhibited by acidotropic agents (37). Also, it has been shown that some basolaterally targeted secretory proteins (12) or the membrane bound VSVG protein's basolateral distribution (22) are disrupted by chloroquine treatment (24). Targeting via acidic compartments or lysosomes could be tested using

acidotropic agents to increase the pH of the intracellular compartments and determine if RLP secretion follows this route. Conversely, it may be possible to correlate RLP secretion with the apical, membrane bound protein influenza virus HA (75), or apically secreted gp 80 (91), neither of which are affected by chloroquine treatment. Alternatively, cells could be treated with tunicamycin or transfected with glycosylation mutants to see if targeting is dependent upon protein glycosylation, as has been recently reported (45, 79). However, coronavirus sorting is unaffected by tunicamycin treatment (77). It may be possible to demonstrate co-localization of RLPs with Rab proteins involved in vesicle transport. Rab proteins have specific subcellular locations in the secretory and endocytic pathways (1). Also, co-localization with the transferrin-receptor/transferrin complex or IgA, IgG or thyroglobulin receptors (if present) could implicate or rule out the involvement of endosomes in RLP secretion.

4.2. Assembly of RLPs in mammalian cells

The molecular biological techniques used to study RV infection, mark the advent of a new level at which the virus can be understood. Many antibodies have been raised to epitopes involved in virion fusion and infection, and the precise location of these epitopes has been mapped in some cases (99-101). Similarly, recombinant DNA technology has been used to delineate the nucleotide sequence of the genomic (96) and subgenomic (15) viral RNAs.

Much work is being done to determine how the structural proteins assemble into virus particles. Targeting of coordinately expressed proteins C-E2 or C-E2-E1, i.e., proteins expressed from the same plasmid, seems to differ from targeting of proteins coexpressed, i.e., coexpression of capsid and E2 proteins. In the former case, capsid was found in the Golgi whereas in the latter case, capsid remained in the ER (3). Presumably some interaction takes place between

C/E2/E1 during coordinate expression that does not take place during coexpression (3). In CHO cells, E2 localizes mainly to the ER (41). In COS cells, some Golgi and cell surface staining is seen, but expression levels are so high, mis-targeting can occur (36). In fact, a Golgi targeting and retention signal has been located within the transmembrane region of E2 (42). E1 when expressed alone, primarily localizes to a post ER pre Golgi region (3, 40), but when expressed with C/E2 or E2, localizes to the Golgi (3, 40). Consequently, Golgi localization of E1 is dependent upon coordinate expression of E2.

In the cases of CHO24S, CHO24S-E1ct-, CHO24S-E1Gtmct, CHO24S-E1CD8tmct and CHO24S-E1CD8tm, capsid, E2 and E1 were all shown to be located within the Golgi and vesicular structures, and capsid was noted throughout the cytoplasm by immunofluorescent staining. To investigate capsid staining in vesicles involved in proteolysis, cells could be treated with puromycin or cycloheximide to prevent protein synthesis (1), then monitored for diminished vesicular capsid staining. E2 and E1 glycoproteins remain prevalent within the Golgi for 3 h in cells treated with cycloheximide (41), and as they are protected from cytoplasmic proteases they would serve as an internal positive control for protein stability.

Capsid localization to the Golgi was not dependent upon E1tm or E1ct, so presumably the C/E2 interaction is predominant in these recombinant clones. Similarly, E1 localization to the Golgi was not dependent upon E1tm or E1ct, as has previously been demonstrated (42). However, RLP secretion was dependent upon both the E1tm and E1ct, and this has previously been demonstrated in COS cells transiently transfected with pCMV5-24S-E1ct- and pCMV5-24S-E1Gtmct (37). Golgi localization was necessary but not sufficient for assembly of structural proteins, which appears to be dependent upon the presence of E1tmct. It may well be that nucleocapsid formation is uniquely dependent upon E1tmct.

Covalent capsid oligomerization possibly occurs as E1tmct sequesters capsid from the cytoplasm (at a site separate from the putative C/E2 association site), and the E2E1 studded membrane contorts and envelopes the nucleocapsid structure. Alternatively, though covalent capsid oligomerization is not required for budding (49), an E1tmct modulated C/E2 interaction may enhance C/C interaction, and consequently facilitate E1tmct dependent nucleocapsid formation, ultimately leading to RLP assembly.

Preliminary studies with pCMV524S-E2Gtm demonstrate the dependence of RLP secretion upon E2tm. Western blot analysis of transiently transfected CHOK1 cells revealed capsid present in the cell lysate but not in the media. By immunofluorescent staining of transiently transfected CHODG44 cells, E2 was retained in the ER, E1 was localized to the post ER pre Golgi compartment, and capsid was found throughout the cytoplasm. This result seems to lend support to the second hypothesis above, i.e., E2tm is necessary for transport of capsid, E2 and E1 to the Golgi where E1tmct modulates a C/E2 interaction. E2tm may be involved in E2/E1 dimer formation via a putative helix-helix association with E1tm (25), leading to Golgi targeting of C/E2/E1. Expression of C/E1tmct was not sufficient to cause RLP secretion in CHO cells, implying that Golgi localization is required for RLP formation.

4.3. Future perspectives

The experiments above provide us with the basis to study RV secretion characteristics in cultured placental cells. Information on infection and secretion from placental cells may help us learn how to block infection at this level. This information would be especially useful from a medical standpoint.

RLPs may have a potential use as a vaccine. First, the immunological effects of RLPs produced from different cells could be determined in animals.

Next, E2 or E1 domains could be introduced into other glycoproteins to facilitate incorporation of the chimeric proteins into RLPs. Finally, Chimeric RLPs may serve as a multipurpose vaccine. RLP induced immunization could potentially help seronegative women who contract RV infection during pregnancy, as immunization of pregnant women with attenuated virus is inadvisable due to the potential risk to the fetus (99).

The amino acid residues essential for RV assembly can be determined using site directed mutagenesis. For instance, the tyrosine residue in the E1 cytoplasmic tail (ct) may be important, as analogous tyrosine residues in the E2ct glycoprotein of Sindbis virus are essential for virus budding (68). Similarly, arginine residues on the E2ct (putatively involved in capsid association) or cysteine residues on E2 and E1 (putatively involved in fatty acylation) may be important.

Receptor mediated endocytosis of RV could be studied using techniques from the above experiments. RLPs are continually shed from the basolateral surface of cells grown on cell culture inserts. Various cells grown on coverslips could be placed into the basal chamber, underneath the inserts, and RV (or other virion) endocytosis monitored using IF, EM or other procedures.

Figure 1. Synthesis of RV structural proteins

RV non-structural (NS) proteins use the positive (+) polarity, 40S genomic RNA as a template to transcribe negative-polarity RNA, which is subsequently used as a template to make full length and subgenomic positive-polarity RNAs. The subgenomic 24S RNA, which corresponds to the 3' one-third of the genomic RNA, codes for the structural proteins NH₂-capsid-E2-E1-COOH in the form of a polyprotein. Signal peptides direct the translocation of the polyprotein into the endoplasmic reticulum (ER), where it is cleaved by resident signal peptidase on the C-terminal side of both signal peptides. Capsid, E2 and E1 are produced as a result.

figure modified from Oker-Blom, PhD thesis, 1984

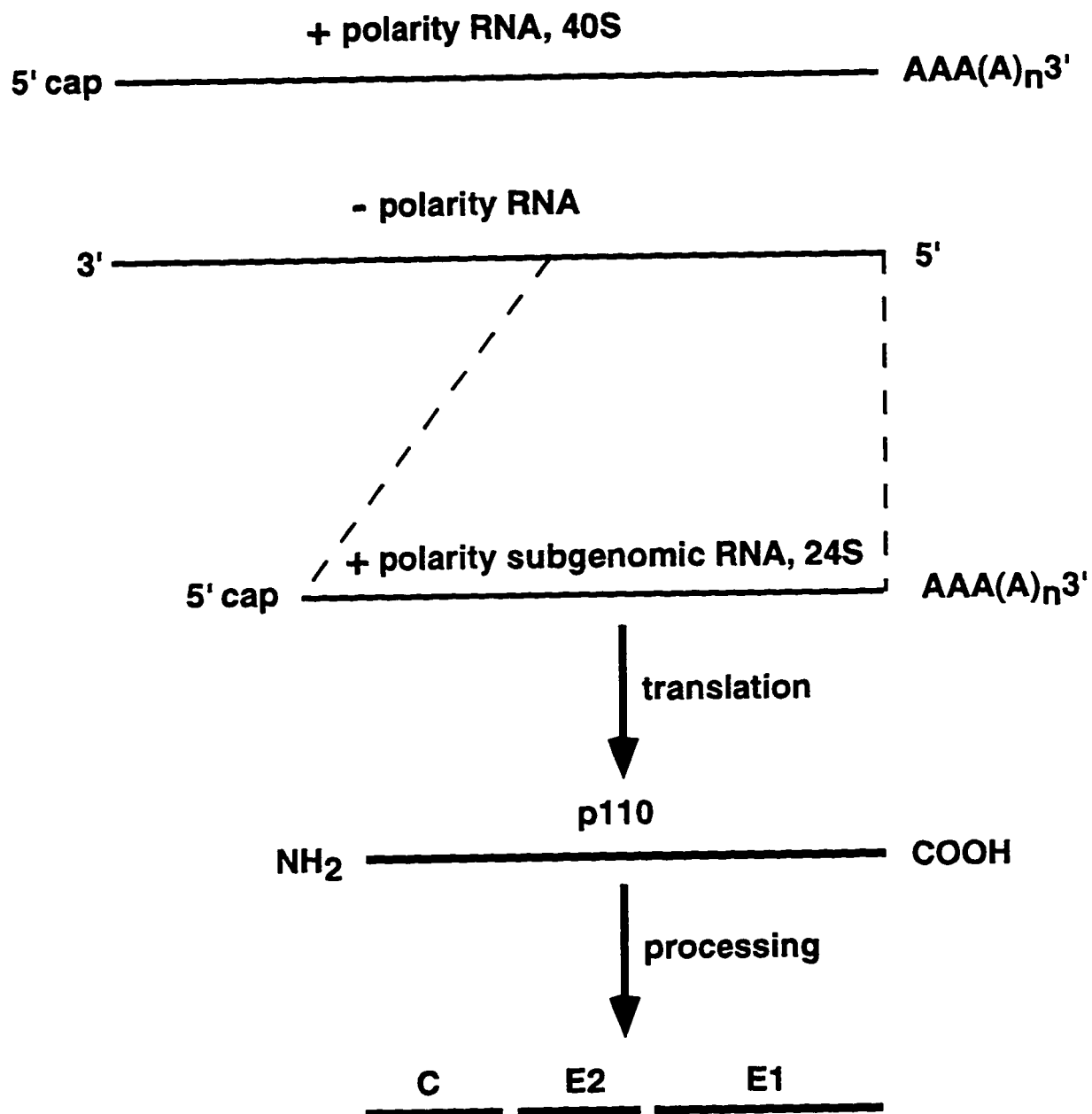
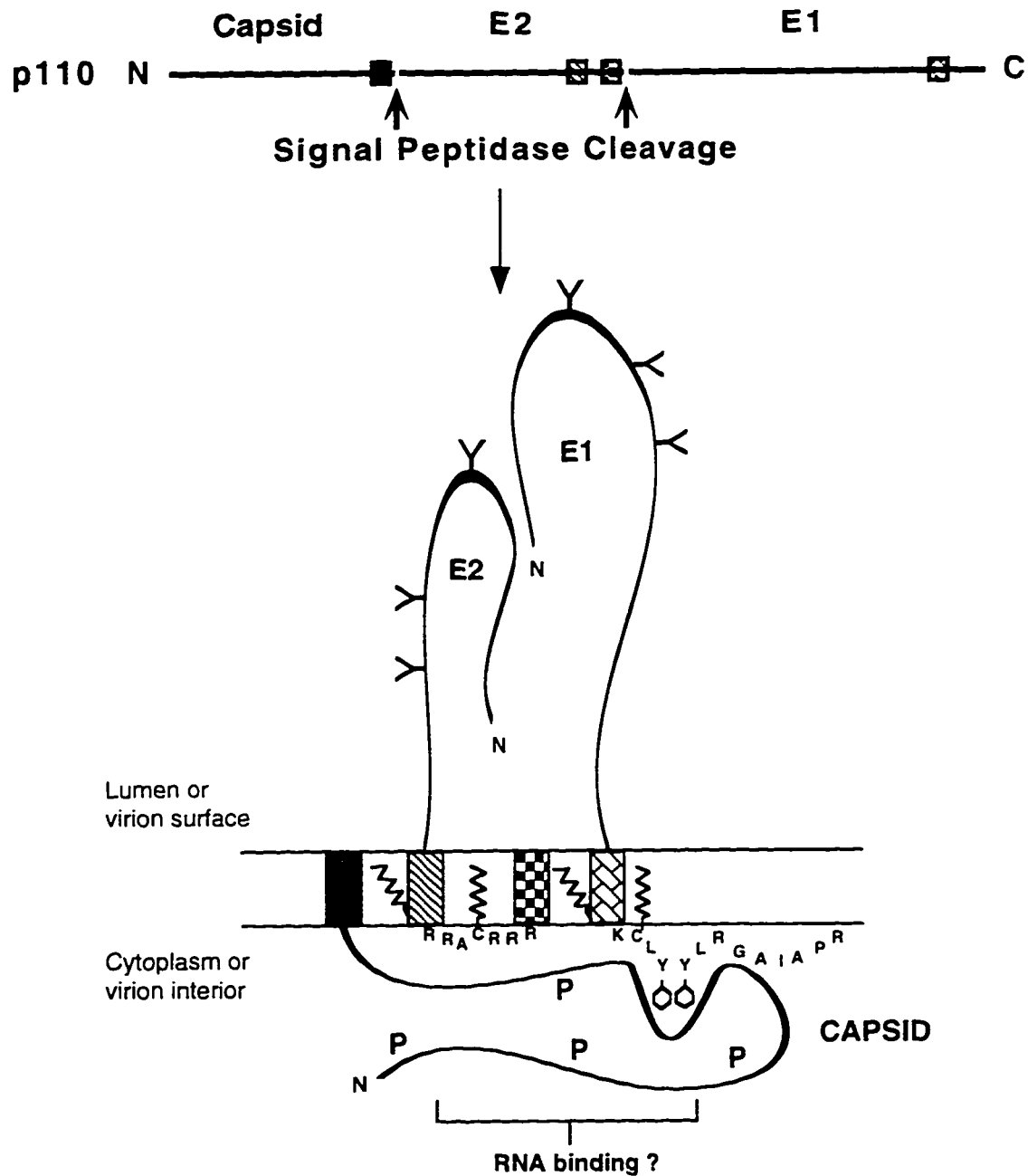
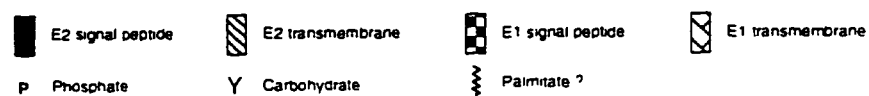


Figure 2. Predicted membrane topology of RV structural proteins

The p110 polyprotein, NH₂-capsid-E2-E1-COOH, is translocated into the lumen of the ER by virtue of E2 and E1 signal peptides, whereupon it is cleaved by signal peptidase. Capsid protein remains on the cytoplasmic side of the ER membrane, the C-terminus being anchored to the ER by virtue of the E2 signal peptide. Capsid proteins are phosphorylated, are rich in arginine and bind to the viral genomic RNA. E2 is a palmitylated, type I membrane spanning glycoprotein, being N-glycosylated at three or four sites and O-glycosylated. E1 is also a palmitylated, type I membrane spanning glycoprotein, N-glycosylated at three sites. N = N terminus, C = C terminus.



Processing of rubella virus structural proteins and predicted membrane topology following translocation into the endoplasmic reticulum/viral membrane.

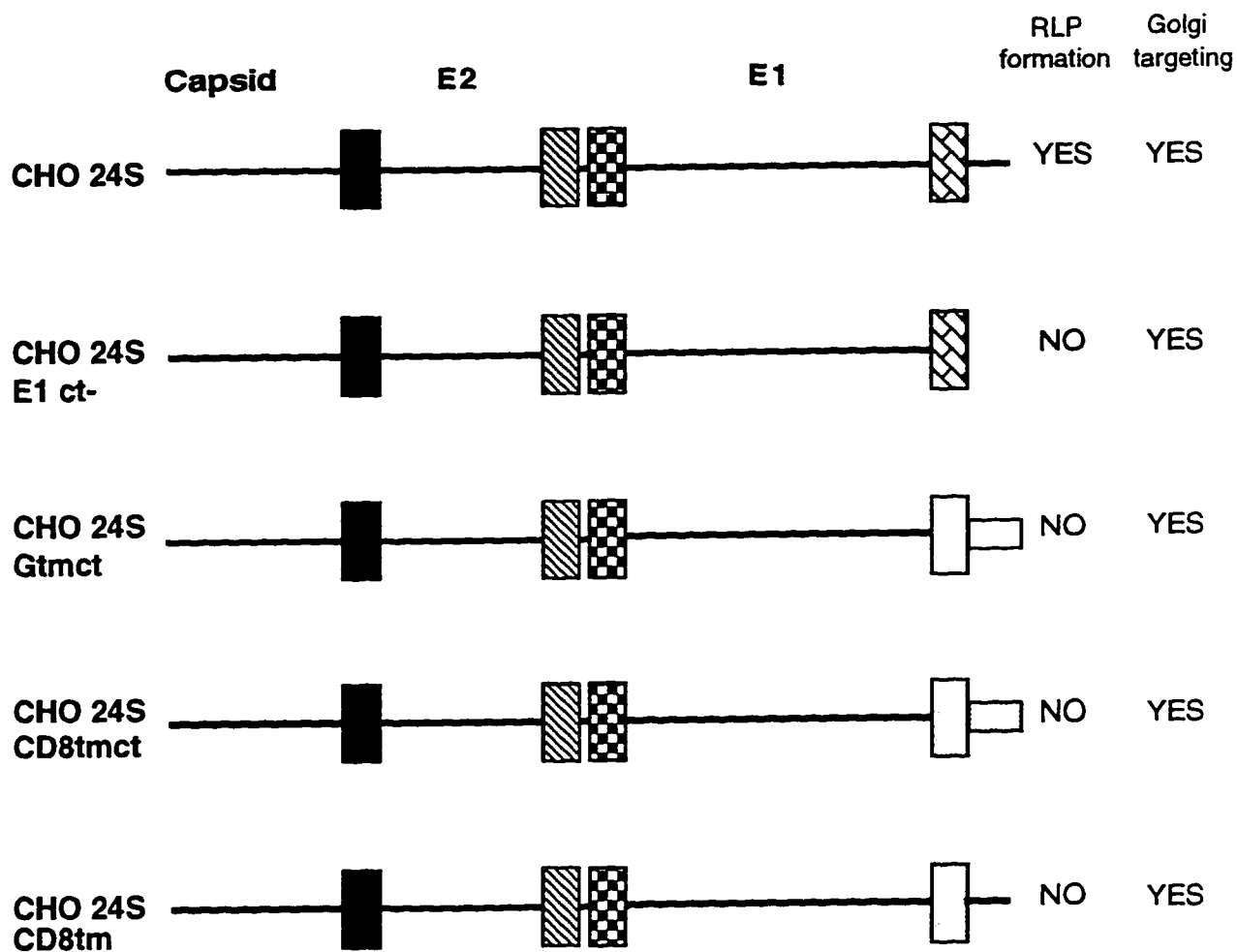


modified from Hobman et al. (1994) *Virology* 202, 574-585

Figure 3. Schematic of RV 24S cDNA constructs

Restriction fragment replacement and site-directed mutagenesis were used to replace or delete E1 transmembrane and/or cytoplasmic domains with analogous domains from CD8 or VSVG. Recombinant 24S cDNA constructs were subcloned into pCMV5 vectors, between the *Eco* RI and *Hind* III or *Bam* HI sites of the polylinker, downstream from the CMV promoter. Expression of RV structural proteins in stably transfected CHO cells revealed Golgi targeting of proteins, but RLP formation was inhibited.

List of Constructs



E2 signal peptide



E2 transmembrane



E1 signal peptide

E1 transmembrane
and cytoplasmic domainE1 transmembrane
onlyVesicular Stomatitis
virus G protein
transmembrane and
cytoplasmic domainCD8 transmembrane
and cytoplasmic domainCD8 transmembrane
E1 cytoplasmic domain

Figure 4. RV structural proteins targeted to the Golgi of MDCK II-24S cells

RV structural proteins were targeted to the Golgi in MDCK II cells, stably transfected with 24S cDNA, coding for NH₂-capsid-E2-E1-COOH. Cells were fixed with paraformaldehyde and permeablized with Triton X-100 before being processed for immunofluorescence. Rubella virus specific proteins capsid (A), E2 (C) and E (E), were detected using mouse monoclonal antibodies to capsid, E2 and E1, and co-stained for Golgi specific marker, rabbit anti-Manosidase II (Man II; B, D and F). Texas Red conjugated 2° antibodies specific for mouse IgG and FITC conjugated 2° antibodies specific for rabbit IgG were used to locate RV antigens. Co-localization can be seen in all cases between RV antigens and Golgi marker, as indicated by the arrowheads. Nuclei were noted to fluoresce in the FITC channel under these fixation conditions.

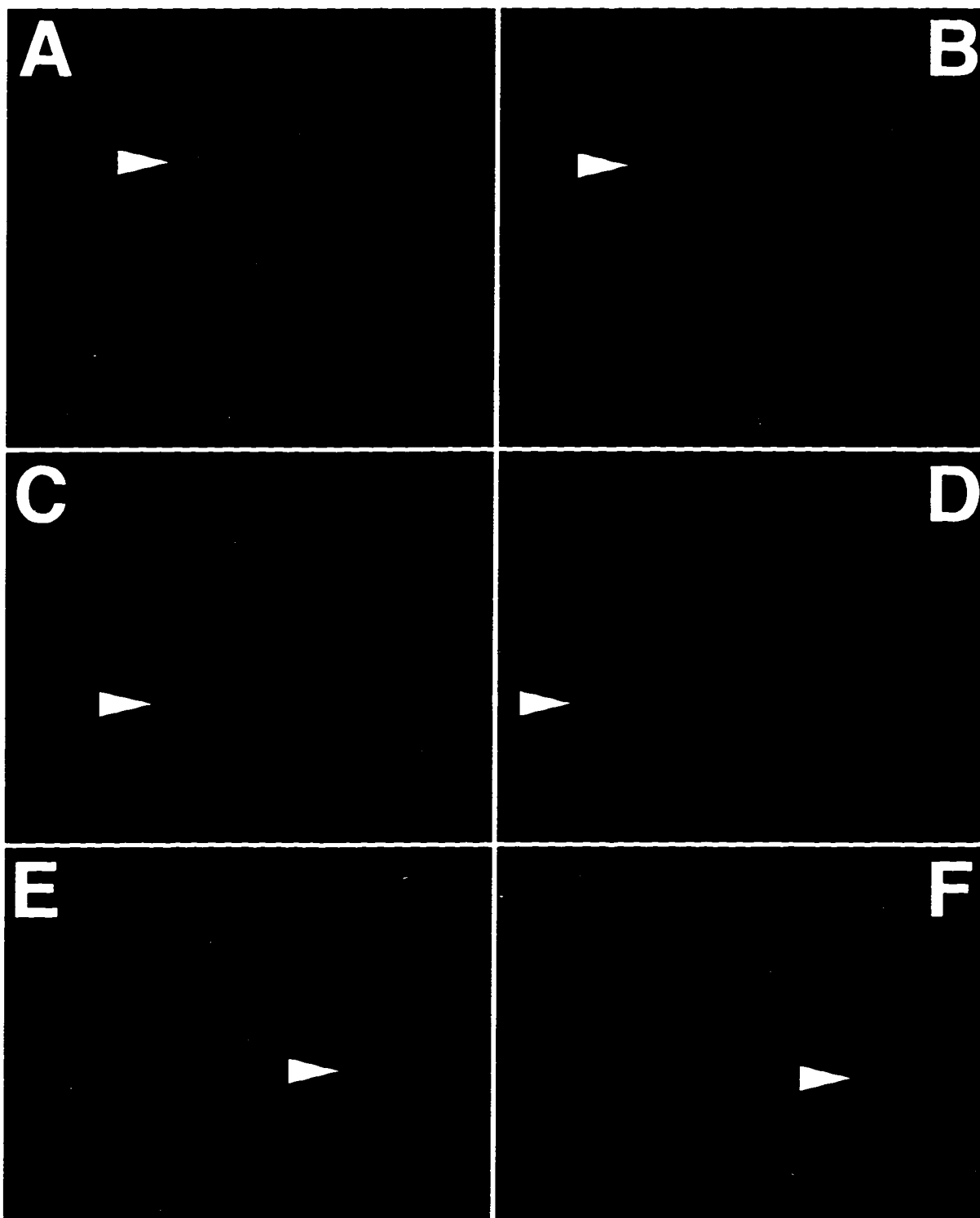


Figure 5. RLP assembly and secretion in MDCK II-24S cells

A. RLPs were noted by EM at both the apical (i) and basolateral (not shown) cell surfaces, and within cytoplasmic vesicles (iii). An RLP could be seen in what was presumed to be an endocytosed vesicle (ii). MDCK II-24S cells were cultured on high pore density cell culture inserts, or glass cover slips.

B. RV structural proteins were released primarily into the apical media from MDCK II-24S cells, cultured on high pore density cell culture inserts. Cells were labeled for 30 min with 100 μ Ci of 35 S cys/met labeling media, then cultured for the indicated times in normal growth media containing 25X cys/met. Apical and basal media were immunoprecipitated with human anti-RV and subjected to SDS-PAGE and fluorography. By 24 h, almost all RV proteins could be found in the apical media. E2 is glycosylated with N- and O-linked sugars, consequently, the mature form of E2 migrates more slowly than the native form. The asterisk indicates the mature form of E2. (for lane headings, C = cell lysate, A = apical media, B = basal media)

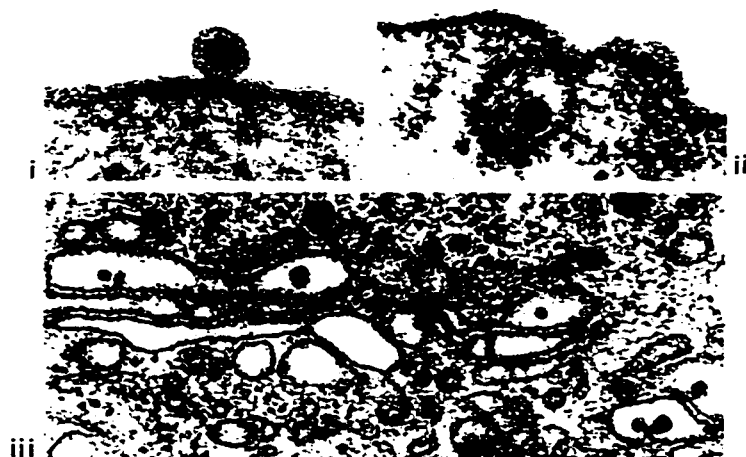
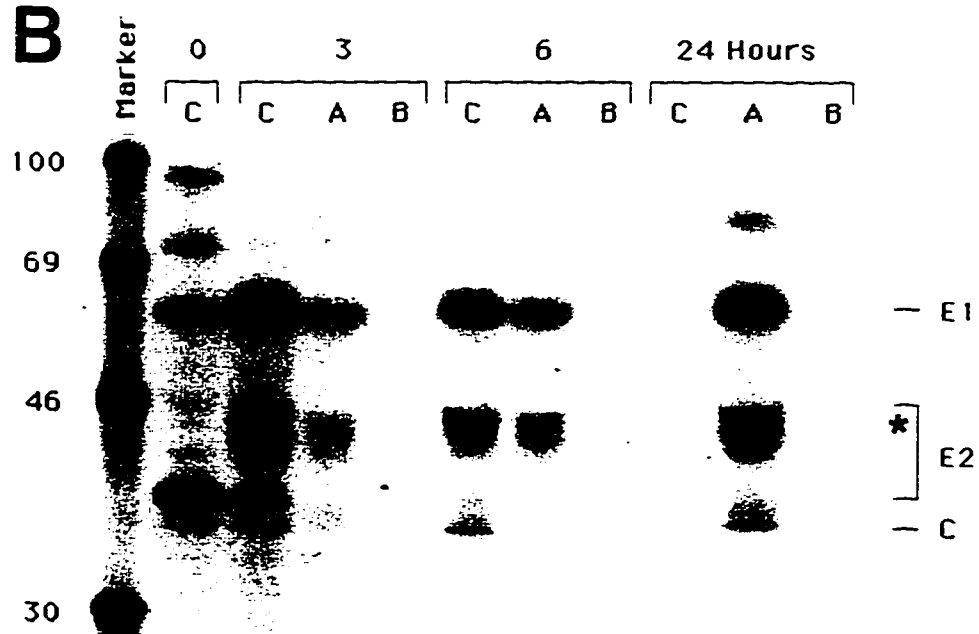
A**B**

Figure 6. RV structural proteins targeted to the Golgi of Vero C1008-24S cells

Co-localization can be seen between RV antigens and the Golgi marker, as indicated by the arrowheads. In addition, capsid can be seen at the peripheral surface of some cells (arrowhead, panel A). Vero C1008 cells were stably transfected with 24S cDNA, coding for RV structural proteins NH₂-capsid-E2-E1-COOH. Cells were fixed and permeablized with methanol before being processed for immunofluorescence. Rubella virus specific proteins capsid (A), E2 (C) and E1 (E), were detected using mouse monoclonal antibodies, and co-stained for the Golgi marker, rabbit anti- β -COP (B, D and F). Texas Red conjugated 2° antibodies specific for mouse IgG and FITC conjugated 2° antibodies specific for rabbit IgG were used to locate RV antigens.

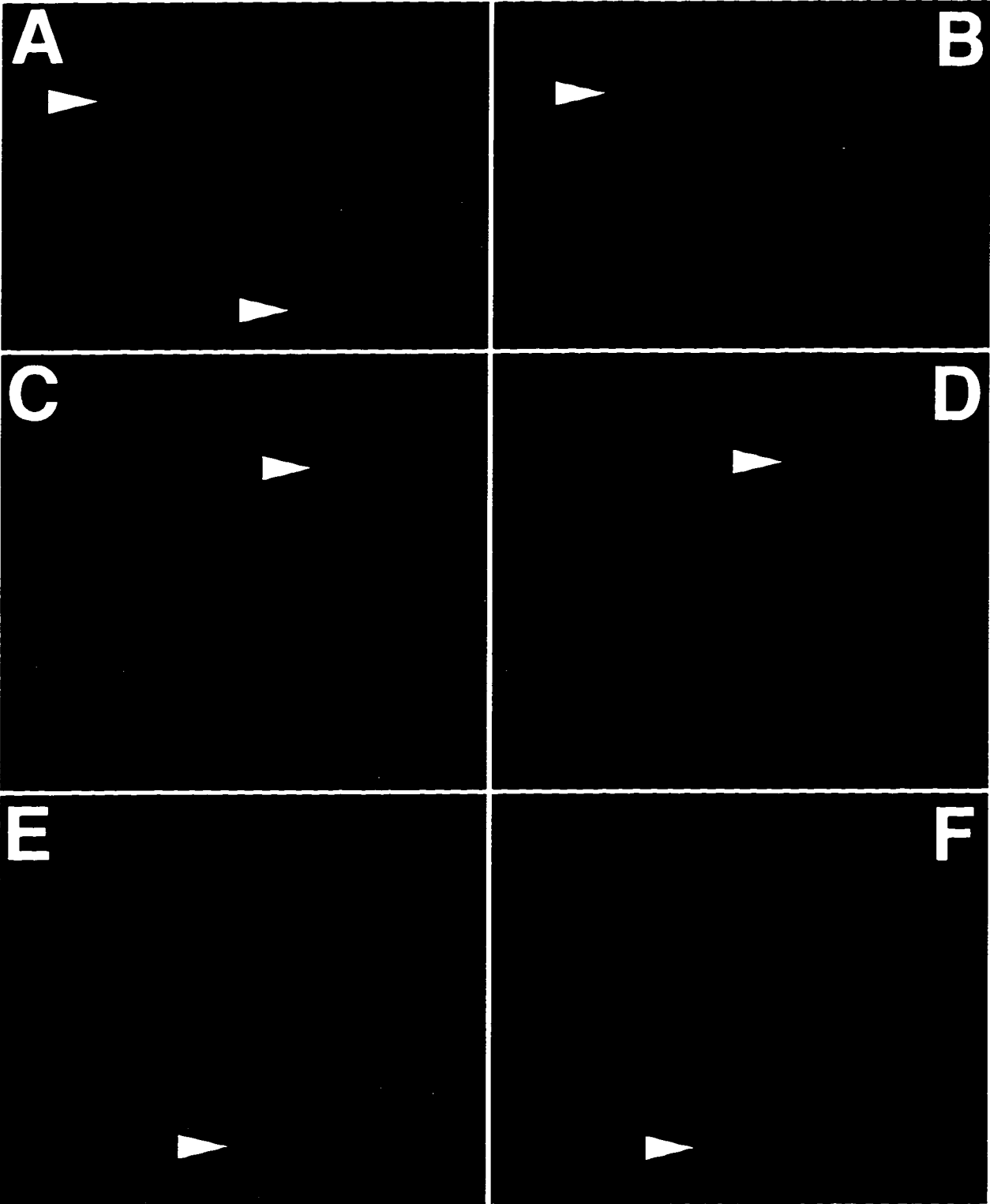


Figure 7. RLP assembly and secretion in Vero C1008-24S cells

Vero C1008-24S cells were cultured on high pore density cell culture inserts, and processed for EM as described in materials and methods. RLPs were found at both the apical (asterisk) and basolateral cell surfaces (not shown), and within cytoplasmic vesicles (arrowhead).



Figure 8. Secretion of RLPs in Vero C1008-24S cells

A. RV structural proteins were released in a non-polarized manner from Vero C1008-24S cells, cultured on high pore density cell culture inserts. Cells were metabolically labeled for 30 min with 100 μ Ci of 35 S cys/met. Labeling media was replaced with growth media containing 25X cys/met, and culture continued for the indicated times. Apical and basal media were immunoprecipitated with human anti-RV and subjected to SDS-PAGE and fluorography. E2 and E1 were present in both the apical and basal media as early as 3 h after labeling. Capsid could barely be detected in the radioimmunoprecipitates, implying that E2/E1 heterodimers recruit both labeled and unlabeled capsid for RLP assembly. (for lane headings, C = cell lysate, A = apical media, B = basal media)

B. Western blot analysis confirmed that capsid protein was present in both the apical and basal media at the same times that metabolically labeled E2 and E1 were immunoprecipitated. It is important to note that capsid protein is only secreted in the form of RLPs.

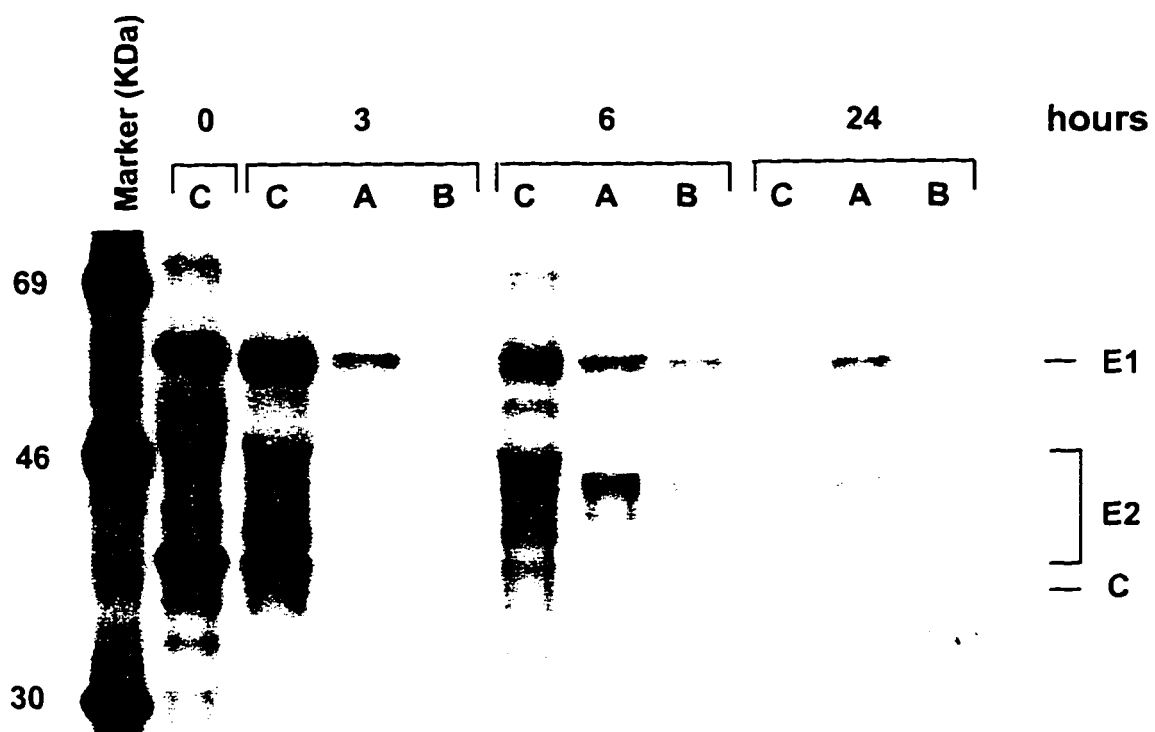
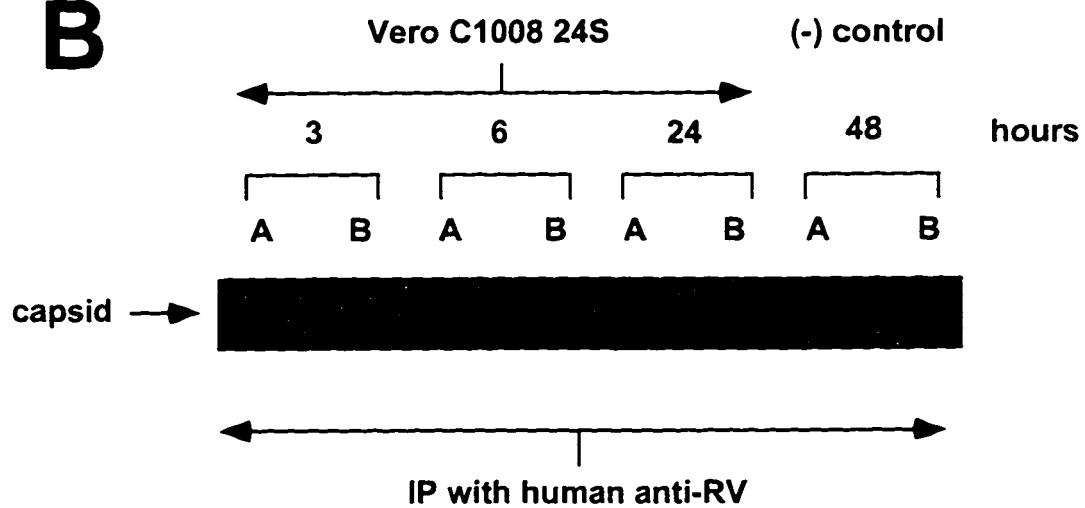
A**B**

Figure 9. Vero C1008-24S cells resist inulin diffusion

Inulin diffusion rates for Vero C1008-24S monolayers more closely resembled Vero C1008 than unpolarized Vero cells. Apical and basal chambers of cells grown on high pore density cell culture inserts, were equilibrated with 1.0 mM unlabeled inulin, after which, the apical chamber was spiked with 2 μ l (40 nCi/89K dpm) 14 C labeled inulin. Aliquots were removed from both the apical and basal chambers (with replacement where necessary) and radioactivity measured by liquid scintillation counter. Inulin diffusion is an indicator of the average permeability through the transcellular space, where low inulin diffusion values indicate tight junction formation. Error bars, \pm 1 SD.

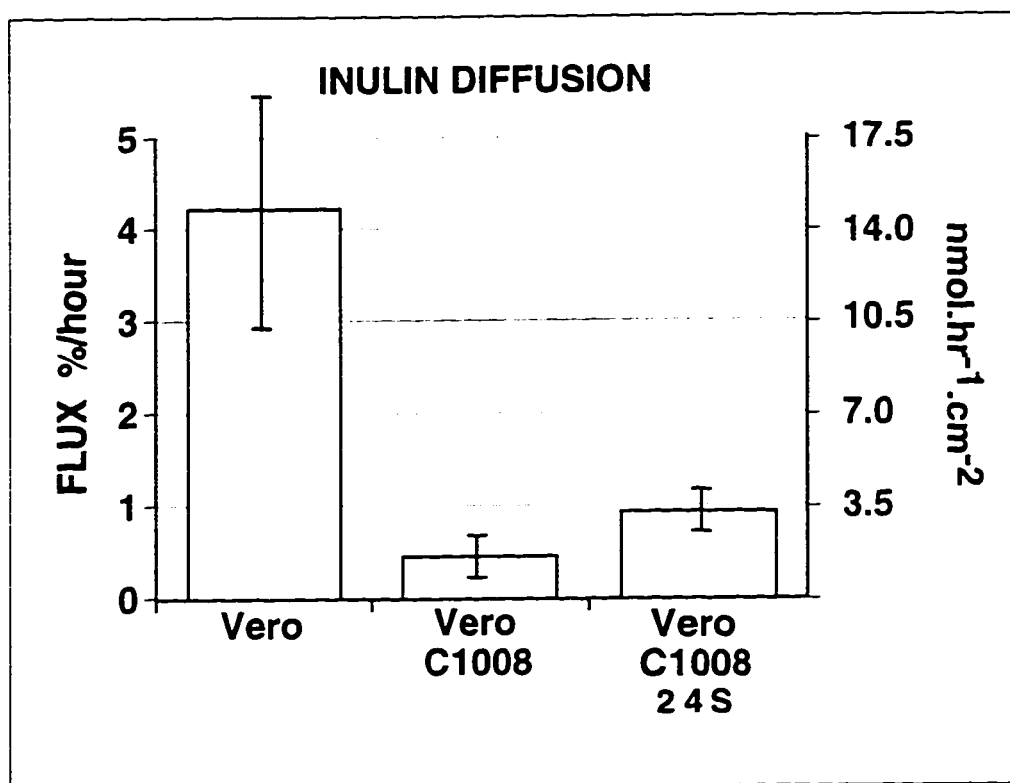


Figure 10. Vero C1008-24S cells demonstrated polarized distribution of cell surface proteins

A. Biotinylation of Vero and Vero C1008-24S cells reveals strikingly different profiles of cell surface moieties. Cells grown on high pore density cell culture inserts were biotinylated on either the apical or basal surface. Cells were lysed, boiled in 2X SDS gel loading buffer, and separated by SDS PAGE. Proteins were blotted onto PVDF membranes, then probed with horseradish peroxidase conjugated to streptavidin. ECL was used to detect biotin/streptavidin complexes.

B. N/K-ATPase distribution is typical of non-polar distribution in Vero cells and of basolateral distribution in Vero C1008-24S cells. Cells grown on high pore density cell culture inserts were processed for immunofluorescence using a rabbit polyclonal antibody specific for N/K-ATPase. Confocal microscopy was employed to scan the cells from the apical to the basal surface. Representative sections are shown.

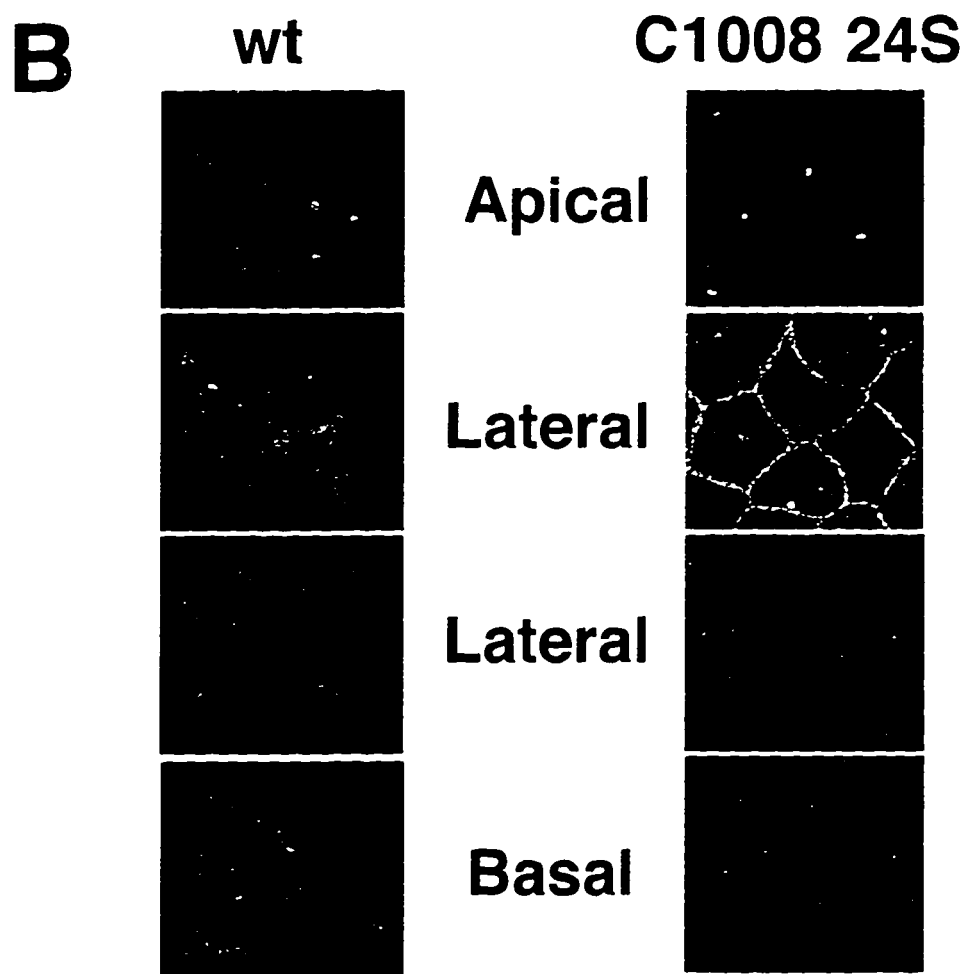
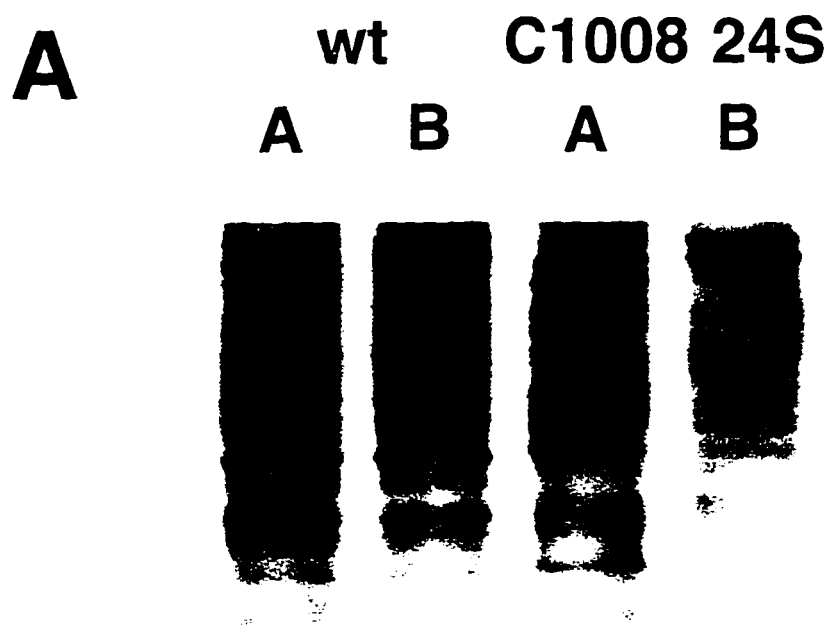


Figure 11. RV virion secretion in Vero and Vero C1008 cells

RV virions are secreted in a non-polarized manner from Vero and Vero C1008 cells. Cells were seeded at 1.0 to 1.5×10^6 and grown for 7 to 9 d on ≈ 4.7 cm^2 , high pore density cell culture inserts, $0.4 \mu\text{m}$ pore diameter. Cells were infected from the apical surface with $200 \mu\text{l}$ of inoculum (M33 RV, approx. $\text{MOI} = 0.1$) for 1 h. Inoculum was removed, monolayer surfaces washed and culture continued for 48 h. Apical and basal media were collected, clarified by centrifugation at $10,000 \text{ g}$, titered out in serial 10 fold dilutions, grown for three days then processed for immunofluorescence. Only wells with four or more plaques were used to assay viral titers, and the highest and lowest apical to basal ratios were discarded prior to preparing histograms. Error bars, ± 1 SD.

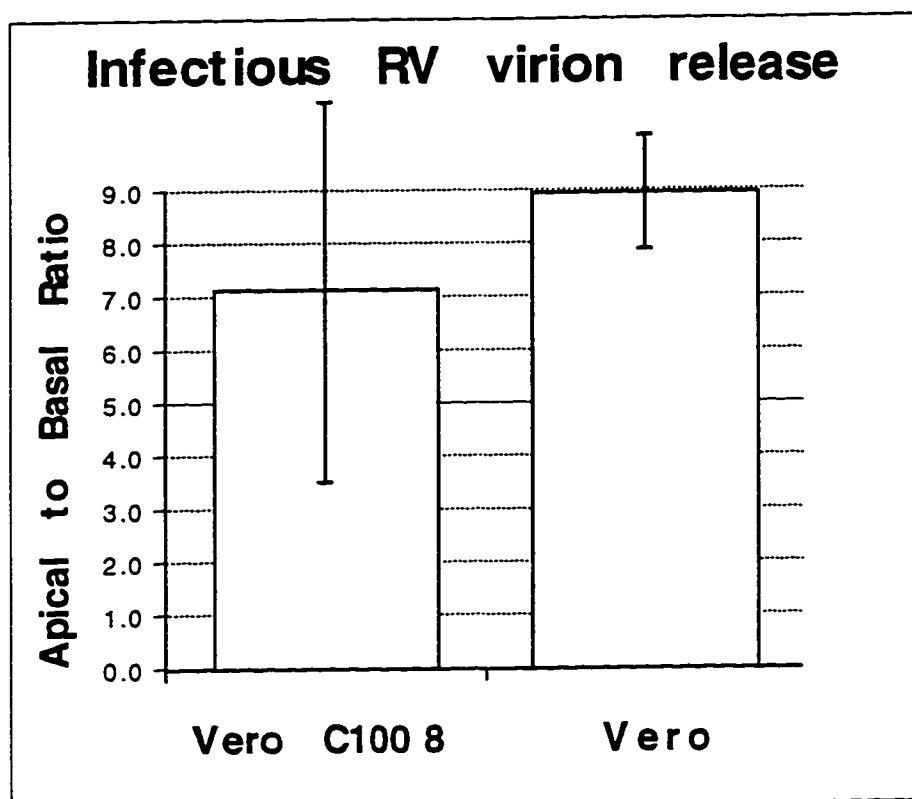
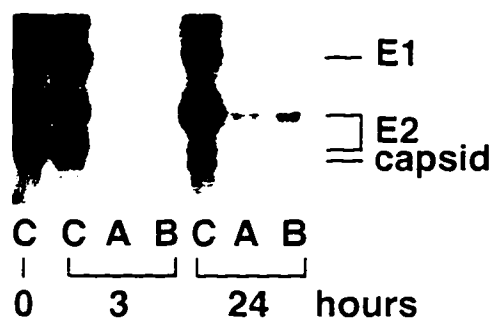
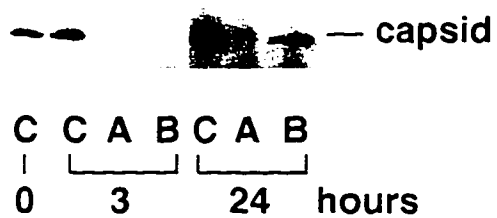


Figure 12. RLP assembly and secretion in Caco-2-24S cells

A. Caco-2-24S cells were cultured on high pore density cell culture inserts, and processed for EM as described in materials and methods. RLPs were evident at both the apical (i) and basolateral cell surfaces (not shown), and within cytoplasmic vesicles (ii and iii). The membrane pore (arrowhead) visible in panel iii is much wider than the RLPs (asterisk) visible in cytoplasmic vesicles.

B. Metabolic labeling of Caco-2-24S cells revealed that RV structural proteins could be immunoprecipitated at 24 h from both the apical and basal media of cells grown on cell culture inserts. Radiolabeled capsid could not be detected in immunoprecipitates from the media, implying that E2/E1 heterodimers assemble with a pool of labeled and unlabeled capsid, prior to secretion. (C = cell lysate, A = apical media, B = basal media)

C. Western blot analysis confirmed that capsid protein was present in both the apical and basal media at 24 h, the same times that metabolically labeled E2 and E1 were immunoprecipitated. (C = cell lysate, A = apical media, B = basal media)

A**B****C**

**Figure 13. RV structural proteins targeted to the Golgi of CHO 24S,
CHO 24S-CD8tmct, CHO 24S-E1ct- cells**

RV structural proteins were targeted to the Golgi in CHO 24S, CHO 24S-CD8tmct, CHO 24S-E1ct- cells. Cells were grown on fibronectin coated glass coverslips, then fixed and permeablized with methanol before being processed for immunofluorescence. Cells were stained for capsid, E2 and E1 using mouse monoclonal antibodies, and co-stained for the Golgi marker using rabbit anti-Man II. Texas Red conjugated 2° antibodies specific for mouse IgG and FITC conjugated 2° antibodies specific for rabbit IgG were used to locate RV antigens. Co-localization of capsid, E2 (not shown) or E1 with the Golgi marker Man II was present in all cases (indicated by arrowheads in several slides).

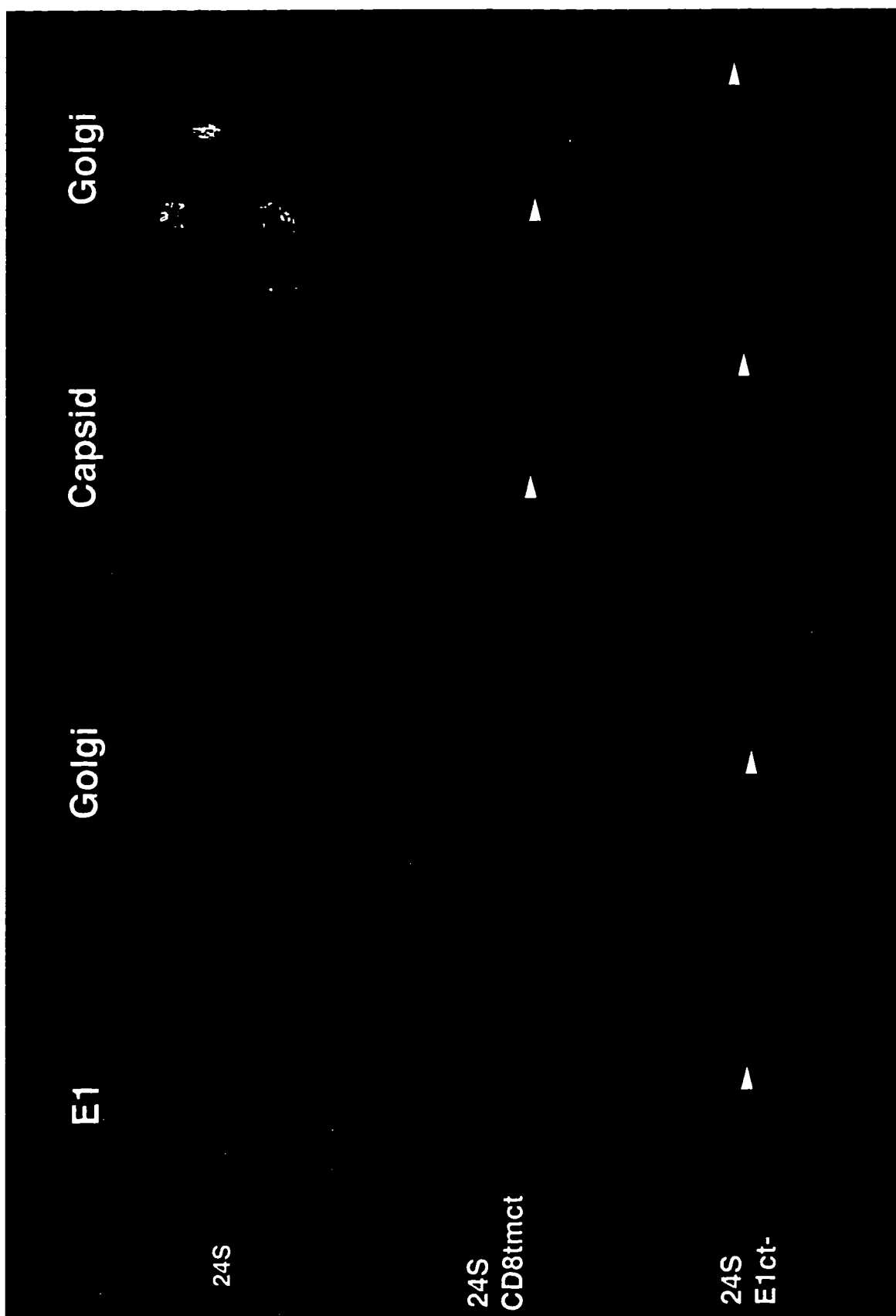


**Figure 14. RV structural proteins targeted to the Golgi of CHO 24S,
CHO 24S-CD8tm, CHO 24S-Gtmct cells**

RV structural proteins were targeted to the Golgi in CHO 24S, CHO 24S-CD8tm, CHO 24S-Gtmct cells. Cells were grown on fibronectin coated glass coverslips, then fixed and permeablized with methanol (CHO 24S and CHO 24S-CD8tm) or were fixed with paraformaldehyde and permeablized with Triton X-100 (CHO 24S-Gtmct) before being processed for immunofluorescence. Cells were stained for capsid, E2 and E1 using mouse monoclonal antibodies, and co-stained for the Golgi marker using rabbit anti-Man II. Texas Red conjugated 2° antibodies specific for mouse IgG and FITC conjugated 2° antibodies specific for rabbit IgG were used to locate RV antigens. Co-localization of capsid, E2 (not shown) or E1 with the Golgi marker Man II was present in all cases (indicated by arrowheads in several slides).

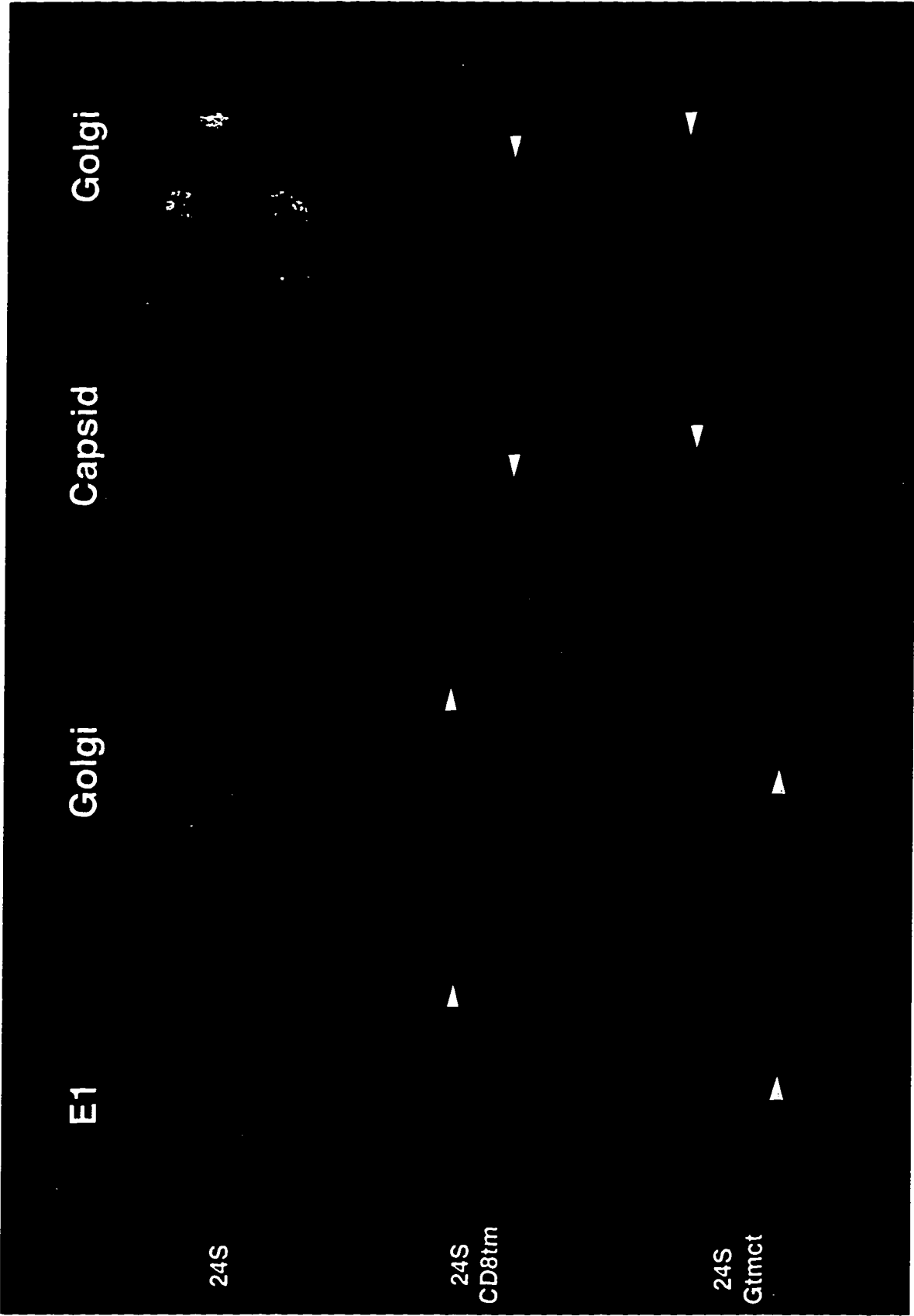


Figure 15. RLP secretion is dependent upon E1tmct

Transfected CHO cells were processed for ^{35}S and ^{32}P metabolic labeling, and for Western blot analysis. Capsid, E2 and E1 were secreted in CHO 24S cells only. However, all other clones expressed capsid, E2 and E1 at levels detectable by any and all of the three assay types employed.

Cells were labeled with ^{35}S cys/met or ^{32}P orthophosphate, and the media immunoprecipitated with human anti-RV. Proteins were separated by SDS PAGE, and the resulting fluorographs examined. After a 6 h chase period, ^{35}S labeled E2 and E1 could be detected in the media of CHO 24S cells only (A). Similarly, after an 18 h chase period, ^{32}P orthophosphate labeled capsid protein could be detected in the media of CHO 24S cells only (C). Interestingly, capsid is the only stably phosphorylated protein. Western blots were performed in parallel with ^{32}P orthophosphate labeling. Media was immunoprecipitated with human anti-RV serum, and the resulting protein blot probed with mouse monoclonal antibody specific for capsid. ECL analysis of the blots revealed capsid protein in the media of CHO24S cells only (B).

The specificity of the antibodies were demonstrated by using a non-specific antibody in the case of ^{32}P orthophosphate labeling (C) or negative human serum in the case of Western blots (not shown).

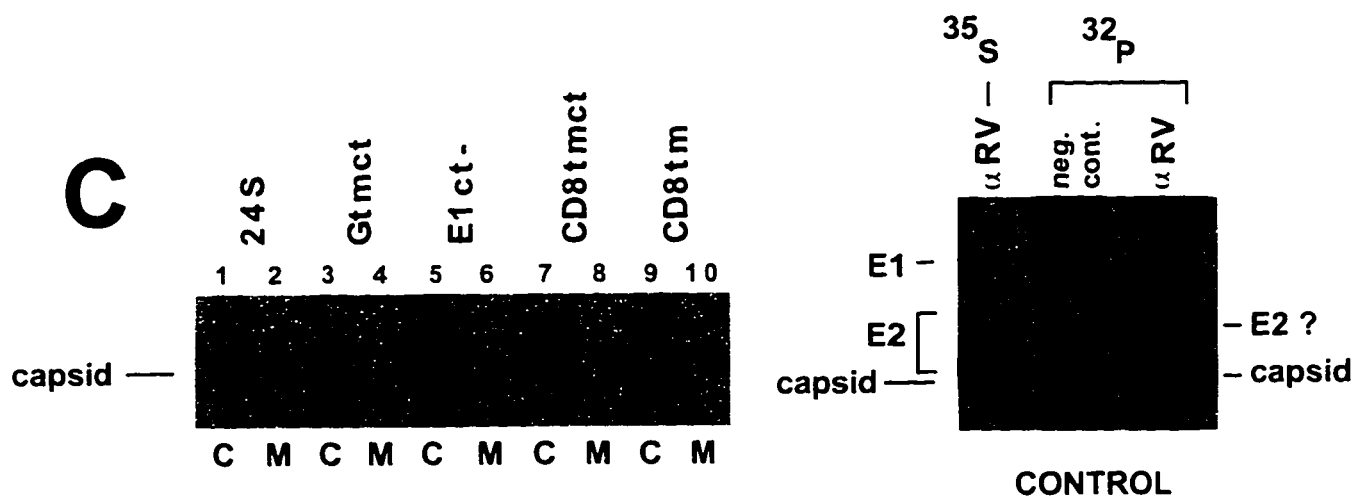
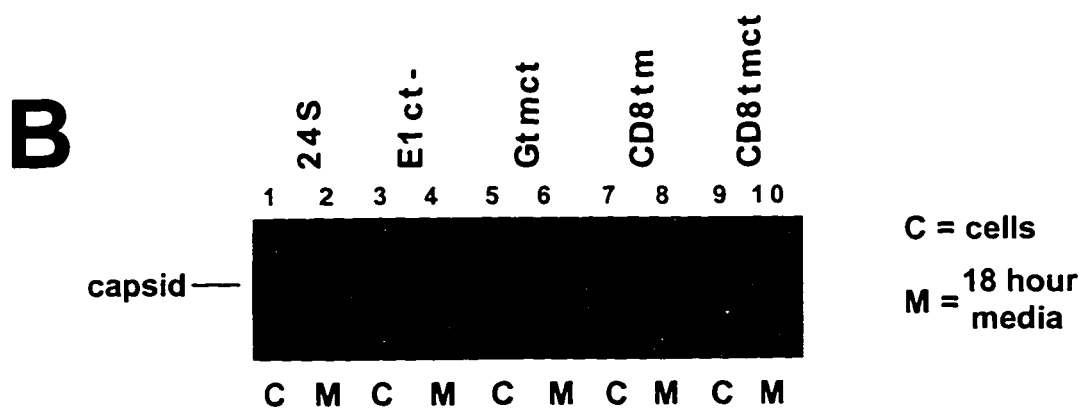
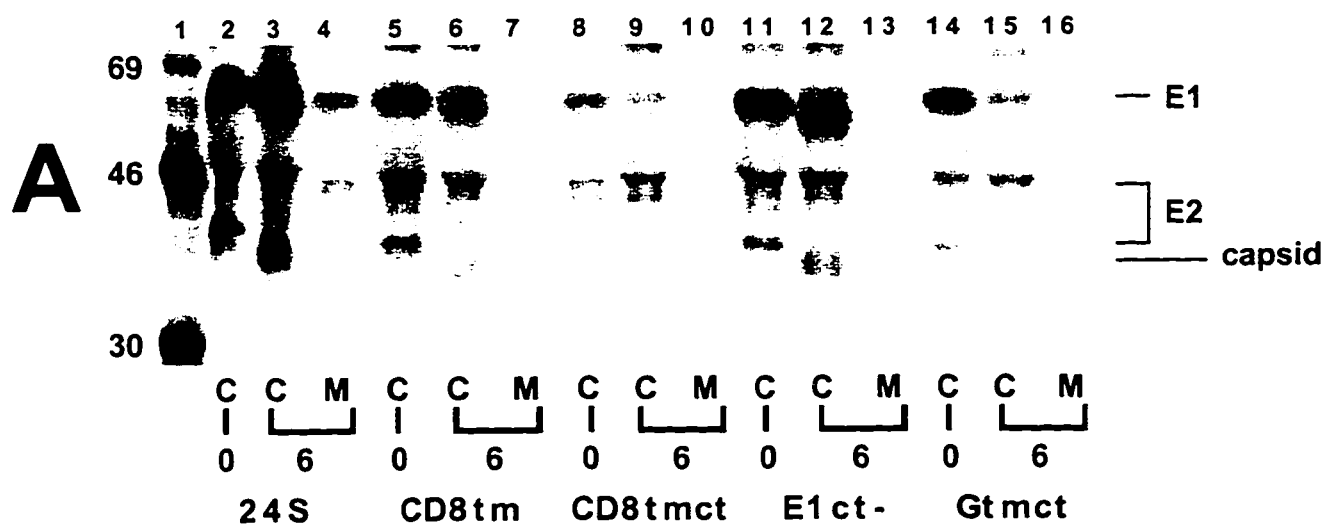


Figure 16. RLP and RV virion secretion, and default secretion pathways in polarized mammalian cells

A cartoon comparing RLP secretion and RV infection release with the default secretion pathways in Vero C1008, MDCK II and Caco-2- cells. In Caco-2 cells, RLPs and RV virions are secreted at both the apical and basolateral surfaces. The default secretion pathway is to the basolateral surface. In Vero C1008 cells RLPs and RV virions are also secreted at both surfaces. The default secretion pathway is unknown. In MDCK II cells, RLPs are secreted primarily at the apical surface. The default secretion pathway is to both the apical and basolateral surfaces.

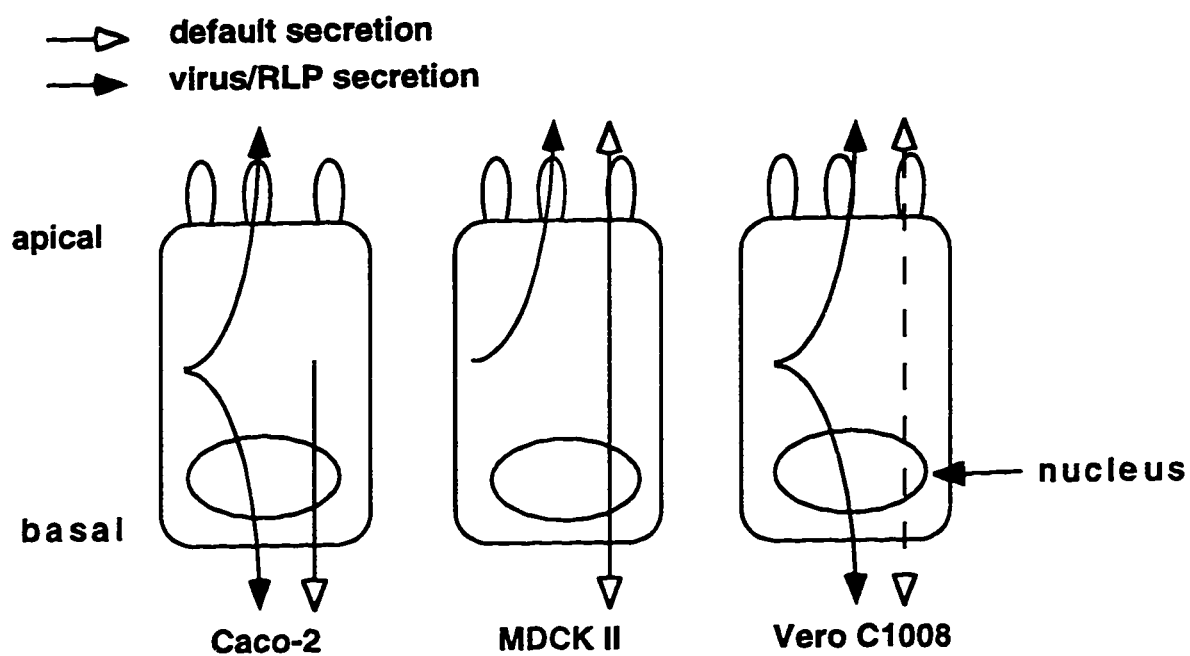


Figure 17. Construction of pCMV5-24SE1-CD8_{tm}

To construct this plasmid, pCMV5-CD8-E1ct was digested with *Eco* RV and *Bam* HI, and the ≈160 bp *Eco* RV/*Bam* HI, CD8_{tm}E1ct fragment purified by agarose gel electrophoresis and elution. pCMV5-24S-Gtmct was digested with *Bam* HI and *Eco* RV and the 415 bp *Bam* HI /*Eco* RV fragment purified by agarose gel electrophoresis and elution. pCMV5-24S-Gtmct was digested with *Bam* HI only, and the large fragment, i.e., the vector-NH₂-capsid-E2-and the N-terminal part of the E1ecto domain, was treated with Shrimp Alkaline Phosphatase (SAP; USB, Cleveland OH). Ligation of the three fragments resulted in a construct which contained pCMV5-24S with the transmembrane region of CD8 in place of the transmembrane region of E1 (CD8_{tm} underlined).

NH₂-...WADIYIWAPLAGTCGVLLLSLVITLYCNHKCLYYLRGAIAPR

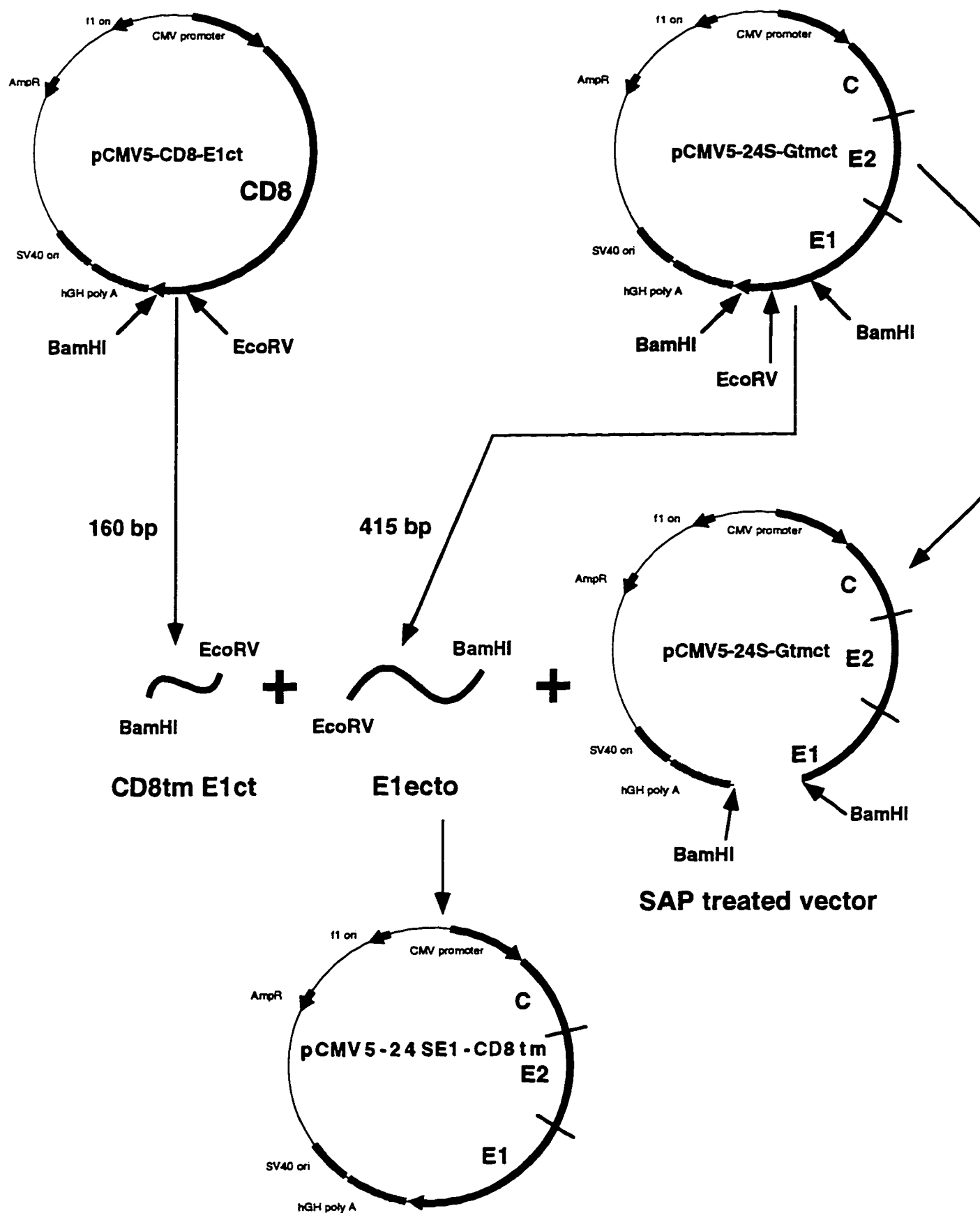


Figure 18. Construction of pCMV5-24SE1-CD8tmct

To construct this plasmid, pCMV5 was digested with *Eco* RI and *Bam* HI; this opened up the 4.7 kb vector at the polylinker. pCMV5-CD8 was digested with *Eco* RV and *Bam* HI, and the 900 bp (approx.) *Eco* RV/*Bam* HI, CD8tmct fragment purified by agarose gel electrophoresis and elution. pCMV5-24S-Gtmct was digested with *Eco* RI and *Eco* RV, and a 3.0 kb (approx.) fragment purified by agarose gel electrophoresis and elution, i.e., NH₂-capsid-E2-E1ecto domain. The three part ligation resulted in a construct which contained pCMV5-24S with the transmembrane and cytoplasmic regions of CD8 in place of the transmembrane and cytoplasmic regions of E1 (CD8tmct underlined).

NH₂-...WADYIWAPLAGTCGVLLLSLVITLYCNHRNRRRVCKCPRPVVKSGDKPSLSARYV

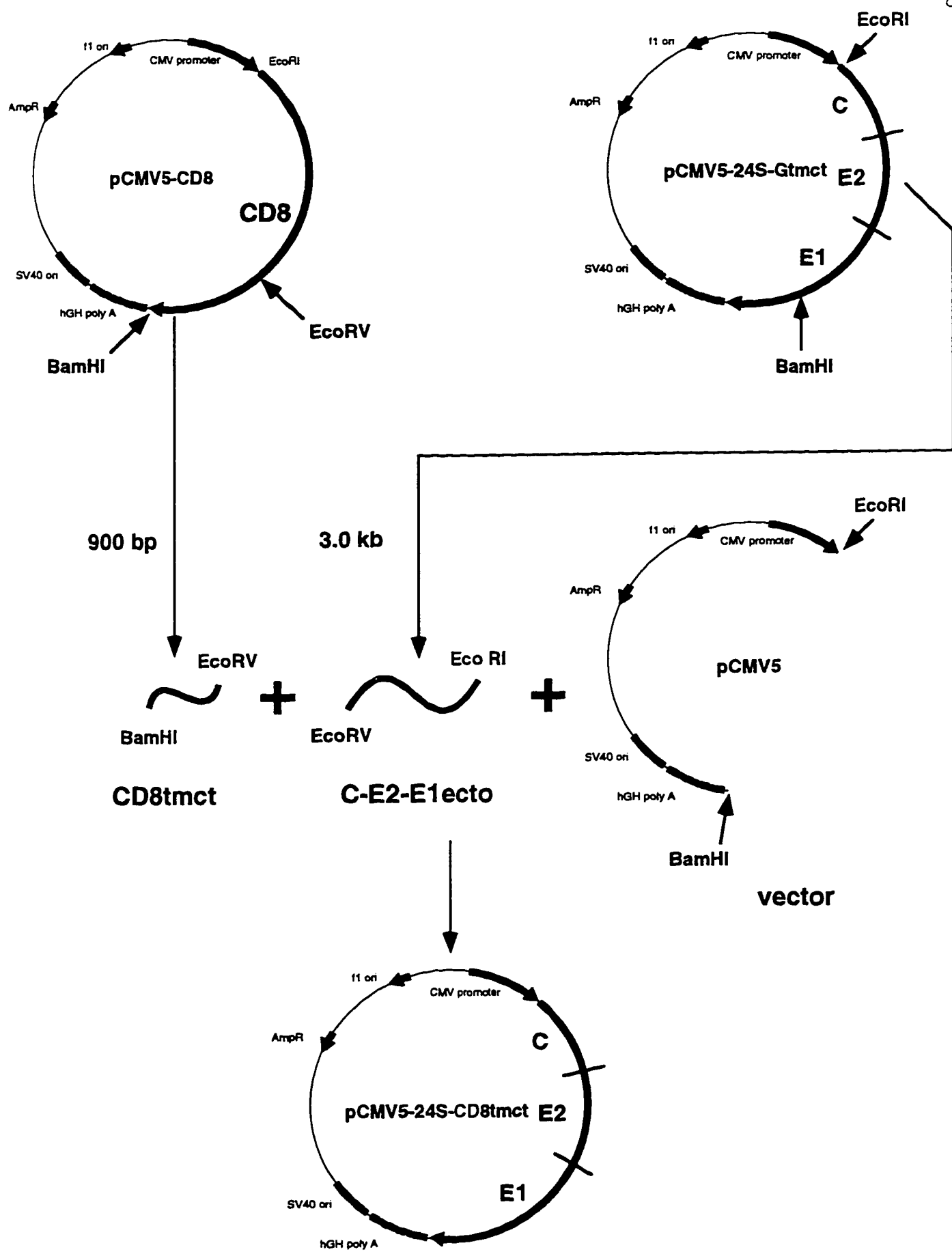


Figure 19. Construction of pCMV5-24SE2-Gtm

pCMV5-E2-Gtm-EI was digested with *Eco* RI and *Bst* EI, and the 7 kb large fragment containing the pCMV5 vector and all except the first 26 N-terminal amino acids of NH₂-E2-E1-COOH was purified by agarose gel electrophoresis and elution. pCMV5-24S was digested with *Eco* RI and *Bst* EI, and the 1 kb fragment containing NH₂-capsid and the first 26 amino acids of E2 was purified by agarose gel electrophoresis and elution. These two fragments were ligated together to produce pCMV5-24S-E2Gtm which contained

NH₂-capsid-E2Gtm-E1-COOH, i.e., E2 tm was replaced by VSVGtm (VSVGtm underlined).

NH₂-...SLDSSIASFFFFIIGLIIGLEFLVLRRA...-COOH

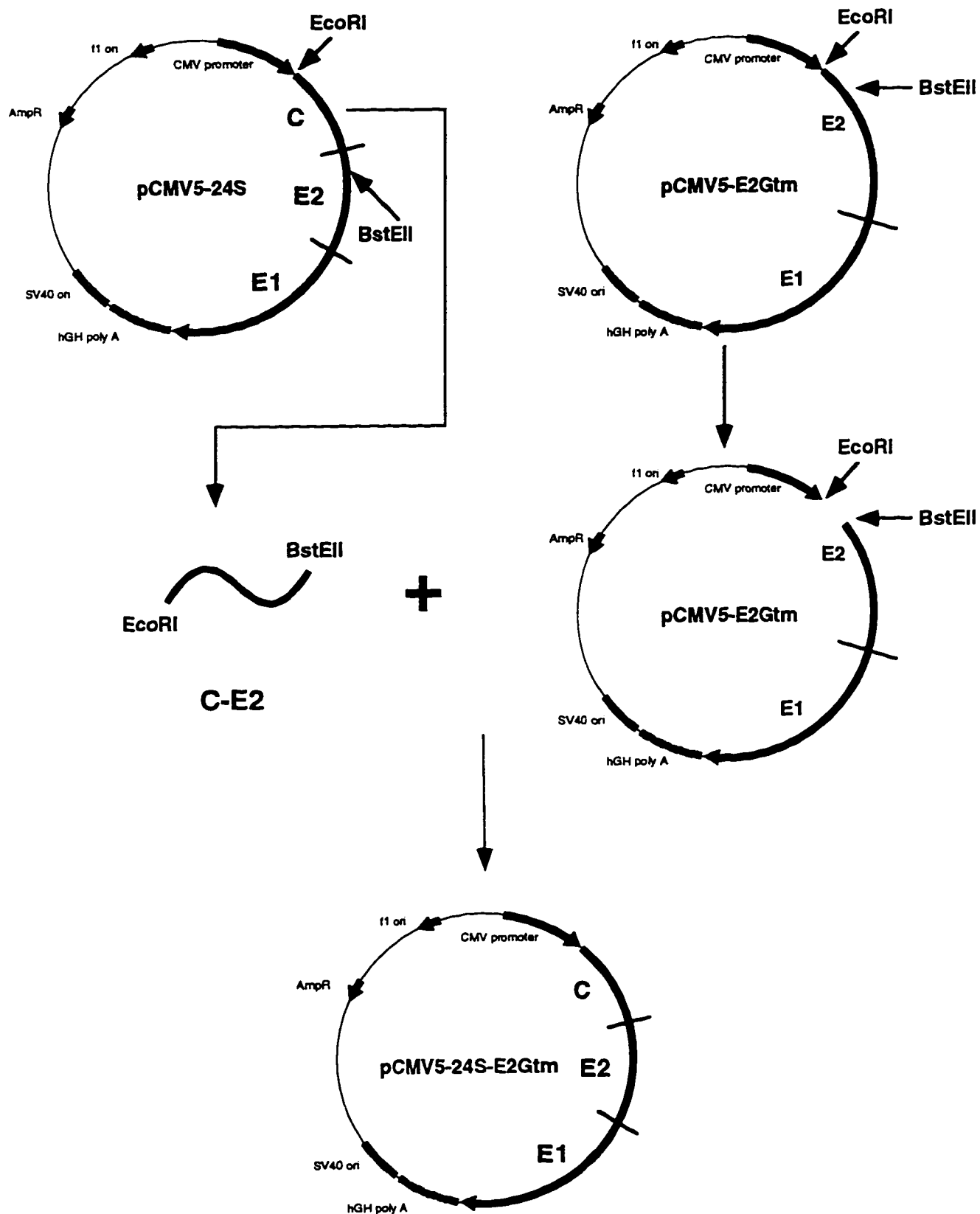
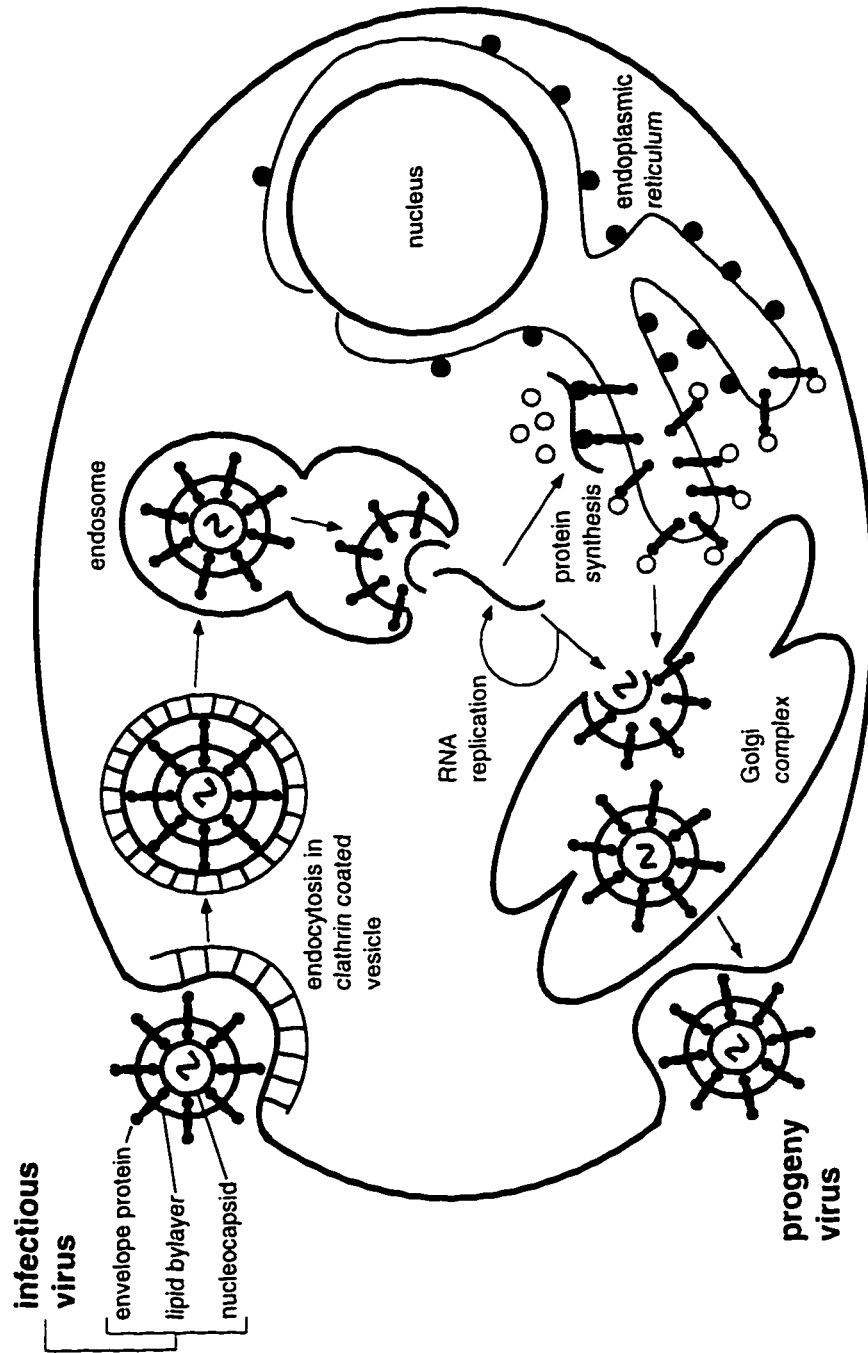


Figure 20. Cartoon of RV infection and replication cycle

Subsequent to attachment, RV virions are internalized and follow the endosomal pathway into the cell. The low pH of the endosome is believed to cause capsomere solubility after fusion of the viral envelope with the endosome. Positive polarity viral RNA is released into the cytoplasm, and the 5' proximal ORF is translated by host enzymes to produce non-structural (NS) RV proteins. NS proteins use the genomic RNA as a template to make full length and subgenomic positive polarity RNAs. The 3' one-third of the genomic RNA codes for the structural proteins NH₂-capsid-E2-E1-COOH in the form of a polyprotein. E2 and E1 signal peptides direct the translocation of the polyprotein into the endoplasmic reticulum (ER), where it is cleaved by resident signal peptidase on the C-terminal side of both signal peptides. Capsid protein remains on the cytoplasmic side of the ER membrane, the C-terminus being anchored to the ER membrane by virtue of the E2 signal peptide. Both E2 and E1 are type I membrane spanning glycoproteins. After cleavage of the polyprotein within the lumen of the ER, E2 and E1 ectodomains are core glycosylated. Ultimately, E2 is N- and O-glycosylated whereas E1 is N-glycosylated only. E2 is predicted to be attached to the ER by a transmembrane region and the signal peptide of E1, while a single transmembrane region attaches E1 to the ER. E2 and E1 form heterodimers that are targeted to the Golgi. RNA genomes are encapsidated by an icosahedral protein shell, forming a nucleocapsid complex which associates with membrane bound E2/E1. New virions mature by budding into the Golgi membrane, and are subsequently released at the cell surface (not to scale).



The life cycle of rubella virus

5 BIBLIOGRAPHY

1. **Alberts, B., D. Bray, J. Lewis, M. Raff, K. Roberts, and J. D. Watson (ed.).** 1994. *Molecular Biology of the Cell*, third ed. Garland Publishing, Inc., New York and London.
2. **Andersson, S., D. L. Davis, H. Dahlback, H. Jornvall, and D. W. Russell.** 1989. Cloning, structure, and expression of the mitochondrial cytochrome P-450 sterol 26-hydroxylase, a bile acid biosynthetic enzyme. *J. Biol. Chem.* **264**:8222-8229.
3. **Baron, M. D., T. Ebel, and M. Suomalainen.** 1992. Intracellular transport of rubella virus structural proteins expressed from cloned cDNA. *J. Gen. Virol.* **73**:1073-1086.
4. **Baron, M. D., and K. Forsell.** 1991. Oligomerisation of the structural proteins of rubella virus. *Virology.* **185**:811-819.
5. **Bergmann, J. E.** 1989. Propagation of wild-type and temperature -sensitive mutants of VSV, p. 102-105, *Methods Cell Biol.*, vol. 32. Academic Press, Inc.
6. **Blau, D. M., and R. W. Compans.** 1995. Entry and release of measles virus are polarized in epithelial cells. *Virology.* **21**:91-9.
7. **Bowden, D. S., and E. G. Westaway.** 1984. Rubella virus: structural and non-structural proteins. *J. Gen. Virol.* **65**:933-943.
8. **Brakenhoff, G. J., E. A. Van-Spronsen, H. T. M. Van-der-Voort, and N. Nanninga.** 1989. Three-dimensional confocal fluorescence microscopy, p. 379-397, *Methods Cell Biol.*, vol. 30. Academic Press, Inc.
9. **Butor, C., and J. Davoust.** 1992. Apical to basolateral surface area ratio and polarity of MDCK cells grown on different supports. *Exp. Cell. Res.* **203**:115-127.

10. **Caplan, M., and K. S. Matlin.** 1989. Sorting of membrane and secretory proteins in polarized epithelial cells, p. 71-127. *In* K. S. Matlin and J. D. Valentich (ed.), *Functional Epithelial Cells in Culture*, vol. 8. Alan R. Liss, Inc., New York.
11. **Caplan, M. J., H. C. Anderson, G. E. Palade, and J. D. Jamieson.** 1986. Intracellular sorting and polarized cell surface delivery of N/K-ATPase, an endogenous component of MDCK Cell basolateral plasma membranes. *Cell*. 46:623-631.
12. **Caplan, M. J., J. L. Stow, A. P. Newman, J. Madri, H. C. Anderson, M. G. Farquhar, G. E. Palade, and J. D. Jamieson.** 1987. Dependence on pH of polarized sorting of secreted proteins. *Nature*. 329:632-635.
13. **Cereijido, M., J. Ehrenfeld, S. Fernandez-Castelo, and I. Meza.** 1981. Fluxes, junctions and blisters in cultured monolayers of epithelioid cells (MDCK). *Ann. NY Acad. Sci.* 372:422-441.
14. **Chen, S. Y., Y. Matsuoka, and R. W. Compans.** 1991. Assembly and polarized release of Punta Toro virus and effects of brefeldin A. *J. Virol.* 65:1427-39.
15. **Clarke, D. M., T. W. Loo, I. Hui, P. Chong, and S. Gillam.** 1987. Nucleotide sequence and *in vitro* expression of rubella virus 24S subgenomic mRNA encoding the structural proteins E1, E2 and C. *Nucl. Acids Res.* 15:3041-3057.
16. **Clarke, D. M., T. W. Loo, H. McDonald, and S. Gillam.** 1988. Expression of rubella virus cDNA coding for the structural proteins. *Gene*. 65:23-30.
17. **Dong, J., and E. Hunter.** 1993. Analysis of retroviral assembly using a vaccinia/T7-polymerase complementation system. *Virology*. 194:192-199.
18. **Earley, E. M., and K. M. Johnson.** 1988. The lineage of the Vero, Vero 76 and its clone C1008 in the United States, p. 26-29. *In* B. Simizu and T. Terasima

(ed.), Vero Cells - Origin, Properties and Biomedical Applications. Soft Science Publications, Tokyo.

19. **Frazer, I. H.** 1996. Immunology of papillomavirus infection. *Curr. Opin. Immunol.* 8:484-491.
20. **Frey, T. K.** 1994. Molecular Biology of Rubella Virus, p. 69-160, *Advances in Virus Research*. Academic Press.
21. **Frey, T. K., and M. L. Hemphill.** 1988. Generation of defective-interfering particles by Rubella virus in vero cells. *Virology.* 164:22-29.
22. **Fuller, S., C. H. von Bonsdorff, and K. Simons.** 1984. Vesicular stomatitis virus infects and matures only through the basolateral surface of the polarized epithelial cell line, MDCK. *Cell.* 38:65-77.
23. **Gonzalez, S. A., J. L. Affranchino, H. R. Gelderblom, and A. Burny.** 1993. Assembly of the matrix protein of simian immunodeficiency virus into virus-like particles. *Virology.* 194:548-556.
24. **Gotlieb, T. A., S. Gonzalez, L. Rizzolo, M. Rindler, M. Adesnik, and D. D. Sabatini.** 1986. Sorting and endocytosis of viral glycoproteins in transfected polarized epithelial cells. *J. Cell Biol.* 102:1242-1255.
25. **Gross, C., M. Linder, G. Wengler, and G. Wengler.** 1997. Analyses of disulfides present in rubella virus E1 glycoprotein. *Virology.* 230:179-186.
26. **Gstraunthaler, G. J. A.** 1988. Epithelial Cells in Tissue Culture. *Renal Physiol Biochem.* 11:1-42.
27. **Hammerton, R. W., K. A. Krzeminski, R. W. Mays, T. A. Ryan, D. A. Wollner, and W. J. Nelson.** 1991. Mechanism for regulating cell surface distribution of Na/K-ATPase in polarized epithelial cells. *Science.* 254:847-850.
28. **Hammond, C., and A. Helenius.** 1995. Quality control in the secretory pathway. *Curr. Opin. Cell Biol.* 7:523-529.

29. Hayflick, L. 1965. The limited in vitro lifetime of human diploid cell strains. *Ex. Cell Res.* **37**:614-636.
30. Hemphill, M. L., R. Y. Forng, E. S. Abernathy, and T. K. Frey. 1988. Time course of virus specific macromolecular synthesis during rubella virus infection in vero cells. *Viol.* **162**:65-75.
31. Ho-Terry, L., and A. Cohen. 1984. The role of glycosylation on haemagglutination and immunological reactivity of Rubella virus. *Arch. Virol.* **79**:139-146.
32. Ho-Terry, L., and A. Cohen. 1985. Rubella virus haemagglutinin: association with a single virion glycoprotein. *Arch. Virol.* **84**:207-215.
33. Hobbins, T. E., and K. O. Smith. 1968. Fluorescent plaque assay of Rubella Virus infectivity. *Proc. Soc. Exptl. Biol. Med.* **129**:407-412.
34. Hobman, T. C., and S. Gillam. 1989. In vitro and in vivo expression of rubella virus E2 glycoprotein: The signal peptide is located in the C-terminal region of capsid protein. *Virology.* **173**:241-250.
35. Hobman, T. C., H. F. Lemon, and K. Jewel. 1997. Characterization of an ER retention signal in the rubella virus E1 glycoprotein. submitted for publication.
36. Hobman, T. C., M. L. Lundstrom, and S. Gillam. 1990. Processing and intracellular transport of rubella virus structural proteins in COS cells. *Virology.* **178**:122-133.
37. Hobman, T. C., M. L. Lundstrom, C. A. Mauracher, L. Woodward, S. Gillam, and M. G. Farquhar. 1994. Assembly of rubella virus structural proteins into virus-like particles in transfected cells. *Virology.* **202**:574-585.
38. Hobman, T. C., Z. Qiu, H. Chaye, and S. Gillam. 1991. Analysis of rubella virus E1 glycosylation mutants expressed in COS cells. *Virology.* **181**:768-772.

39. **Hobman, T. C., R. Shukin, and S. Gillam.** 1988. Translocation of rubella virus glycoprotein E1 into the endoplasmic reticulum. *J. Virol.* **62**:4259-4264.
40. **Hobman, T. C., L. Woodward, and M. G. Farquhar.** 1992. The rubella virus E1 glycoprotein is arrested in a novel post-ER, pre-Golgi compartment. *J. Cell Biol.* **118**:795-811.
41. **Hobman, T. C., L. Woodward, and M. G. Farquhar.** 1993. The rubella virus E2 and E1 spike glycoproteins are targeted to the Golgi complex. *J. Cell Biol.* **121**:269-281.
42. **Hobman, T. C., L. Woodward, and M. G. Farquhar.** 1995. Targeting of a heterodimeric membrane protein complex to the Golgi: Rubella virus E2 glycoprotein contains a transmembrane Golgi retention signal. *Mol. Biol. Cell.* **6**:7-20.
43. **Jacobs, J. P., C. M. Jones, and J. P. Baille.** 1970. Characteristics of human diploid cell designated MRC-5. *Nature.* **227**:168-170.
44. **Karounos, D. G., J. S. Wolinsky, and J. W. Thomas.** 1993. Monoclonal antibody to rubella virus capsid protein recognizes a β -cell antigen. *J. Immunol.* **150**:3080-3085.
45. **Kitagawa, Y., Y. Sano, M. Ueda, K. Higashio, H. Narita, M. Okano, S.-I. Matsumoto, and R. Sasaki.** 1994. N-Glycosylation of erythropoietin is critical for apical secretion by Madin-Darby Canine Kidney cells. *Exp. Cell Res.* **213**:449-457.
46. **Kreis, T. E.** 1986. Microinjected antibodies against the cytoplasmic domain of vesicular stomatitis virus glycoprotein blocks its transport to the cell surface. *EMBO J.* **5**:931-941.
47. **Leahy, D. J.** 1995. A structural view of CD4 and CD8. *FASEB J.* **9**:17-25.
48. **Lee, J.-Y., J. A. Marshall, and D. S. Bowden.** 1992. Replication complexes associated with the morphogenesis of rubella virus. *Arch. Virol.* **122**:95-106.

49. Lee, J. Y., D. Hwang, and S. Gillam. 1996. Dimerization of rubella capsid protein is not required for virus particle formation. *Virology*. 216:223-227.
50. Lopez-Vancell, R., G. Beaty, E. Stefani, E. E. Rodriguez-Boulan, and M. Cereijido. 1984. Changes in paracellular and cellular ionic permeabilities of monolayers of MDCK cells infected with influenza or vesicular stomatitis viruses. *J. Mem. Biol.* 81:171-80.
51. Lundstrom, M. L., C. A. Mauracher, and A. J. Tingle. 1991. Characterization of carbohydrates linked to rubella virus glycoprotein E2. *J. Gen. Virol.* 72:843-850.
52. Madara, J. L., and K. Dharmasathaphorn. 1985. Occluding junction structure-function relationships in a cultured epithelial monolayer. *J. Cell Biol.* 101:2124-2133.
53. Madara, J. L., and G. Hecht. 1989. Tight (Occluding) junctions in cultured (and native) epithelial cells, p. 131-163. *In* K. S. Matlin and J. D. Valentich (ed.), *Functional Epithelial Cells in Culture*, vol. 8. Alan R. Liss, Inc., New York.
54. Marr, L. D., A. Sanchez, and T. K. Frey. 1991. Efficient in-vitro translation and processing of the Rubella Virus structural proteins in the presence of microsomes. *Virology*. 180:400-405.
55. Mastromarino, P., L. Cioe, S. Rieti, and N. Orsi. 1990. Role of membrane phospholipids and glycolipids in the vero cell surface receptor for rubella virus. *Medical Microbiology and Immunology*. 179:105-114.
56. Mauracher, C. A., S. Gillam, R. Shukin, and A. J. Tingle. 1991. pH-dependent solubility shift of Rubella virus capsid protein. *Virol.* 181:773-777.
57. Mays, R. W., K. A. Siemers, B. A. Fritz, A. W. Lowe, G. van Meer, and W. J. Nelson. 1995. Hierarchy of mechanisms involved in generating Na/K-ATPase polarity in MDCK epithelial cells. *J. Cell Biol.* 130:1105-1115.

58. McDonald, H., T. C. Hobman, and S. Gillam. 1991. The influence of capsid protein cleavage on the processing of E2 and E1 glycoproteins of rubella virus. *Virology*. 183:52-60.
59. McRoberts, J. A., M. Taub, and M. H. Saier Jr. 1981. The Madin Darby Canine Kidney (MDCK) cell line. In G. Sato (ed.), *Functionally Differentiated Cell Lines*. Liss, Alan R., New York.
60. Mebatsion, T., M. Konig, and K.-K. Conzelmann. 1996. Budding of rabies virus particles in the absence of the spike glycoprotein. *Cell*. 84:941-951.
61. Mellinger, A. K., J. D. Cragan, W. L. Atkinson, W. W. Williams, B. Kleger, R. G. Kimber, and D. Tavis. 1995. High incidence of congenital rubella syndrome after a rubella outbreak. *Ped. Infect. Dis. J.* 14:573-578.
62. Neutra, M., and D. Louvard. 1989. Differentiation of Intestinal Cells In Vitro, p. 363-398. In K. S. Matlin and J. D. Valentich (ed.), *Functional Epithelial Cells in Culture*, vol. 8. Alan R. Liss, Inc., New York.
63. Oker-Blom, C. 1984. PhD Thesis. University of Helsinki.
64. Oker-Blom, C., N. Kalkkinen, L. Kaariainen, and R. F. Pettersson. 1983. Rubella virus contains one capsid protein and three envelope glycoproteins, E1, E2a and E2b. *J. Virol.* 46:964-973.
65. Oker-Blom, C., I. Ulmanen, L. Kaariainen, and R. F. Pettersson. 1984. Rubella virus 40S genome RNA specifies a 24S subgenomic RNA that codes for a precursor to structural proteins. *J. Virol.* 49:403-408.
66. Orci, L., M. Ravazzola, M. Amherdt, A. Perrelet, S. K. Powell, D. L. Quinn, and H.-P. Moore. 1987. The trans-most cisternae of the Golgi complex: A compartment for sorting of secretory and plasma membrane proteins. *Cell*. 51:1039-1051.
67. Oshiro, L. S., N. J. Schmidt, and E. H. Lennette. 1969. Electron microscopic studies of Rubella Virus. *J. Gen. Virol.* 5:205-210.

68. **Owen, K. E., and R. J. Kuhn.** 1997. Alphavirus budding is dependent on the interaction between the nucleocapsid and hydrophobic amino acids on the cytoplasmic domain of the E2 envelope glycoprotein. *Viol.* **230**:187-196.
69. **Pascale, M. C., N. Malagolini, F. Serafini-Cessi, G. Migliaccio, A. Leone, and S. Bonatti.** 1992. Biosynthesis and oligosaccharide structure of human CD8 glycoprotein expressed in Rat epithelial cell line. *J. Cell Biol.* **267**:9940-9947.
70. **Petruzzello, R., N. Orsi, S. Macchia, S. Rieti, T. K. Frey, and P. Mastromarino.** 1996. Pathway of rubella virus infectious entry into Vero cells. *J. Gen. Virol.* **77**:303-308.
71. **Qiu, Z., T. C. Hobman, H. L. McDonald, N. O. Seto, and S. Gillam.** 1992. Role of N-linked oligosaccharides in processing and intracellular transport of E2 glycoprotein of rubella virus. *J. Virol.* **66**:3514-3521.
72. **Richardson, J. C. W., V. Scalera, and N. L. Simmons.** 1981. Identification of two strains of MDCK cells which resemble separate nephron tubule segments. *Biochim. Biophys. Acta.* **673**:26-36.
73. **Roberts, D.** 1997. Manitobans warned of rubella epidemic, *Globe and Mail*.
74. **Roberts, S. R., R. W. Compans, and G. W. Wertz.** 1995. Respiratory syncytial virus matures at the apical surfaces of polarized epithelial cells. *J. Virol.* **69**:2667-73.
75. **Rodriguez-Boulan, E., and D. D. Sabatini.** 1978. Asymmetric budding of viruses in epithelial monolayers: A model system for study of epithelial polarity. *Proc. Natl. Acad. Sci.* **75**:5071-5075.
76. **Rodriguez-Boulan, E., P. Salas, J., M. Sargiacomo, M. Lisanti, A. Lebivic, Y. Sambuy, D. Vega-Salas, and L. Graeve.** 1989. Methods to estimate the polarized distribution of surface antigens in cultured epithelial cells, p. 37-56, *Methods Cell Biol.*, vol. 32. Academic Press, Inc.

77. **Rossen, J. W. A.** 1996. PhD Thesis. University of Utrecht.
78. **Schalich, J., S. L. Allison, K. Stiasny, C. W. Mandl, C. Kunz, and F. X. Heinz.** 1996. Recombinant subviral particles from tick-borne encephalitis virus are fusogenic and provide a model system for studying flavivirus envelope glycoprotein functions. *J. Virol.*:4549-4557.
79. **Scheiffele, P., J. Peranen, and K. Simons.** 1995. N-glycans as apical sorting signals in epithelial cells. *Nature.* 378:96-98.
80. **Schlesinger, S., and M. J. Schlesinger.** 1996. *Togaviridae* : The viruses and their replication, p. 825-841. *In* B. N. Fields and D. M. Knipe and P. M. Howley (ed.), *Virology*, Third ed. Raven Press Ltd., New York.
81. **Sherris, J. C. (ed.).** 1990. *Medical Microbiology*, Second ed. Elsevier, New York.
82. **Sicard, D., D. Salmon-Ceron, and L. Finkielsztejn.** 1997. Search for a HIV vaccine. *Presse Med.* 26:248-254.
83. **Strauss, J. H., and E. G. Strauss.** 1994. The alphaviruses: gene expression, replication, and evolution. *Microbiol Rev.* 58:491-562.
84. **Suomalainen, M., H. Garoff, and M. D. Baron.** 1990. The E2 signal sequence of Rubella virus remains part of the capsid protein and confers membrane association in vitro. *J. Virol.* 64:5500-5509.
85. **Tashiro, M., N. L. McQueen, J. T. Seto, H.-D. Klenk, and R. Rott.** 1996. Involvement of the mutated M protein in altered budding polarity of a pantropic mutant, F1-R of Sendai virus. *J. Virol.*:5990-5997.
86. **Terry, G. M., L. Ho-Terry, P. Londesborough, and K. R. Rees.** 1988. Localization of the rubella E1 epitopes. *Arch. Virol.* 98:189-197.
87. **Tingle, A. J., M. Allen, R. E. Petty, G. D. Kettyls, and J. K. Chantler.** 1986. Rubella-associated arthritis. 1. Comparative study of joint manifestations

associated with natural rubella infection and RA 727/3 rubella immunization.

Ann. Rheum. Dis. 45:110-114.

88. Tooze, J., S. A. Tooze, and S. D. Fuller. 1987. Sorting of progeny coronavirus from condensed secretory proteins at the exit from the trans-Golgi network of AtT-20 cells. J. Cell Biol. 105:1215-1226.

89. Tucker, S. P., C. L. Thornton, E. Wimmer, and R. W. Compans. 1993. Bidirectional entry of poliovirus into polarized epithelial cells. J. Virol. 67:29-38.

90. Tucker, S. P., C. L. Thornton, E. Wimmer, and R. W. Compans. 1993. Vectorial release of poliovirus from polarized human intestinal epithelial cells. J. Virol. 67:4274-82.

91. Urban, J., K. Parczyk, A. Leutz, M. Kayne, and C. Kondor-Koch. 1987. Constitutive apical secretion of an 80-kD sulfated glycoprotein complex in the polarized epithelial Madin-Darby canine kidney cell line. J. Cell Biol. 105:2735-2743.

92. Vennema, H., G.-J. Godeke, J. W. A. Rossen, W. F. Voorhout, M. C. Horzinek, D.-J. E. Opstelten, and P. J. M. Rottier. 1996. Nucleocapsid-independent assembly of coronavirus-like particles by coexpression of viral envelope protein genes. EMBO J. 15:2020-2028.

93. von Bonsdorff, C.-H., and A. Vaheri. 1969. Growth of rubella virus in BHK-21 cells: Electron microscopy of morphogenesis. J. Gen. Virol. 5:47-51.

94. von Bonsdorff, C. H., S. Fuller, and K. Simons. 1985. Apical and basolateral endocytosis in MDCK cells grown on nitrocellulose filters. EMBO J. 4:2781-2792.

95. Wagner, R. R., and J. K. Rose. 1996. Rhabdoviridae: the viruses and their replication, p. 1121-1135. In B. N. Fields and D. M. Knipe and P. M. Howley (ed.), Virology, Third ed. Raven Press Ltd., New York.

96. **Wang, C.-Y., G. Dominguez, and T. K. Frey.** 1994. Construction of rubella virus genome-length cDNA clones and synthesis of infectious RNA transcripts. *J. Virol.* 68:3550-3557.
97. **Waxham, M. N., and J. S. Wolinsky.** 1985. A model of the structural organization of rubella virus virions. *Rev. Infect. Dis.* 7:S133-S139.
98. **Wheater, P. R., H. G. Burkitt, and V. G. Daniels.** 1987. *Functional Histology: a text and colour atlas*, second ed. Churchill Livingstone, New York.
99. **Wolinsky, J. S.** 1996. Rubella, p. 899-929. *In* B. N. Fields and D. M. Knipe and P. M. Howley (ed.), *Virology*, Third ed. Raven Press Ltd., New York.
100. **Wolinsky, J. S., M. McCarthy, D. Allen-Cannady, W. T. Moore, R. Jin, S. Cao, A. Lovett, and D. Simmons.** 1991. Monoclonal antibody-defined epitope map of expressed rubella virus protein domains. *J. Virol.* 65:3986-3994.
101. **Wolinsky, J. S., E. Sukholutsky, W. T. Moore, A. Lovett, M. McCarthy, and B. Adame.** 1993. An antibody- and synthetic peptide-defined rubella virus E1 glycoprotein neutralization domain. *J. Virol.* 67:961-968.
102. **Zurzolo, C., C. Polistina, M. Saini, R. Gentile, L. Aloj, G. Migliaccio, S. Bonatti, and L. Nitsch.** 1992. Opposite polarity of virus budding and of viral envelope glycoprotein distribution in epithelial cells derived from different tissues. *J. Cell Biol.* 117:551-564.